Transthyretin Amyloidosis Therapy: A possibility in "Brahmi" (*Centella asiatica* and *Bacopa monnieri*) phytochemicals

Eze Fredrick Nwude

A Thesis Submitted in Fulfillment of the Requirements for the Degree of Doctor of Philosophy in Biochemistry
Prince of Songkla University
2020

Transthyretin Amyloidosis Therapy: A possibility in "Brahmi" (*Centella asiatica* and *Bacopa monnieri*) phytochemicals

Eze Fredrick Nwude

A Thesis Submitted in Fulfillment of the Requirements for the Degree of Doctor of Philosophy in Biochemistry
Prince of Songkla University
2019

Thesis Title	Transthyretin Amyloidosis Therapy: A possibility in "Brahmi" (*Centella asiatica and Bacopa monnieri*) phytochemicals
Author	Mr. Eze Fredrick Nwude
Major Program	Biochemistry

Major Advisor

.....
(Assoc. Prof. Dr. Porntip Prapunpoj)

Examining Committee :

.....Chairperson
(Asst. Prof. Dr. Phisit Prapunwattana)

.....Committee
(Assoc. Prof. Dr. Porntip Prapunpoj)

.....Committee
(Asst. Prof. Dr. Ladda Leelawatwattana)

The Graduate School, Prince of Songkla University, has approved this thesis as fulfillment of the requirements for the Doctor of Philosophy Degree in Biochemistry

.....
(Prof. Dr. Damrongsak Faroongsarng)
Dean of Graduate School

This is to certify that the work here submitted is the result of the candidate's own investigations. Due acknowledgement has been made of any assistance received.

.....Signature
(Assoc. Prof. Dr. Porntip Prapunpoj)
Major Advisor

.....Signature
(Mr. Eze Fredrick Nwude)
Candidate

I hereby certify that this work has not been accepted in substance for any degree, and is not being currently submitted in candidature for any degree.

.....Signature
(Mr. Eze Fredrick Nwude)
Candidate

Thesis Title	Transthyretin Amyloidosis Therapy: A possibility in "Brahmi" (*Centella asiatica* and *Bacopa monnieri*) phytochemicals
Author	Mr. Eze Fredrick Nwude
Major Program	Biochemistry
Academic Year	2019

ABSTRACT

Transthyretin (TTR) is a 55 kDa multifunctional plasma protein. Human native TTR is a β-sheet-rich homotetramer with monomers comprising of 127 amino acid residues. Its canonical functions include the transport of thyroid hormones and vitamin A, aided by retinol-binding protein within the blood and cerebrospinal fluid. Under certain conditions, TTR acquires a gain in toxic function role associated with the development of a severe disorder, transthyretin (ATTR) amyloidosis. ATTR amyloidosis are a group of progressive, debilitating and often fatal disease for which there is currently no cure. They are characterized by systemic deposition and accumulation of abnormal, misfolded/mis-aggregated TTR in vital organs leading to degeneration and dysfunction. With limited therapeutic options there is need for investigations aimed at developing safe and effective remedies for these ailments. Given that they key molecular event underlying the etiopathogenesis of TTR amyloidogenesis is the dissociation of the homotetramer into monomers only which could enter the amyloid cascade, preventing tetramer dissociation using small ligands or stabilizers which enhance the kinetic barrier for dissociation had been promoted as a pragmatic therapeutic strategy to combat ATTR amyloidosis. The primary objective of this work was to determine and elucidate the TTR amyloidogenic inhibitory activities of two popular nervines, *Centella asiatica* and *Bacopa monnieri*. Chemical characterization showed that both extracts were replete with antioxidant bioactive compounds. Tetramer stability assays by urea- and acid-mediated denaturation revealed that both extracts protected against tetramer dissociation into monomers. Aggregation-inducing assays suggest that both extracts inhibited the formation of mature amyloid fibrils from TTR. However, only *B. monnieri* extract prevented

formation of TTR aggregates. From the ANS and NBT-redox cycling assays, it could be inferred that both extracts were able to bind at the hydrophobic thyroxine-binding sites putatively increasing dimer-dimer interactions. While the binding interactions between TTR and *C. asiatica* seems to be covalent, that between the protein and *B. monnieri* extract was weak and non-covalent. Together, these findings suggest that *C. asiatica* and *B. monnieri* inhibited TTR amyloidogenesis in vitro and highlighted the potential of these bioactives as plausible therapeutic candidates and sources for the mining of novel drug scaffolds targeted against TTR amyloidosis.

ACKNOWLEDGEMENT

I give thanks to Jehovah, the Source of all that is good. Foremost, I am grateful to my supervisor, Assoc. Prof. Dr. Porntip Prapunpoj for the creating this special opportunity, giving me the support and allowing me to draw form her wealth of wisdom, knowledge and generosity. Also, I would like to thank Asst. Prof. Ladda Leelawatwattana for creating a conducive environment for me to perform my research and making sure I get all the materials needed. Thanks for your kindness, advice and encouragements. I would like to extend my sincere appreciation to the academic and administrative staff of the department of biochemistry, for your hospitality and warmth. To my Lab mates at ST420, I am thankful for your camaraderie. To the Graduate School, National Research Council of Thailand, Prince of Songkla University and the Excellent Biochemistry Program Fund of Prince of Songkla University, Thailand and Thailand's Education Hub for ASEAN Countries, I am grateful for the financial support during my program. To the Chairperson of my thesis examination committee, Asst. Prof. Dr. Phisit Prapunwattana, thank you for finding time out of your busy schedule and the valuable critique you brought to bear on this work. To my family, who had endured my absence without withholding their love and encourage, I would always be in your debt. To my soulmate, Eze Roseline thanks for your patience and love.

Eze Fredrick Nwude

CONTENTS

LIST OF TABLES

LIST OF FIGURES

LIST OF ABBREVIATIONS AND SYMBOLS

BME	*Bacopa monnieri* extract
CAP	*Centella asiatica* bioactives
CSF	cerebrospinal fluid
° C	degree Celsius
EDTA	ethylenediaminetetraacetic acid
FAC	familial amyloidotic cardiomyopathy
FAP	familial amyloidotic polyneuropathy
HPLC	high-performance liquid chromatography
LC-MS	liquid chromatography coupled to mass spectrometry
kDa	kilodalton
kg	kilogram
L55P	leucine-55 substituted by proline
M	molar
mg	milligram
ml	milliliter
PAGE	polyacrylamide gel electrophoresis
RBP	retinol binding protein
SDS	sodium dodecyl sulfate
T4	thyroxine
TBG	thyroxine-binding globulin
TBP	thyroxine-binding pocket
TTR	transthyretin
V30M	valine substituted by methionine at position 30
WT	wild type

CHAPTER 1

Introduction and Literature Review

1.1 Introduction

Proteins are some of the most interesting biomolecules found in nature. With a long list of physiological roles including locomotion (actin and myosin filaments), transport (hemoglobin), storage (ferritin), signal transduction (G-proteins), enhancement and regulation of metabolic reactions (enzymes), just to mention a few, it is clearly indicative of the fact that they are vital to the survival of living systems on earth. Biosynthesis of a fully functional protein requires the folding of its polypeptide(s) into the appropriate three-dimensional structure, a process that is tightly regulated by the cell. Aberration in this process leads to several protein folding diseases in humans (Gutteridge and Thornton, 2005).

The delicate balance between properly folded proteins and misfolded proteins or non-native toxic aggregates in nature may have necessitated cells to evolve highly complex mechanisms to ensure the structural fidelity of functional proteins vital for life. These systems are collectively known as protein homeostasis or "proteostasis", and comprise a vast network that ranges from synthesis and folding (i.e., ribosomes, chaperones, etc.) to degradation (i.e., proteases, autophagy, lysosomal targeting, etc) (Blancas-Mejía and Ramirez-Alvarado, 2013). For example, the presence of incorrectly folded protein would normally trigger complex biological responses such as heat shock response and unfolded protein response (UPR), which assist with protein folding and degradation (Powers et al., 2009). When the equilibrium between properly folded proteins and misfolded proteins is disturbed due to overloading or failure in proteostasis, it leads to: 1) loss in protein function such as in Marfan syndrome and cystic fibrosis or 2) gain-of-toxic function protein misfolding diseases characterized by unfolding/misfolding, aggregation and/or accumulation of the non-native protein, which might induce cellular and tissue damage such as in many neurodegenerative diseases e.g., Alzheimer's and Parkinson (Greenwald and Riek, 2010).

Protein misfolding is at the center of many human diseases, one of the most common being amyloidosis or amyloid diseases (Johnson et al., 2012). A major

feature of amyloidosis is the presence of fibrillar amyloid aggregates composed of the originator protein. The amyloid fibril protein is a protein that is deposited as insoluble fibrils, mainly in the extracellular spaces of organs and tissues as a result of changes in protein the protein conformation (Sipe et al., 2014). Generally, amyloid fibrils irrespective of the precursor protein share some common features such as binding to Congo Red dye and exhibiting a green, yellow or orange birefringence under polarized light microscopy. Isolated amyloid fibrils display a characteristic cross-β diffraction pattern when analyzed by x-ray diffraction (Sipe et al., 2014). To date, over 30 different amyloid precursor proteins have been identified in human involved in various types of amyloidosis such as amyloid beta (Aβ) peptide in Alzheimer's disease (AD), α-synuclein in Parkinson disease and transthyretin in transthyretin (ATTR) amyloidosis (Benson et al., 2018).

Transthyretin (TTR) is a major protein in extracellular fluids that binds to thyroid hormone (TH). In human, it carries virtually all the retinol binding protein (RBP) (hence vitamin A) in the blood and 15% of total thyroxine in plasma. It is the only thyroid hormone binding protein synthesized in the cells of the blood-CSF. Most of the TTR found in the blood is synthesized in the liver. Extracellular misfolding, misassembly and subsequent aggregation of TTR are associated with systemic organ dysfunction, including peripheral neuropathy, cardiomyopathy, nephropathy, ophthalmopathy and central nervous system (CNS) amyloidosis (for review, see Johnson et al., 2012). Deposition of wild-type TTR- containing amyloid fibrils, preferentially in the heart leads to sporadic amyloid disease called senile systemic amyloidosis in individuals over 65 years of age, often leading to heart failure. An earlier onset and often more severe familial amyloidotic polyneuropathy (FAP) and cardiomyopathy (FAC), in which an amino acid substitution from a single point mutation in the TTR gene results in deposition of amyloid aggregate composed of the variant protein in peripheral and autonomous nervous system and heart, respectively. In FAC and senile systemic amyloidosis (SSA), the fibrils are accumulated at the heart of the patient resulting in cardiomyopathy, a chronic and progressive condition that leads to arrhythmias, biventricular heart failure, and death. FAP typically causes length-dependent polyneuropathy that starts in the feet with loss of temperature and pain sensation, progresses with gastro-intestinal, cardiac or even renal dysfunction

leading up to cachexia and death within a decade on average (Sekijima, 2014). Over a hundred *TTR* gene mutations have been reported with several variants of the protein exhibiting tissue selective deposition and pathology. TTR Y78F is the most aggregate-prone variant under physiological conditions while, TTR V30M in addition to having a high tendency to aggregate and deposit in peripheral nerves, heart, eye and carpal tunnel, also happens to be the most frequent of all the variants, while TTR L55P is known to be associated with the most aggressive form of TTR amyloidosis (Benson and Kincaid, 2007). It is worth mentioning that TTR can also have anti-amyloidogenic activity in the context of Alzheimer's disease (Rios et al., 2019).

At the moment, there is no cure for TTR amyloidosis. Conventional therapy for FAP had been orthotopic liver transplantation since liver is the major source of the mutated protein in the blood. Besides minor secretions of variant TTR from retinal pigment epithelial cells and choroid plexus, which contribute to post-transplantation clinical manifestations of the disease, liver transplantation is also very invasive and unsuitable for some patients, thus, an alternative less invasive treatment is needed. A new drug called Tafamidis was recently approved for the treatment of early stage (stage I) V30M FAP in Europe and FAP of every stage in Japan. However, little is known about the efficacy of Tafamidis in non-V30M FAP as well as its long term side effects (Bulawa et al., 2012).

Familial TTR amyloidosis was for a long time considered a rare and endemic disease; however, recent improvements in diagnosis using genetic and immunochemical tests have indicated that it is a pandemic phenomenon (Sekijima, 2014). Advancement in medical technology and healthcare delivery is increasing the geriatric population globally and hence SSA. With no cure for TTR amyloidosis, there is a need for more research in the development of safe, effective and suitable therapies.

Although there are still some gaps in current understanding of the precise molecular mechanism of TTR fibrillation, it is widely accepted that it is preceded by tetramer destabilization followed by a rate-limiting tetramer dissociation leading to the formation of partially unfolded monomers with low conformational stability, which self-assemble into non-fibrillar aggregates, protofibrils and mature fibrils (Quintas et al., 2000; Cardoso et al., 2001). This understanding favored the

development of the therapeutic approach involving the use of small molecules referred to as kinetic stabilizers to stabilize the soluble native TTR tetramers. Subsequently, several non-steroidal anti-inflammatory drugs (NSAIDs) and natural products have been investigated. Tafamidis is the first and only pharmaceutical agent to be approved in this category (Ueda and Ando, 2014).

Much research in the identification and development of anti-amyloidogenic plants-derived agents had involved the use of phytochemicals. For example, epigallocatechin 3-gallate (EGCG), the most abundant polyphenol in green tea was shown to inhibit TTR aggregation and amyloid fibril formation *in vitro* and *in vivo* in a well-characterized animal model (Ferreira et al., 2012). Also, curcumin the major bioactive polyphenol in turmeric was reported to strongly suppress TTR fibril formation in an *in vitro* study either by stabilization of TTR fibril formation or by generating innocuous non-fibrillar intermediates. *In vivo,* using a well characterized FAP animal model, it was indicated that curcumin significantly increased TTR resistance and reduced TTR load in as much as 70% and lowered cytotoxicity associated with aggregation (Ferreira et al., 2013).

For multifactorial and complex disease like TTR amyloidosis with a plurality of toxic species, there are several factors driving its origin and pathogenicity. When this is taken together with the heterogeneous genetic and clinical nature of the disease, it becomes clear that it is unlikely that a single therapeutic approach will adequately and effectively address all the TTR-related amyloidosis. A synergy of different therapeutic strategies, targeted at different aspects molecular mechanisms of the disease has thus envisaged as a viable alternative (Hammarström et al., 2003; Azevedo et al., 2011). This may involve protection against TTR-induced cellular toxicity in addition to stabilization of soluble TTR, inhibition of aggregation of amyloidogenic intermediates and disruption of insoluble deposits (Saraiva, 2002). A plant extract which is by nature a multicomponent entity has the potential to serve as a multitarget agent against ATTR amyloidosis. In this work, the anti-TTR amyloidosis activities of two popular medicinal plants *Centella asiatica* and *Bacopa monnieri* are explored in view of validating their potential as candidates for therapeutic development.

1.2 Amyloidosis

The native protein structure is vital for its physiological performance in living systems. The folding process is a crucial step in the development of mature and functional proteins and thus, cells have evolved complex mechanisms to protect folding and avoid any related malfunction (Blancas-Mejía and Ramirez-Alvarado, 2013). More than 40 proteins are known to misfold into different aggregates such as oligomers, protofibrils and amyloid fibrils (Dobson 2001; Chiti and Dobson, 2006). Protein misfolding is at the centre of a significant number of human diseases such as Alzheimer's disease, Parkinson disease and Huntington's disease. A relevant group of protein misfolding diseases is amyloidosis (Eisele et al., 2015).

Amyloidoses are associated with tissue, organ or systemic dysfunction resulting from accumulation of extracellular deposits of insoluble protein fibrils known as amyloids, for example, beta amyloid (Aβ) fibrils implicated in the pathology of Alzheimer's disease (AD) (Sipe et al., 2014).

All amyloid fibril proteins share very similar properties in terms of morphology and structural features: They occur in tissue deposits as rigid, non-branching fibrils of approximately 7-10 nm in diameter; the fibrils bind to Congo Red dye and exhibit a green, yellow or orange birefringence under polarized light microscopy; they are mainly constituted by polypeptide chains arranged in a β-sheet extended shape, with the β-strands perpendicular to the axis of the fibril (Figure 1 below). In addition, they form fluorescent complexes with thioflavin S and T (Sipe et al., 2014).

The word, "amyloid" was first introduced in the 19th century for what was observed as microscopic tissue deposit originally thought to be cellulose but characterized as starch as it stained with iodine. Later, Friedreich and Kekule' demonstrated that amyloids are actually proteinaceous in nature. Further investigation revealed that amyloids are also fibrous (Cohen and Calkins, 1959). Later, the composition of amyloid fibrils was analyzed. The first amyloid fibrils constituent protein was TTR or prealbumin (Costa et al., 1978; Skinner et al., 1982).

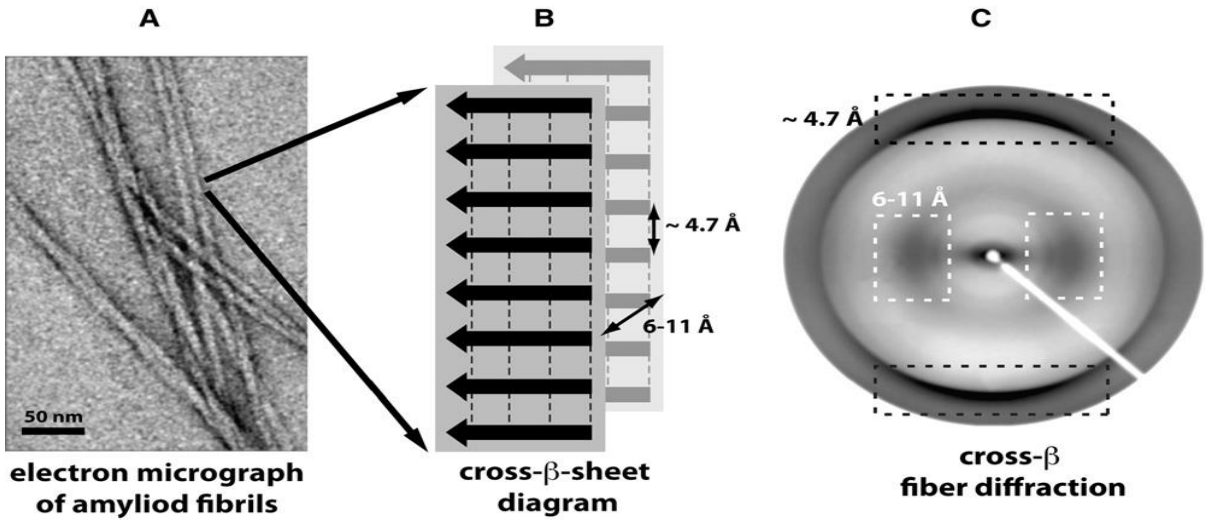

Figure 1. Detailed structure of amyloids (A) Long amyloid fibrils filaments that are visible in negatively stained TEM micrographs. (B) Schematic representation of the cross-β sheets in a fibril, with the backbone hydrogen bonds represented by dashed lines. (C) The typical fibre diffraction pattern. Source: Greenwald and Riek, (2010)

Currently, over 31 amyloidogenic proteins have been identified in human. Two of these are iatrogenic in nature and nine have also been identified in animals (Sipe et al., 2014).

1.3 Transthyretin

Transthyretin (TTR) is an extracellular protein synthesized in the liver hepatocytes, choroid plexus and retina pigment epithelial cells. TTR binds to thyroid hormones (THs) and is involved in the extracellular transport of retinol binding proteins (RPB), and by extension, vitamin A. In human, TTR serves as an auxiliary transporter of thyroxine (T4) in plasma and the main transporter in the cerebrospinal fluid (CSF) (Johnson et al., 2012).

1.3.1 Transthyretin structure

TTR exists *in vivo* mainly as a tetrameric protein with a molecular mass of 55 KDa. Each of the four identical subunits comprises 125 to136 amino acid residues, depending on the animal species (for review, see (Prapunpoj and Leelawatwattana, 2009). The TTR monomer has a β-sandwich conformation consisting of eight β-

strands (designated A to H) arranged into two β-sheets (labelled DAGH and CBEF), and a short α-helix between the E and F strands, as shown in Figure 2 (Pinto et al., 2011).

The β-strands are connected by loops to form a barrel structure. Dimers are formed through hydrogen bonds between H-H and F-F strands of two monomers. Homotetramers are composed of two dimers linked through hydrophobic interactions between AB loop of one monomer and the H-strand of the adjacent dimer (Blake et al., 1978)(Blake et al., 1978). This TTR tetramer presents a central channel in the dimer-dimer interface where the two equivalent binding sites which display negative cooperativity are located. The two binding sites can accommodate simultaneously two molecules of the natural ligand, thyroxine (T4) as well as other small molecules. The outer surface of the molecule houses four binding sites for the vitamin A specific carrier, retinol-binding protein (Monaco et al., 1995).

TTR is produced in the liver and secreted into the circulation. In the central nervous system (CNS), the choroid plexus synthesizes TTR and releases it to the cerebrospinal fluid. Transthyretin is also produced in the retinal pigment epithelial cells, alpha (glucagon) cells of the islets of Langerhans in the pancreas as well as skin and peripheral Schwann cells (Murakami et al., 2010; Westermark and Westermark, 2008).

The established function of transthyretin in the blood is to transport holoretinol binding protein; without binding to TTR, most of RBP will be lost in glomerular filtration due to its small molecular weight (Monaco et al., 1995). TTR transports about 15 percent of total plasma thyroxine and plays an important role in thyroxine homeostasis (Sousa et al., 2000). The other thyroxine carrier proteins are albumin and thyroxine-binding globulin (TBG). Of these three proteins, albumin has the highest concentration ([albumin]=620μM; [TTR]=5μM; [TBG]=0.3μM), and TBG has the highest affinity for T4 (K_{dTBG}=0.1nM; K_{dTTR}=15nM; $K_{dalbumin}$=1.5μM) (Bartalena and Robbins, 1992).

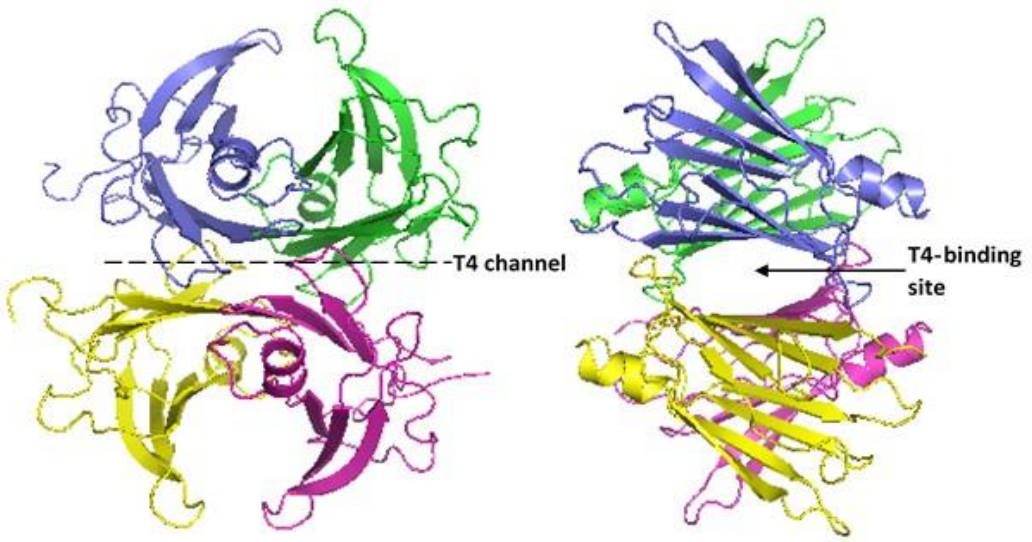

Figure 2 X-ray structure of TTR tetramer. Adapted from a model PDB ID :1RLB Source: (Monaco et al., 1995).

These in addition to the low T4 concentration in the blood (0.1μM), mean that only a minor fraction (<10%) of T4 in human blood is bound to TTR while virtually all (>99%) of T4-binding sites in TTR remain unoccupied and available for small molecule binding. Moreover, other small organic molecules such as drugs (diflunisal), phytochemicals (polyphenols) and toxic compounds (polychlorinated biphenyls) have been shown to bind with TTR, suggesting its role in the clearance of these compounds from the system (Monaco et al., 1995).

1.3.2 Transthyretin production and physiological functions

Besides its main role as transport of thyroid hormones and vitamin A, recent findings has indicated that TTR is involved in the cleavage of beta-amyloid peptide, apolipoprotein A-I, neuropeptide Y and protection against apolipoprotein CIII-induced β-cell apoptosis, for detailed review, see (Prapunpoj and Leelawatwattana, 2009; Refai et al., 2005).

1.4 Transthyretin (ATTR)-related amyloidosis

Toxicity of abnormal TTR is implicated in a number of amyloid diseases such as familial amyloid polyneuropathy (FAP), familial amyloid cardiomyopathy (FAC), central nervous system-selective amyloidosis, and senile systemic amyloidosis (SSA).

For SSA, the deposited (mainly wild-type TTR protein) can be found in the brain, pancreas, spleen, and especially, the heart. This disease has onset at 65 years and affects about 25 percent of the population over 80 years (Sekijima, 2014).

Regarding familial TTR-related amyloidosis, more than 100 mutations have been reported for the TTR protein, of which only 13 are non-pathologic (Steven et al., 2012). The mutations are distributed along all the protein sequence, but the most amyloidogenic aggressive mutations are related to residue55 (Sant'anna et al., 2013). Y78F TTR is the most aggregate-prone variant under physiological conditions while, V30M TTR in addition to having a high tendency aggregate and deposit in the peripheral nerves, heart, eye and carpal tunnel, also happens to be the most frequent of all the variants. L55P TTR is known to be associated to the most aggressive form of TTR amyloidosis (Benson and Kincaid, 2007; Jacobson et al., 1992; Redondo et al., 2000). These mutations are presumed to alter the stability of TTR resulting in various familial TTR amyloidosis. Familial ATTR amyloidosis are generally more severe and have earlier onset than SSA.

The first identified cause of familial amyloidotic polyneuropathy (FAP) was V30M mutation. The penetrance and age in the onset of FAP among people carrying the same mutation vary between countries. FAP typically causes a nerve length-dependent polyneuropathy that starts in the feet with loss of temperature and pain sensation, along with gastro-intestinal, cardiac or even renal dysfunction leading to cachexia and death within 10 years on average (see Figure 3 below) (Ueda and Ando, 2014).

In familial amyloid cardiomyopathy (FAC) the fibrils are accumulated in the heart of the patients. TTR-related cardiomyopathies are chronic and progressive conditions that lead to arrhythmias, biventricular heart failure, and death. Both the wild-type TTR protein and the mutant V122I can produce this disease. This single point mutation is present in about 3-4 percent of the Afro-American population (for review, see (Sekijima, 2014).

Strikingly, not all transthyretin mutations lead to pathology. Non-amyloidogenic mutations, such as the T119M mutation, have been identified and shown to stabilize the native fold of transthyretin. These mutations have also been shown to have a protective effect against the development of disease in compound

heterozygotic individuals i.e., individuals with different mutations in both alleles of the transthyretin gene (Hammarström et al., 2003).

1.5 Pathophysiology of TTR-related amyloidosis

The exact molecular mechanism for TTR fibrillation is still poorly characterized though it is generally accepted that it involves several steps preceded by a rate-limiting tetramer dissociation (Ferreira et al., 2012) as represented in Figure 3 below. *In vivo* conditions for the formation of amyloid fibrils are still unknown, but many studies have revealed that the crucial point in this pathway is the low TTR tetramer stability (Sekijima, 2014).

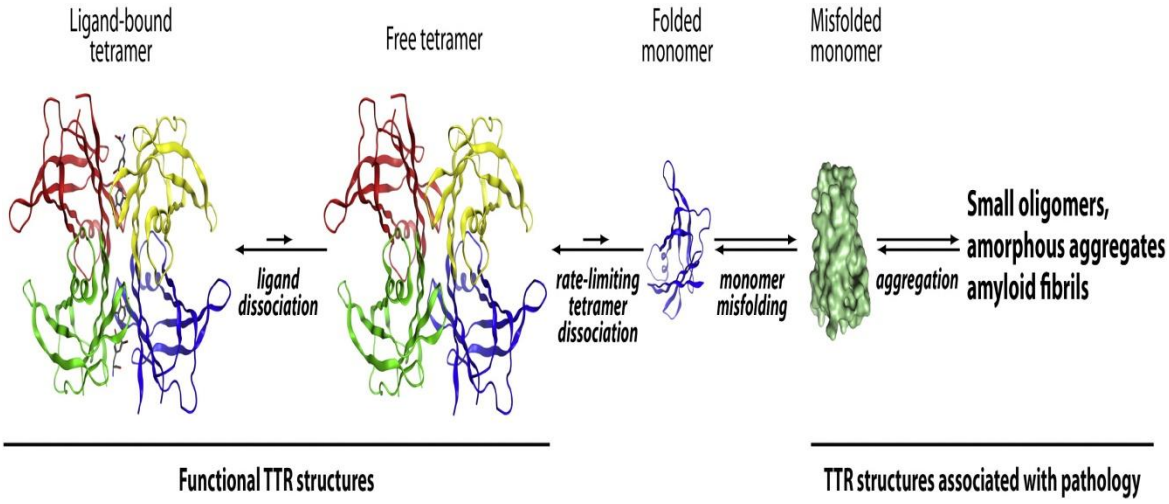

Figure 3 Transthyretin amyloidogenic pathway. Source:(Johnson et al., 2012)

In vivo, the formation of fibrils may be triggered by decreasing the pH of the medium. It is even possible to correlate the pH value at which amyloidogenicity is induced and the pathogenicity of a given TTR tetramer (Kelly and Lansbury, 1994) as shown in Table 2 below.

Table 1. Stability of transthyretin in relation to disease pathology and onset

TTR	pHm*	Disease	Age of onset
WT	4.4	SSA	>80
V30M	4.7	FAP	~30
L55P	5.4	FAP	Teens

pHm - midpoint of the equilibrium tetramer-monomer. Adapted from Kelly and Lansbury, 1994

Many questions linger regarding the molecular mechanisms that triggers TTR amyloid-induced cytotoxicity. Sousa et al. reported that neuronal stress in FAP patients begins at a very early stage with soluble prefibrillar aggregates inducing cytotoxicity similar to Alzheimer's disease pathology (Sousa et al., 2001). In AD, there exists a correlation between soluble beta-amyloid levels and disease severity; these transient toxic soluble oligomers are not peculiar to Alzheimer's disease alone but are common to proteins involved in amyloid diseases including TTR. Kayed et al. (2003) demonstrated that soluble oligomers from different amyloidogenic proteins are more toxic than fibrils. In the same vein, TTR amyloid fibrils larger than 100KDa were shown to be innocuous. The non-native monomeric TTR or relatively small, rapidly formed aggregates of a maximum size of six subunits were the major cytotoxic species (Reixach et al., 2004). Cytotoxicity of these pre-amyloid aggregates had been linked to their large exposed hydrophobic surfaces, which may inappropriately interact with a wide range of cellular components stimulating inflammatory responses and oxidative stress that can lead to neuronal death (Sousa and Saraiva, 2003). It is unclear whether this was due to the activation of a specific signaling cascade or was a general stress response. Although increased oxidative stress and increased pro-inflammatory cytokines had been observed in FAP patients (Cardoso and Saraiva, 2006; Sousa et al., 2001)), recently, it was demonstrated that TTR aggregates induced intracellular oxidative stress by promoting pro-oxidative activities. The study reported that TTR aggregates stimulate the production of reactive nitrogen and oxygen species in human Schwannoma cells, lead to a reduction in levels of glutathione and catalase, and decrease overall cellular antioxidant capacity (V.-H. Fong and Vieira, 2013; V. H. Fong and Vieira, 2013). Thus, perhaps, phytochemicals with antioxidant capacity may counteract this pro-oxidative activity and protect the cell by restoring oxidative balance.

In addition, TTR mutants that exhibit increased aggregation, e.g., L55P and V30M, are known to increase membrane fluidity (Hou et al., 2007), and such changes may affect cell function and contribute to toxicity. Also, V30M reportedly

compromises cell membrane integrity and results in increased LDH release (Reixach et al., 2006).

Interestingly, TTR has both amyloidogenic and anti-amyloidogenic properties under physiological conditions (Schwarzman et al., 2004) (Schwarzman and Tsiper et al., 2004). TTR itself contributes to its own set of disease; it has also been demonstrated to sequester other amyloidogenic factors such as beta-amyloid peptide in the brain. TTR can bind and cleave beta-amyloid (Costa et al., 2008), decrease amyloid formation and amyloid-induced toxicity in the brain (Schwarzman et al., 1994). This may have therapeutic implications for Alzheimer's disease.

1.6 Diagnosis of TTR-related amyloidosis

Accurate diagnosis is a pre-requisite for the effective treatment of any disease. The diagnosis of TTR-related amyloidosis typically relies on target organ biopsies, followed by histopathological staining of the excised tissue using Congo red dye and microscopic examination under polarized light. Given a positive result, immunohistochemical staining or amino acid sequence analysis is then performed to ensure that the precursor protein is indeed transthyretin. A rapid method of identifying the type of precursor protein and classify the type of amyloid disease including TTR amyloidosis from tissue biopsies using tandem mass spectrometric analysis had earlier been reported (Dogan, 2015; Vrana et al., 2009). For familial forms of the disease, demonstration of mutation in the gene encoding TTR is needful for diagnosis to be conclusive.

1.7 Therapeutic strategies for TTR-associated amyloidosis

The cure for TTR-related amyloidosis is still elusive. Current therapeutic approaches can be grouped based on what step of the disease pathology they target (see Figure 4).

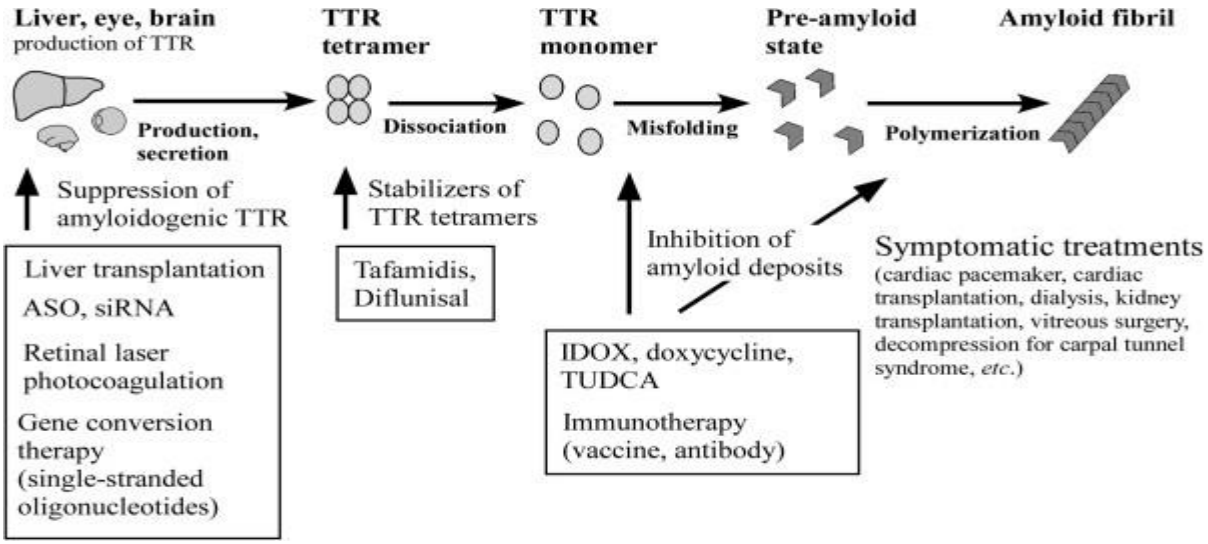

Figure 4 TTR amyloid formation and therapies for FAP. Source: Ueda and Ando, 2014.

1.7.1 Prevent or decrease the production and secretion of amyloidogenic TTR

Liver transplantation (LT) is the standard care for TTR FAP. Exchange of a FAP patient's diseased liver with a healthy liver from a donor causes the mutant TTR in circulation to be replaced by wild-type, except for CSF and eyes into which mutant TTR is secreted by choroid plexus and retinal pigment epithelial cells, respectively (Ando et al., 2004). It has been reported that V30M FAP patients who underwent LT had a decrease in the progression of the disease and lived longer (Ericzon et al., 2009). It is worth noting that LT is not applicable to mutants that develop amyloidosis in the CNS where TTR is also synthesized (Ueda and Ando, 2014). Furthermore, LT has a number of disadvantages which include: slowing down rather than completely treating the disease because TTR mutants can also be synthesized in the choroid plexus and RPE cells; symptomatology is not improved due to the already existing amyloid deposits; high difficulty of finding organ donors and the concomitant risk of surgery; expensive cost; lifelong administration of immunosuppressants, and sometimes, development of cardiac and ocular disorders.

Because of ocular complications after LT (Ando et al., 2004), retinal laser photocoagulation (RLP) was investigated for the suppression of TTR-related ocular disorders. RLP is a technique used to treat retinal diseases which damage the retinal epithelial cells. It was reported that RLP prevented the progression of amyloid

deposition in vitreous and on the retinal surface in certain FAP patients, without any negative side effects (Kawaji et al., 2010).

Gene therapies to suppress TTR expression is a specific approach to the inhibition of amyloidogenic TTR production by gene silencing. Two of the most popular tools include the use of small interfering RNAs (siRNA) and antisense oligonucleotides (ASO). siRNA and ASO therapies inhibit both mutant and wild-type TTR in several studies (Ackermann et al., 2012). ASO reportedly suppressed TTR mRNA levels in the liver and choroid plexus of the brain (Benson et al., 2010). Because wild-type TTR also contribute to the formation of amyloid in FAP, especially after LT, it is hoped that gene therapy will provide a better alternative to LT. A phase II/III study evaluating the efficacy of ASO and siRNA in FAP patients was underway in 2014 (Ueda and Ando, 2014).

1.7.2 Stabilization of native TTR tetramers

Tetramer dissociation is the proposed rate-limiting step in the formation of amyloid fibrils. The therapeutic implication for this is that stabilizing the soluble TTR tetramer would prevent the progression to amyloidosis (Johnson et al., 2012). Proof of principle was provided by the observation that various non-steroidal anti-inflammatory drugs (NSAID) stabilized the tetrameric form of TTR (Baures et al., 1999). Through a structure-based drug design strategy, Dr. Jeffrey W. Kelly and colleagues developed a very effective kinetic stabilizer known as Tafamidis. In clinical trials, patients treated with Tafamidis had less neurological deterioration than patients who began using the drug later; they also had some preservation of function as measured by the Neuropathy Impairment Score-Lower Limb The drug is approved in Europe for the treatment of early stage V30M FAP disease and in Japan for the treatment of FAP disease of all stages (Coelho et al., 2012).

At the moment, little progress had been made pertaining to the effectiveness of Tafamidis in non-V30M FAP patients with the exception of WT-TTR cardiac amyloidosis. In a phase II study involving twenty one patients with various non-V30M variants who received 20 mg QD of Tafamidis for a period of 12 months; it was reported that neurological function degenerated with a median increase of total NIS by 5.3 within the period of study (Adams et al., 2014). Though Tafamidis is well

tolerated, side effects such as urinary tract infections (UTI) and diarrhea have been reported (Coelho et al., 2012).

Diflunisal, a NSAID can stabilize TTR tetramers and is currently undergoing clinical development. Diflunisal reportedly reduced the rate of progression of neurological impairment and preserved quality of life (Berk et al., 2013). However, data on the effects of Tafamidis and diflunisal on long-term outcomes, cardiac functions and ophthalmic symptoms are scanty. This is even more important considering that these drugs will be consumed by the patients for a long time.

In addition to the aforementioned kinetic stabilizers, a number of structurally diverse small molecules have been shown to bind and increase TTR stability, and therefore inhibit amyloid fibrillogenesis. Examples include various dietary phytochemicals like epigallocatechin 3-gallate, the most abundant polyphenol in green tea (Ferreira et al., 2011).

1.7.3 Inhibition of amyloid deposits.

These are potential therapeutic agents targeted against the misfolding and polymerization of non-native monomers and pre-amyloid state aggregates, respectively. 4'-iodo-4'-deoxydoxorubicin (IDOX) and tauroursodeoxycholic acid (TUDCA) are some of the drug molecules that have been investigated (Macedo et al., 2008). Doxycycline influences many functions of mammalian cells such as proliferation, migration, apoptosis, and matrix remodelling (Bendeck et al., 2002). Cardoso and coworker investigated the therapeutic potentials of doxycycline in ATTR V30M transgenic mice (Cardoso and Saraiva, 2006). TUDCA is a unique natural compound with potent anti-apoptotic, antioxidant agent, and neuroprotective effects. TUDCA treatment reportedly caused a significant decrease in the deposition of TTR toxic aggregates in FAP mice (Macedo et al., 2008).

Serum amyloid P component (SAP) is a major component in amyloid deposits in all amyloidosis. Recently, Bodin et al. (2010) investigated therapeutic effects of anti-human SAP antibodies on AA amyloid deposition using a human SAP transgenic mouse model. The antibodies removed AA amyloid deposits in the mouse model. This antibody therapy might be applicable to FAP.

Putting the afore mentioned findings together, at least two inferences can be drawn: first, most of the therapies are still in their development, and second, it is not likely that any one therapeutic option can effectively treat the wide TTR-related amyloidosis. The genetic and clinical heterogeneity of the disease further complicates the development of a single drug for all TTR amyloidosis; a synergy of various therapeutic options each focusing perhaps on a different molecular mechanism, and yet complementing one another seem a more plausible strategy for treating the disease. As such there is need for further research effort targeted at the development of effective, non-invasive and safe therapeutic agents that focus on different molecular mechanisms underlying TTR-associated amyloidosis. These therapies must equally be available, accessible and affordable to everybody; features which cannot be attributed to liver transplantation and Tafamidis. With rising acceptance and use of herbal medicine globally, a lot of interest have been shown in the use of medicinal plants and their phytochemicals for combating various diseases.

1.7.4 Phytochemicals as potential therapeutic agents for amyloidosis

A good number of organic molecules have been investigated for their anti-amyloidogenic potential. Curcumin, the major bioactive constituent in turmeric strongly suppressed amyloid fibril formation in an *in vitro* study, either by stabilization of TTR tetramer or by generating innocuous non-fibrillar intermediates. The same investigators demonstrated that curcumin significantly increases TTR tetramer resistance, reduced amyloid load by 70 percent and lowered cytotoxicity associated with TTR aggregation *in vivo* in a well-characterized FAP mouse model (Ferreira et al., 2013). Epigallocatechin 3-gallate (EGCG) the most abundant polyphenol in green tea inhibited TTR aggregation and amyloid fibril formation in both *in vitro* and *in vivo* studies (Ferreira et al., 2012). Hirohata et al. tested various dietary phytochemicals in assays of beta-amyloid fibril formation, fibril extension, and fibril inhibition. The greatest inhibitory effect of tested compounds was observed on the fibril formation step (Hirohata et al., 2007). It was demonstrated in an *in vitro* study that several organic compounds (e.g., wine-related polyphenols and NSAIDs) not only inhibit beta-amyloid fibril formation and extension, but also destabilize beta-amyloid fibrils dose-dependently (Naiki et al., 2010). Earlier, it was shown that the

stilbene, resveratrol, inhibited beta-amyloid fibril formation and enhanced fibril destabilization. Resveratrol decreased beta-amyloid-induced cell death as well as moderated cell viability from exposure to toxic forms of TTR (Reixach et al., 2006). Recent studies have confirmed the pro-oxidative effect of TTR aggregates (Fong and Vieira, 2013). So, in addition to the direct effect on aggregate formation and stability, another possibility for phytochemical protection against TTR amyloidosis is related to the antioxidant effects of these compounds. The antioxidant phytochemical may be beneficial in terms of neutralizing some of the reactive chemical species or otherwise moderating cellular oxidative stress and re-establishing redox balance. Brahmi represent two of such plants with phytochemicals capable of producing anti-amyloidogenic effect by inhibiting fibrillogenesis and countering pro-oxidative cellular damages

1.8 "Brahmi" (*Centella asiatica* and *Bacopa monnieri*)

The Indian traditional system of medicine known as Ayurveda, one of the most ancient worldwide describes the application of herbs for the treatment of CNS disorders and relief(Singh et al., 2008). One of such alleged boosters of brain function protection is "Brahmi" or *Bacopa monnieri*. *Bacopa monnieri* (BM) or water hyssop is known locally as "phrommi" in Thailand. Early references to Brahmi are also directed to *Centella asiatica* (CA) locally known in Thailand as "Boi-bok" (Chomchalow, 2013; Kulkarni et al., 2012).

Bacopa monnieri is a small medicinal herb with oblong leaves and purple flowers, commonly found in marshes, and indigenous to Australia and India. The whole plant is used in folk medicine. In Ayurveda, it is used as a nervine, for the enhancement of memory, adaptogen and for promoting general vitality (Russo and Borrelli, 2005). The pharmacological effects of *B. monnieri* have been largely attributed to the presence of triterpenoid saponins in the plant with jujubogenin or pseudojujubogenin moieties as aglycone units (Sivaramakrishna et al., 2005). Based on the result of several pharmacological studies (Nathan et al., 2001; Stough et al., 2001), extracts of *Bacopa monnieri* claimed to contain bacosides A and B are now widely available in the international nutraceuticals market. Besides, *B. monnieri*

possesses other phytochemicals including polyphenols, alkaloids and betulic acid (Russo and Borrelli, 2005).

Centella asiatica is a small perennial herb that is widely grown in many parts of Asia for its medicinal value. In traditional Chinese medicine it is used as an antipyretic, diuretic and antidote in the treatment of stroke, diarrhea, ulceration, and traumatic disease. As already stated, it is one of the most important rejuvenating herbs for nerve and brain cells in Ayurveda and is believed to be capable of improving intelligence, longevity and memory (Cheng et al., 2004). In Thai traditional recipes, 'boi-bok' is regularly used as vegetable and herbal tonic sold as a popular refreshing drink in most local markets (Maquart et al., 1990). The major active principles of *C. asiatica* are triterpenoid saponins which include asiaticoside and madecassoside. Other phytochemicals in *C. asiatica* include brahmoside, Brahminoside, cetelloside and its derivatives. In addition, the plant extract contains sterols, flavonoids and other components, largely polyphenols (Alqahtani et al., 2015).

Plant bioactives have shown anti-amyloidogenic activities in several studies. Polyphenols have been reported as being rich antioxidants, a property which can modulate the pro-oxidative effects of TTR aggregates in the body. Likewise, asiaticoside derivatives were shown to reduce hydrogen peroxide-induced cell death, decreased free-radical concentrations and inhibit beta-amyloid-induced cell death *in vitro*. *C. asiatica* reversed beta-amyloid pathology in the brains of PSAAP mice and (Dhanasekaran et al., 2009; Gray et al., 2015). Similarly, *B. monnieri* extracts protected neurons from amyloid beta induced cell death by inhibiting cellular acetylcholine esterase activity (Limpeanchob et al., 2008).

Given the similarity in molecular pathogenesis of beta-amyloid and TTR, it is plausible that Brahmi phytochemicals can also modulate TTR-related amyloidogenesis. The high safety profile of both plants, widespread availability and accessibility in local Asian communities and several parts of the world further add to the appeal of these botanical as prospective candidates for investigation.

1.9 Aim of this thesis

Although there are still several points of contention pertaining to the molecular mechanisms driving ATTR amyloidosis, it is widely accepted however, that

dissociation of the native tetramer is the initial and critical step in the amyloid cascade. As such, preventing tetramer dissociation had been promoted as a pragmatic strategy to mitigate TTR amyloidogenesis. The success of this strategy was demonstrated in the development and approval of the drug Tafamidis, for the treatment of early-stage FAP. Tafamidis is a small molecule that binds at the T4-binding sites and stabilize the native tetramer from dissociation. It slows but do not prevent the progression of the disease, and the long-term side effects are yet to be established. It is therefore pertinent to sustain the research efforts that could lead to the development of novel therapies.

The general aim of this work was to search for novel therapeutic agents targeting ATTR amyloidosis. The specific aims were to 1) determine the potential of *C. asiatica* and *B. monnieri* to modulate transthyretin amyloidogenesis and, 2) elucidate the plausible mechanism of inhibition.

CHAPTER 2

Research Methodology

2.1 Material

2.1.1 Instruments

Instrument	Model	Manufacturer
HPLC system	1100 Series	Hewlwtt-Packard
LC-MS	micrOTOF-QII™ESI-Qq-TOF	Bruker Daltonics
Microcentrifuge	260D	DENVILLE
micropipette		Gilson Labmate Labnet Nichipet EX
Microplate reader	Synergy™ HT	BioTek
Oven	240 Litre	Binder
Orbital shaking incubator		GallenKamp SANYO
Orbital shaker	SH 30	FINEPCR
Orbital shaker	MS-OR	Major Science
pH meter	713	Metrohm
Rotary evaporator	Liftbasis	Heidolph
Rotational vacuum concentrator	RVC 2-25 CDPlus	CHRiST
Preparative gel electrophoresis	Mini protean 3 system	Bio-Rad
	Mini protean system	Bio-Rad
Spectrophotometer	8453	Hewlett-Packard
Spectrophotometer	G20	Thermo
Stirrer		Corning
Vortex-mixer	VX 100	Labnet
Water bath	WB-710M	Optima

2.1.2 Chemicals

Analytical grade reagents

Reagent	Manufacturer
Absolute ethanol	Normapur
Methanol	Lab Scan
Acetic acid	Lab Scan
Acrylamide	Fluka
B-mercaptoethanol	Gibco
Bis-acrylamide	Fluka
Bovine serum albumin	Sigma
Bromophenol blue	Bio-Rad
Coomassie brilliant blue G-250	Bio-Rad
Coomassie brilliant blue R-250	Bio-Rad
D-glucose	Univar
Dimethyl sulfoxide (DMSO)	ACS
Di-potassium hydrogen phosphate	J.T.Baker
Dithiothretol (DTT)	Fisher
Ethylenediaminetetraacetic acid (EDTA)	Carlo
Folin & Ciocalteu's Phenol Reagent	LABAChemie
Formaldehyde	Sigma
Glutaraldehyde	Sigma
Glycerol	Fisher Chemical
Glycine	Fisher
HEPES, Free Acid	Omni Pur Calbiochem
Hydrochloric acid	J.T.Baker
N,N,N',N'-tetramethylenediamine (TEMED)	Bio-Rad
Low molecular weight (protein marker)	GE Healthcare
High molecular weight (protein marker)	GE Healthcare

Peptone	Criterion
Potassium dichromate	Sigma
Potassium dihydrogen phosphate	Fisher
Silver nitrate	Merck
Sodium carbonate	Merck
Sodium chloride	Lab Scan
Sodium dodecyl sulfate (SDS)	J.T.Baker
Tris (Hydroxymethyl)-methylamine	Bioland Scientific
Yeast extract	Criterion

2.2 Methods

2.2.1 Protein purification

2.2.1.1. Purification of human transthyretin from plasma

Human transthyretin was purified from plasma in a series of steps. The crude human plasma was first thawed on ice and filtered through a Whatman No.1 paper. To reduce the albumin content prior to purification, the filtered human plasma was loaded on a Cibacron blue 3GA affinity column pre-equilibrated in 50 mM phosphate buffer pH 7.4. The unbound fraction was eluted from the gel using 50 mM PB, pH 7.4 at 1 mL/6 min while the bound fraction was later eluted using phosphate buffered saline. Both fractions were analyzed on native-PAGE to confirm the reduction of albumin in the unbound fraction. This pretreated human plasma was then concentrated using a stirred ultrafiltration unit with a 30 kDa MWCO membrane filter. The concentrated plasma was subsequently purified on preparative discontinuous native PAGE having a stacking gel layer with 4 % acrylamide and a resolving gel layer of 12 % acrylamide. Purification was initiated by running the plasma through the stacking layer at 20 W followed by separation on the resolving gel at 17 W. The resolved protein fractions were collected at a flow rate of 1 mL/min after dye elution using 50 mM Tris-HCl buffer, pH 7.5. All fractions were analyzed on 10 % native-PAGE to followed by silver staining for visualization of protein bands. Fractions containing only TTR were pooled and concentrated by ultrafiltration. Purity was determined by

SDS-PAGE followed by Coomassie brilliant blue-R250 staining. The concentration of the purified hTTR was determined by Bradford assay as modified.

2.2.1.2 Purification of recombinant L55P TTR from P. pastoris culture supernatant

Preparation of L55P TTR was accomplished via the P. pastoris expression system following the manufacturer's instruction (Invitrogen). Briefly, a colony of P. pastoris clone grown on YPD agar plate was transferred (inoculated) into BMGY medium (10 mL) and grown in a shaker incubator at 30 °C, 200 rpm to an OD600 of 2 to 4 within 16 to 18 hours. The P. pastoris culture was then transferred to 200 mL of BMGY in 1-liter Erlenmeyer flask and further grown for 8 to 10 hours to reach an OD600 of 2 to 6. The Pichia culture was centrifuged at 300 rpm for 10 min at 4 °C and the pellets resuspended in BMMY medium. The Pichia culture was allowed to grow in the medium and expression of L55P TTR was instigated by the presence of daily added 0.5 % methanol in the medium. After 2 days of incubation, the L55P containing Pichia culture supernatant was collected by centrifuging at 10000 rpm for 30 min at 4 °C. The supernatant was concentrated by stirred ultrafiltration unit equipped with 30 kDa MWCO membrane filter. Purification of L55P TTR from the concentrated supernatant was accomplished as described above for hTTR.

2.2.2 Preparation of plant extracts

2.2.2.1 Preparation of *Centella asiatica* extract

Fresh aerial parts of *C. asiatica* was washed with reverse osmosis water and rinsed with distilled water. The fresh plant was air dried for 12 hours and oven dried for another 12 hours at 50 °C. Dried *C. asiatica* was ground into fine powder using an industrial blender and extracted with acetone/methanol/water (2:2:1; v/v/v) at a plant to solvent ration of 1:4.5 (w/v) for 2 hours using an overhead stirrer. The extract was then filtered through a Buchner funnel layered with Whatman No. 1 filter paper. The filtrate collected was fractionated with n-hexane to remove fats and further fractionated with dichloromethane to remove chlorophyll and other pigments. The residual aqueous layer was concentrated to one-third of the initial extract volume and further exposed to speed-vac under vacuum in order to ensure all organic solvents are

evaporated. The extract was then lyophilized into a light brown powder which is hereafter referred to as *C. asiatica* bioactives (CAB).

2.2.2.2 Preparation of *Bacopa monnieri* extract

Bacopa monnieri extract used in this work was a generous gift from Assoc. Prof. Dr. Kornkanok Ingkaninan. The extract was prepared from *B. monnieri* shoot that had been oven-dried in a hot air oven for 24 hours at 50 °C. The dried plant material was blended into powder and extracted with 95 % ethanol at a plant to solvent ratio of 1:6 (w/v). Extraction was carried out by sonication for 10 minutes. The mixture was then filtered and the marc re-extracted. The combined filtrate was subsequently dried under vacuum using rotary evaporator at 40 °C.

2.2.3 SDS-PAGE analysis

SDS-PAGE of proteins was performed according to Laemmli. Briefly, the protein was mixed with loading buffer (containing 2 % SDS and 2.5 % β-mercaptoethanol, final concentrations) and boiled at 100 °C for 30 minutes. Thereafter, the protein solution was resolved on polyacrylamide gel containing 0.1 % SDS (4% acrylamide in the stacking layer and 12 % acrylamide in the resolving layer) and resolved under 100 V for 85 minutes. Separated bands on the gel were visualized by staining with Coomassie brilliant blue-R250.

2.2.4 Tricine-SDS-PAGE analysis

Tricine-SDS-PAGE of TTR samples were carried out as previously reported. The protein solution was initially mixed with loading dye containing 0.2 % SDS before resolving on a 10 or 14 % Tricine-SDS-PAGE gel using running buffer (concentration of SDS: 0.025%). These SDS concentrations had been reported to be sufficient for clear resolution of TTR into its different quaternary structures without favoring its dissociation under electrophoresis condition. The separated protein bands were identified with Coomassie brilliant blue R-250 staining.

2.2.5 Glutaraldehyde chemical cross-linking assay

The quaternary structural conformations of TTR was determined by glutaraldehyde cross-linking assay as previously reported. To protein solution containing 1 µg of protein in 9 µL of buffer was added 1 µL of 25 % glutaraldehyde

solution (final concentration 2.5 %) and incubated for 4 min at ambient temperature. Cross-linking was quenched by addition of 1 µL of 7 % $NaBH_4$ in 0.1 M sodium hydroxide. The protein solution was immediately solubilized with SDS loading buffer containing 2 % SDS and 2.5 % β-mercaptoethanol and boiled for 10 min. Cross-linked protein solution was resolved on 10 % Tricine-SDS-PAGE followed by Coomassie blue R-250 staining for protein band visualization.

2.2.6 Urea-mediated denaturation assay

TTR at a final concentration of 0.1 µg/µL was exposed to 6 or 7 M urea in phosphate buffer, pH 7.4 for a period of 72 hour at 4 °C in the dark. Thereafter, Tricine-SDS sample loading buffer was added to aliquot of the TTR solution and resolved on 10 % Tricine-SDS-PAGE. Bands of folded TTR (i.e. tetramers, trimers and dimers) will migrate a single band, distinct from the monomers. Separated protein bands were visualized by staining with Coomassie blue R-250. The bands of folded TTR was quantified via densitometry using gel documentation and taken for an indication of the relative stability of the protein under denaturation stress.

2.2.7 Acid-mediated denaturation assay

In vitro, mild acidic conditions promote tetramer dissociation – required for transthyretin amyloidogenesis. Thus, to determine the stability of TTR under aggregation prone conditions, the pH of the protein solution was reduced to 4 by addition 200 mM acetate buffer, pH 4. The protein solution was then incubated under aseptic conditions at 37 °C for 7 or 14 days. Aliquot of the protein solution was mixed with SDS loading buffer without β-mercaptoethanol and resolved on 12 % SDS-PAGE. Under these conditions, tetrameric transthyretin migrates as an apparent dimer distinct from the monomer. Separated protein bands were detected by Coomassie blue R-250 staining and the tetrameric bands were quantified by using densitometry gel documentation and taken for an inference for protein stability.

2.2.8 Protein fibril disruption assay

TTR fibril dissociation assay was performed using pre-formed fibrils. Fibrils were performed under acid mediated denaturation conditions as described above. The pre-formed fibrils were subsequently co-incubated with the extracts for 24 hours at 37

°C. The extent of fibril disruption was ascertained by transmission electron microscopy (TEM).

2.2.9 Transmission electron microscopy

To determine the morphology of TTR under aggregation prone-conditions, protein samples were subjected to acid-mediated aggregation conditions and fibril disruption conditions as described above. Aliquot of TTR solution (1 µL) was added to 99 µL of Milli-Q water. A drop of this diluted protein solution (obtained as 10 µL) was added to Formvar coated TEM copper grid for 3 min. Excess fluid was carefully blotted away with a wedge of Whatman No. 1 filter paper. The grid was briefly rinsed with a drop of Milli-Q water and stained with 2 % uranyl acetate solution in 70 % methanol for 2 min. Excess stain was blotted and the grid and dried at ambient temperature for 24 h. Micrographs were obtained using JEOL-JEM 2010 electron microscope (JEOL Ltd. Tokyo, Japan) operating at 120 keV.

2.2.10 NBT-redox cycling assay

NBT redox cycling assay was used to determine initial binding interactions of the TTR and the extracts by observing the formation of a colored product as earlier described. TTR was co-incubated with the extract at 37 °C for 4 hours. Aliquot was resolved on SDS-PAGE after boiling with SDS sample loading buffer for 10 minutes. The gel was removed and proteins electroblotted on nitrocellulose membrane. The membrane was then briefly rinsed with distilled water and stained with Ponceau S dye for 1 hour. Ponceau S dye was destained from the membrane by washing with TBS-T buffer and distilled water. The clear membrane was the re-stained with NBT dye in glycinate buffer.

2.2.11 ANS binding displacement assay

ANS is a small fluorescent dye widely used for probing native TTR binding interactions with small-molecule ligands. ANS in aqueous solution produces a weak fluorescence. However, upon binding at the thyroxine binding sites of TTR which are hydrophobic, the change in polarity of the microenvironment causes ANS to produces a strong fluorescence intensity accompanied by a blue shift in maximum emission wavelength from about 500 nm to 480 nm. To determine the possible binding

interaction between extracts and TTR, native TTR solution was co-incubated with ANS and subsequently, extracts with increasing concentrations. Solutions without TTR was used as to control for blank. Fluorescence intensities were recorded at excitation wavelength of 360/40 nm and emission wavelength of 460/40 nm on Synergy HT microplate reader.

2.2.12 Chemical characterization of extracts

2.2.12.1 Total phenolic content

Total phenolic content was determined by the widely reported Folin-Ciocalteu assay with minor modifications. Extract (10 µg/µL) and gallic acid (1 µg/µL) were solubilized in methanol. Gallic acid (0 to 80 µg) was used as standard. Aliquot of the extract, standard or blank (100 µL) was added to test tube followed by 10 % Folin-Ciocalteu reagent (200 µL). The solution was vortexed and incubated for 5 min before adding 700 mM sodium carbonate solution (800 µL). The mixture was incubated for 2 hours in the dark and absorbance was read at 765 nm using Synergy HT microplate reader (Bio-Tek Instruments, Winooski, USA). The total phenolic content of extract was obtained from gallic acid standard.

2.2.12.2 Total flavonoid content

The content of flavonoid in extracts was determined by aluminum chloride colorimetric assay. Extract was solubilized in 50 % methanol while quercetin (standard) was prepared in 100 % methanol. Extract, standard or blank (30 µL) was added to a test tube followed by methanol (160 µL) and 10 % methanolic aluminum chloride solution (30 µL). The solution was vortexed, and 1 M sodium acetate was added followed by distilled water to make up the final volume to 1100 µL. The solution was incubated for 30 minutes in the dark, absorbance was read at a wavelength of 415 nm. The amount of flavonoid present in the extract was obtained from a quercetin standard curve and expressed in mg quercetin equivalent per gram of extract in dry weight.

2.2.12.3 Ferric reducing antioxidant power (FRAP) assay

The antioxidant ability of extracts was determined using FRAP assay as described by Benzie and Strain. FRAP solution was freshly prepared containing 300

mM acetate buffer pH 3.6, 10 mM 2,4,6-Tri (2-pyridyl)-s-triazine (aka TPTZ), 20 mM FeCl3.6H_2O solution (10:1:1, v/v/v) and preincubated in the dark for 30 min at 37 °C. The extracts were prepared in 50 % methanol. Trolox or $FeSO_4$ was used as standard. The assay was performed by adding extract, standard or blank (10 µL) into 96-well microplate followed by FRAP solution (200 µL). The plate was incubated at 37 °C in the dark for 30 min. Absorbance of the solution was obtained at 593 nm. The antioxidant activity was represented as FRAP value expressed as µmol Trolox equivalent or mM Ferrous equivalent per gram of extract in dry weight.

2.2.12.4 DPPH radical scavenging assay

The capacity of extracts to scavenge free radical species was determined by $DPPH^{\cdot}$ assay. Extract was solubilized in 50 % methanol and Trolox (standard) was diluted with distilled water. The extract, standard or blank (10 µL) was added to 96-well microplate followed by methanol (140 µL). DPPH radical dissolved in methanol (0.1 mM, 150 µL) was added to the sample in microplate. For blanks, 150 µL of methanol replaced $DPPH^{\cdot}$ solution. The sample was incubated for 30 min in the dark at room temperature before reading absorbance at 515 nm. The DPPH radical scavenging activity of extract or Trolox was expressed as IC_{50}, that is, the extract concentration that scavenged 50 % of the DPPH radical.

2.2.12.5 LC-qTOF-ESI-MS analysis

Sample for the LC-MS analysis was prepared by solubilizing extract in methanol (40mg/mL), centrifuged at 5000 rpm for 10 min and filtered through a 0.22 µm nylon filter. The clear, filtered extract was used for analysis. LC-MS analysis was performed using Agilent Technologies Poroshell 120 EC-C18 column (4.6 x 150 mm, 2.7 µm) with water (eluent A) and acetonitrile (eluent B) both containing 0.1 % formic acid as solvents. The separation gradient was maintained as follows: 0 to 5 min, 0 % B; 5 to 50 min, increased linearly to 80 % B; 50 to 53 min, maintained at 80 % B; 53 to 55 min, decreased to 0 % B; 55 to 60 min, re-equilibrated in 0 % B at a constant flow rate of 0.3 mL/min. The separated analyte was detected on micrOTOF-QII™ESI-Qq-TOF mass spectrometer (Bruker Daltonics, Bremen, Germany) in a negative ionization mode over a mass range of 50 to 1500 Da. Acquisition parameters for the mass spectra included a capillary voltage of 3500 V, nebulizer pressure of 2.0 Bar and

drying gas of 8.0 L/min. To ensure accuracy of the system calibration was performed using 10 mM sodium formate solution. Data analysis was performed using Bruker Compass DataAnalysis 4.0 software (Bruker Daltonics, Bremen, Germany). The plausible compound identities were obtained using a combination of accurate mass, retention time, reported bibliography on C. asiatica as well as online databases such as ChemSpider and METLIN.

2.2.13 Statistical analysis

Data of the hTTR stability assays are presented as the mean ± standard error of the mean (for the effects *Centella asiatica*) or the mean ± standard deviation (for the effects of *Bacopa monnieri*) after having been statistically analysed via one-way ANOVA followed byTukey-Kramer test. Differences were statistically significant at $P<0.05$.

CHAPTER 3

Inhibition of human transthyretin amyloidogenesis by *Centella asiatica* (L.) Urban extract

An adaptation from a published journal article (Eze et al. Biomolecules. 2019 Apr; 9(4): 128)

3.1 Introduction

Formation of transthyretin aggregates of various sizes and morphologies had been associated with the development of transthyretin amyloidosis. TTR amyloidogenesis is known to be mediated by a downhill polymerization mechanism. Here, the amyloidogenic species or oligomers formed are more energetically stable than their precursors which are formed by tetramer dissociation. Also, given that the process is dependent on the concentration of amyloid competent monomers, preventing the formation of the monomers by increasing the tetramer stability have been promoted as a reliable strategy for mitigating amyloidogenesis, for review see (Johnson et al., 2012). In this section, we describe the TTR amyloidogenesis inhibitory activities of *C. asiatica*, a small medicinal herb widely popular in Thailand, Asia and many other parts of the tropics and subtropical regions of the world (for detailed review, see Chapter 1).

3.2 CAB promotes the stability of native human transthyretin

TTR was successfully purified from human plasma using preparative discontinuous native-PAGE and concentrated on a stirred ultrafiltration unit. The purity of the TTR was confirmed using SDS-PAGE (Figure 5) and concentration by a Bradford assay with slight modifications (Ernst and Zor, 2010).

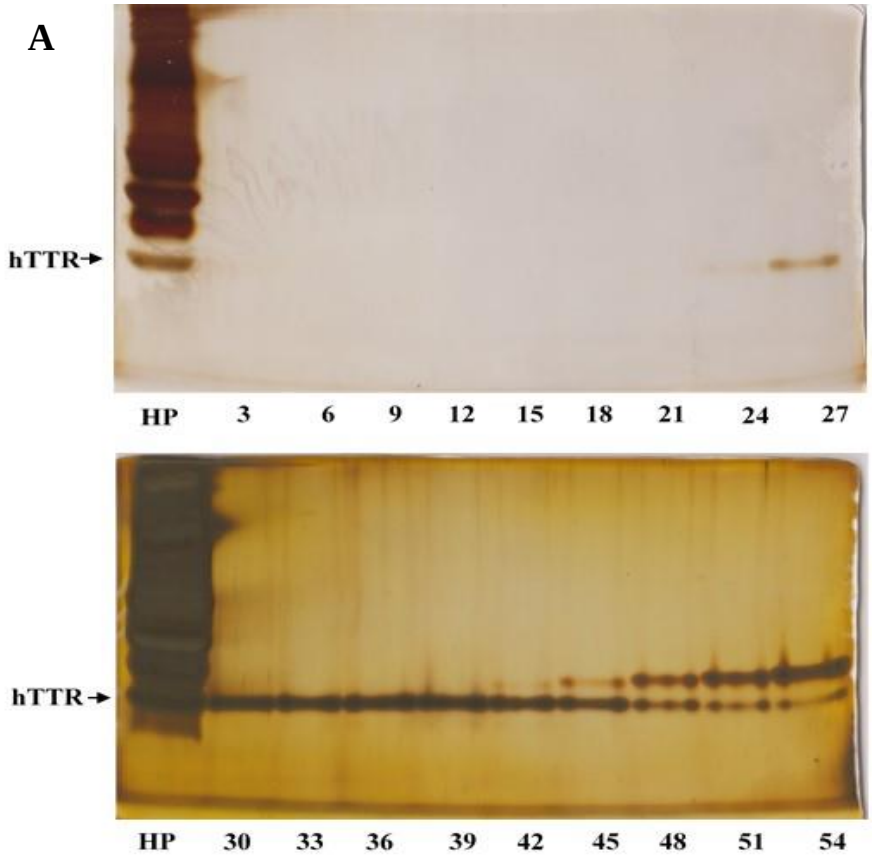

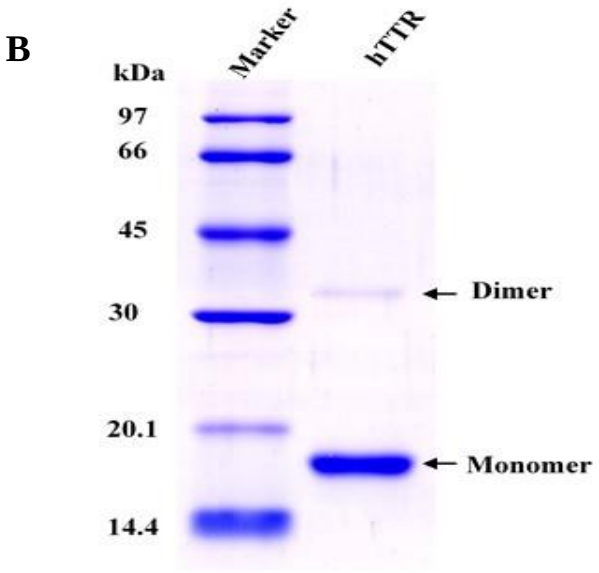

Figure 5 Purification of human TTR from plasma. (A) Silver-stained native PAGE gels of collected fractions from preparative discontinuous PAGE. (B) SDS-PAGE analysis of purified human TTR under reduced conditions.

To determine the influence of CAB on hTTR structural stability, the purified protein was preincubated with or without CAB and thereafter subjected to urea-mediated denaturation assay. The urea-mediated denaturation is a reliable method for estimating the relative stability of native TTR *in vitro*. Although a slightly weaker denaturant than guanidine hydrochloride, urea is often the preferred reagent for TTR stability assay. This is because while guanidine hydrochloride can cause the denaturation of TTR regardless of its quaternary structure, urea only denatures TTR in its monomeric form. The implication is that urea-mediated denaturation requires the dissociation of TTR. By linking the quaternary structural changes to the tertiary structural changes, the rate-limiting tetramer dissociation can be determined. This was accomplished by incubating TTR with or without CAB in 6 M urea at 4 °C. The low temperature enhances tetramer dissociation while the high urea concentration (>5 M, beyond post-transitional region for tertiary structural changes) ensures that the unfolding of the monomer remain irreversible. Under these conditions, WT TTR has an extremely slow tetramer dissociates rate ($t_{1/2}$ = 9.6 h) (Hammarström et al., 2002) followed by a rapid monomer denaturation ($t_{1/2}$ = 69 ms) (Jiang et al., 2001), giving a five-magnitude fold increase. Thus, measuring the fraction of undissociated or non-monomeric TTR (folded TTR) left in solution after 72 of denaturation stress using Tricine-SDS-PAGE, an estimate of the relative stability of the native protein. could be obtained. (Hammarström et al., 2002; Kelly et al., 1997). As shown in Figure 6, the intensity of the folded hTTR band was more in the presence of CAB than in its absence (GMSO). GMSO solution was a mixture of DMSO and GF buffer (1:1, v/v), while GF buffer was 10 mM sodium phosphate buffer with 100 mM KCl and 1 mM EDTA, pH 7.4). The percentage of folded hTTR left at the end of urea denaturation stress in the presence of CAB was 89.65 ± 4.6 compare to 58.87 ± 4.37 in its absence (Figure 6, B).

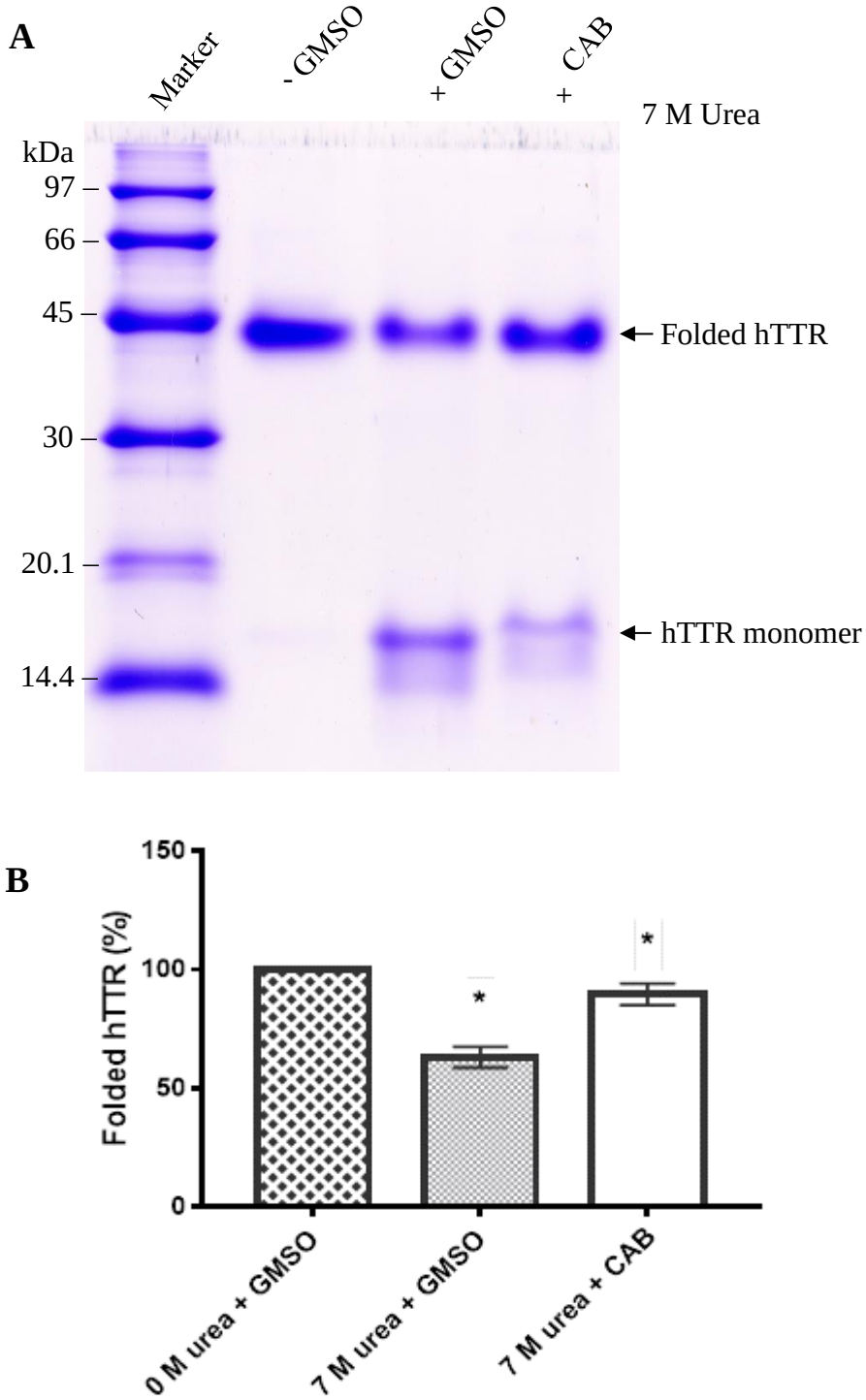

Figure 6 Resistance to urea-mediated dissociation of native hTTR in the presence and absence of *C. asiatica* bioactives (CAB). (A) Tricine-SDS-PAGE gel image (14%) of resolved hTTR after denaturation and (B) Bar chart represents means of hTTR with or without CAB (protein: CAB ratio of 1:100), and standard errors.

To determine the effect of CAB on hTTR quaternary structural changes, the protein solution was cross-linked with glutaraldehyde prior to Tricine-SDS-PAGE analysis. Upon resolution of protein solution on gels, it was revealed that the intensity of hTTR tetrameric band increases in a dose-dependent manner in the presence of CAB. Correspondingly, monomeric band intensity decreases in similar manner. From these results it can be inferred that CAB enhanced the quaternary structural stability of hTTR (Figure 7).

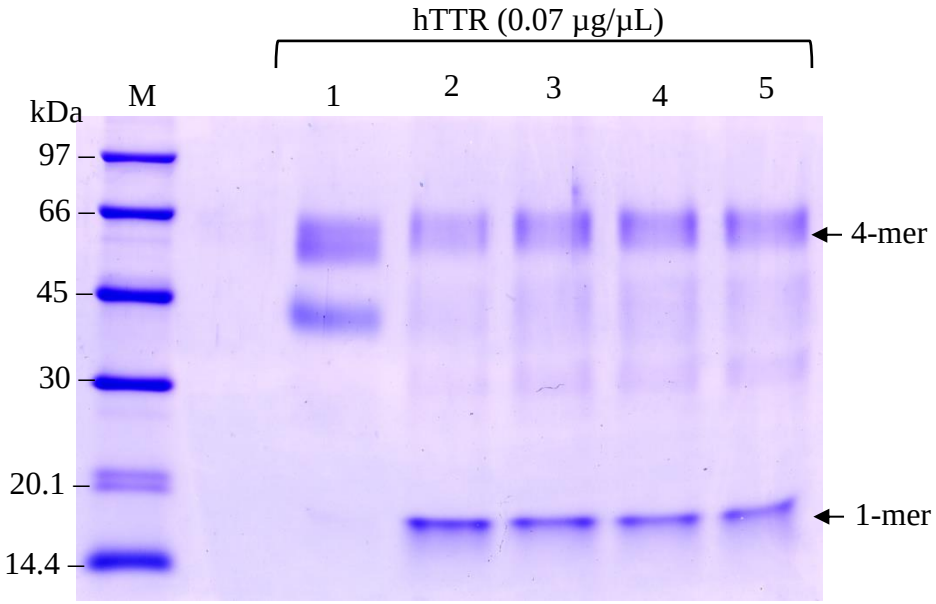

Figure 7. Tricine-SDS-PAGE (10%) gel representation of quaternary structural analysis of hTTR without or with increasing concentrations of CAB by glutaraldehyde cross-linking. M: Protein molecular weight marker; 1: 0 M urea + GMSO only; 2: 7 M urea + GMSO only; 3: 7 M urea + CAB (3.33 µg/µL); 4: 7 M urea + CAB (6.66 µg/µL); 5: 7 M urea + CAB (13.33 µg/µL).

Further evidence of the role of CAB in hTTR amyloidogenesis was obtained using acid-mediated denaturation assay. TTR dissociates and self-assemble into cytotoxic aggregates when subjected to conditions of mild acidity (pH 4 to 5) *in vitro*. The impact of CAB on hTTR stability under these aggregation-promoting conditions was ascertained via acid-mediated denaturation assay (Figure 8). Glutaraldehyde cross-linking followed by Tricine-SDS-PAGE of hTTR with or without CAB subjected to acid denaturation stress revealed far more intense bands for hTTR tetramers and trimers in the presence of CAB than in its absence. Quantification of band intensities by gel documentation show that the percentage of hTTR tetramers was higher in the presence of CAB (68.32 ± 0.81) than in its absence (30.24 ± 0.78). The decrease in hTTR dissociation in the presence of CAB is thus suggestive of its tetramer stabilizing activities and further supported the results earlier obtained using urea-mediated denaturation.

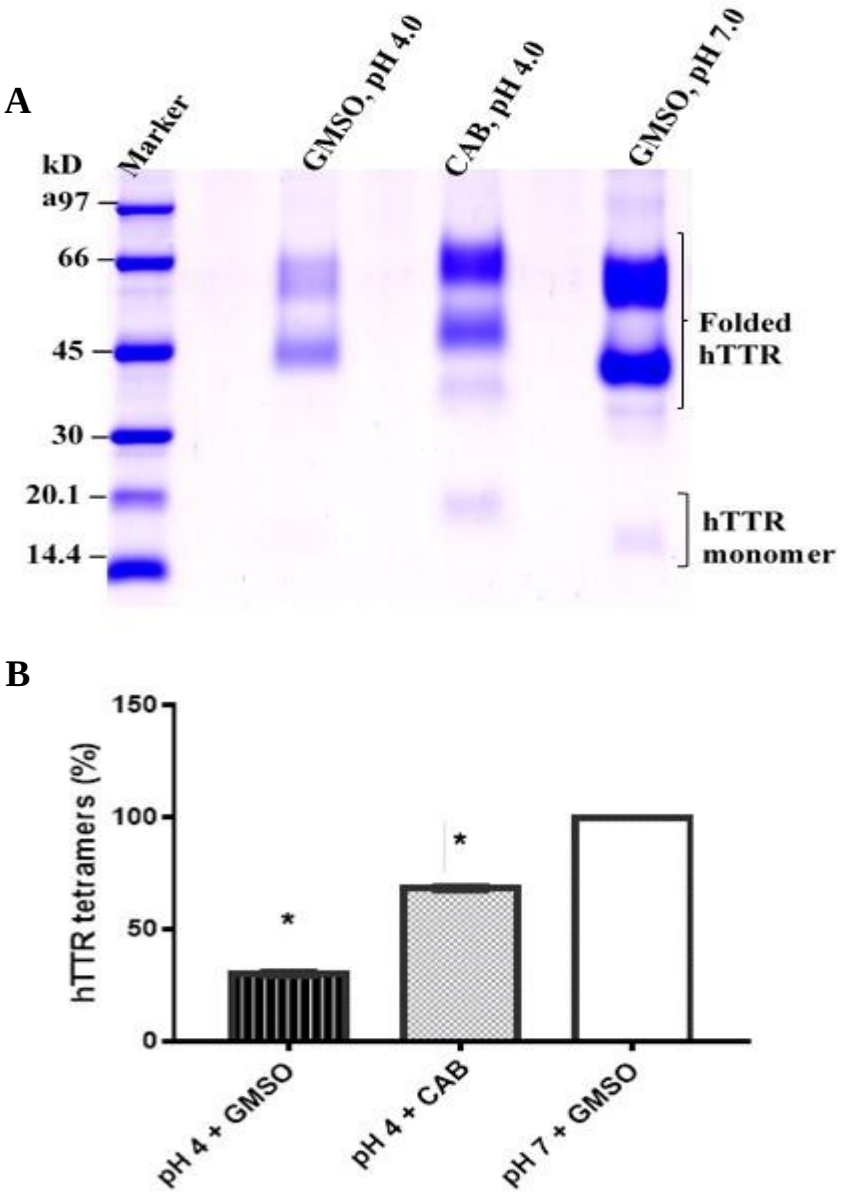

Figure 8. The resistance of human transthyretin in the absence or presence of CAB against acid-mediated denaturation. hTTR (0.5 µg/µL) was incubated with or without CAB (50 µg/µL) and subjected to acidic denaturation conditions for 2 weeks. (A) The image represents the resolved protein mixtures on 10% Tricine SDS-PAGE gels after cross-linking with glutaraldehyde. M: Protein molecular weight marker; 1: huTTR with GMSO only, pH 4.0; 2: huTTR with CAB, pH 4.0; 3: huTTR with GMSO only, pH 7.0. (B) The percentage of tetramers (%) left after denaturation

3.3 CAB attenuated TTR fibril formation

The effect of CAB on TTR fibril formation was determined using acid mediated fibril formation monitored by transmission electron microscopy. The TEM images obtained revealed the different morphological changes in TTR under aggregation-promoting conditions. From the electron micrograph Figure 9, it was revealed that in the absence of CAB, TTR formed mature fibrils and heterogenous amorphous aggregates. However, when CAB was co-incubated with TTR, there was no mature fibril formed, nevertheless, oligomers of various sizes could be observed. Thus, it can be deduced that CAB mitigated the formation of hTTR fibrils but does not prevent the aggregation process.

3.4 CAB binds to the TBS of human transthyretin

Bioactive compounds possessing a catechol moiety for example flavonoids and several other polyphenols are capable of forming quinone adducts with proteins. If the protein-ligand complex formed are SDS-resistant, it can be detected by NBT staining. In brief, the preincubated protein solution containing the bioactive compounds are separated on SDS-PAGE and then electroblotted on nitrocellulose membrane. The membrane is then stained with an alkaline buffer containing glycine and NBT dye. Under these conditions, the bioactive compound autoxidizes into a quinone and subsequently reacts with glycine with the concomitant release of superoxide anion. The superoxide anion then reduces NBT into formazan which produces a purple spot on the membrane.

In the presence of CAB (Figure 10B, Lane 2), a purple formazan band was situated at ~38 kDa suggestive of the presence of a tightly bound SDS-stable ligand with the hTTR tetramer. Correspondingly, no such band was observed in the absence of CAB (Figure 10B, Lane1). Thus, CAB reacted with TTR in a manner indicative of a covalent interaction.

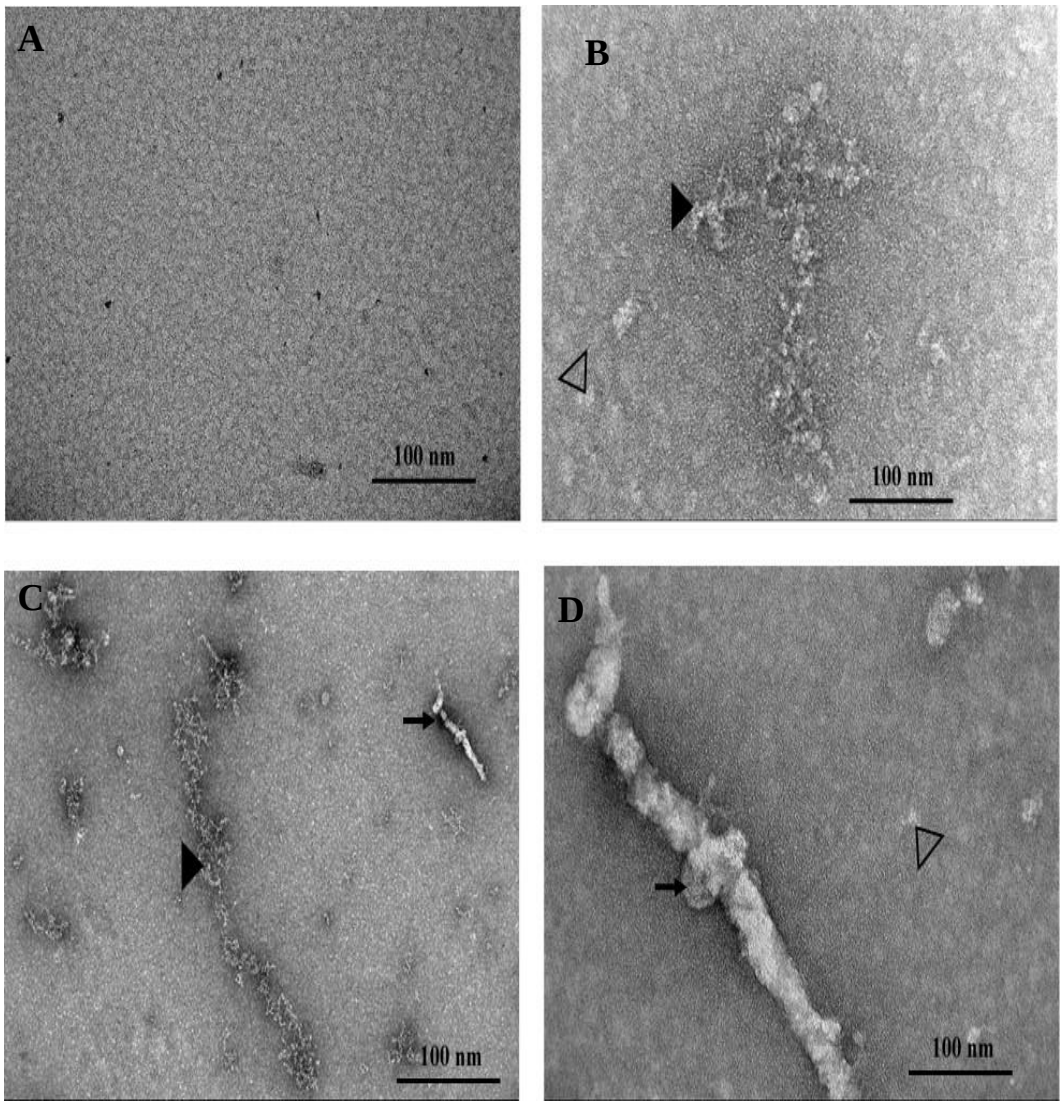

Figure 9. Electron micrograph of hTTR with or without CAB after acid mediated aggregation. A. Human TTR in GF buffer, pH 7.4 with buffer only (GMSO) incubated at −20 °C. B. Human TTR with CAB, final pH 4.0 and incubated at 37 °C for 7 days. C. Human TTR with GMSO, pH 4.0 and incubated at 37 °C for 7 days. D. Same image as C, but with higher magnification

To further explore the nature of CAB binding with TTR, ANS binding displacement assay was performed. The propensity of ANS to bind to the thyroxine-binding sites of TTR accompanied by a blue shift and increase in fluorescence intensity have been exploited as a reliable probe for determining ligand interaction with tetrameric TTR. As shown in Figure 11, in the absence of TTR, ANS produces a weak fluorescence signal. When TTR was present, there was a dramatic increase in the fluorescent intensity, which could be due to ANS binding to the hydrophobic T4-binding sites of TTR. When CAB was included into the mixture, there was a dose-dependent decrease in the fluorescence intensities of the ternary complex which could be attributed to the displacement of ANS from the T4-binding sites by the bioactive compound(s). From these results it can be surmised that CAB bound to the T4-binding sites of hTTR and the interaction of CAB with the protein was partly covalent.

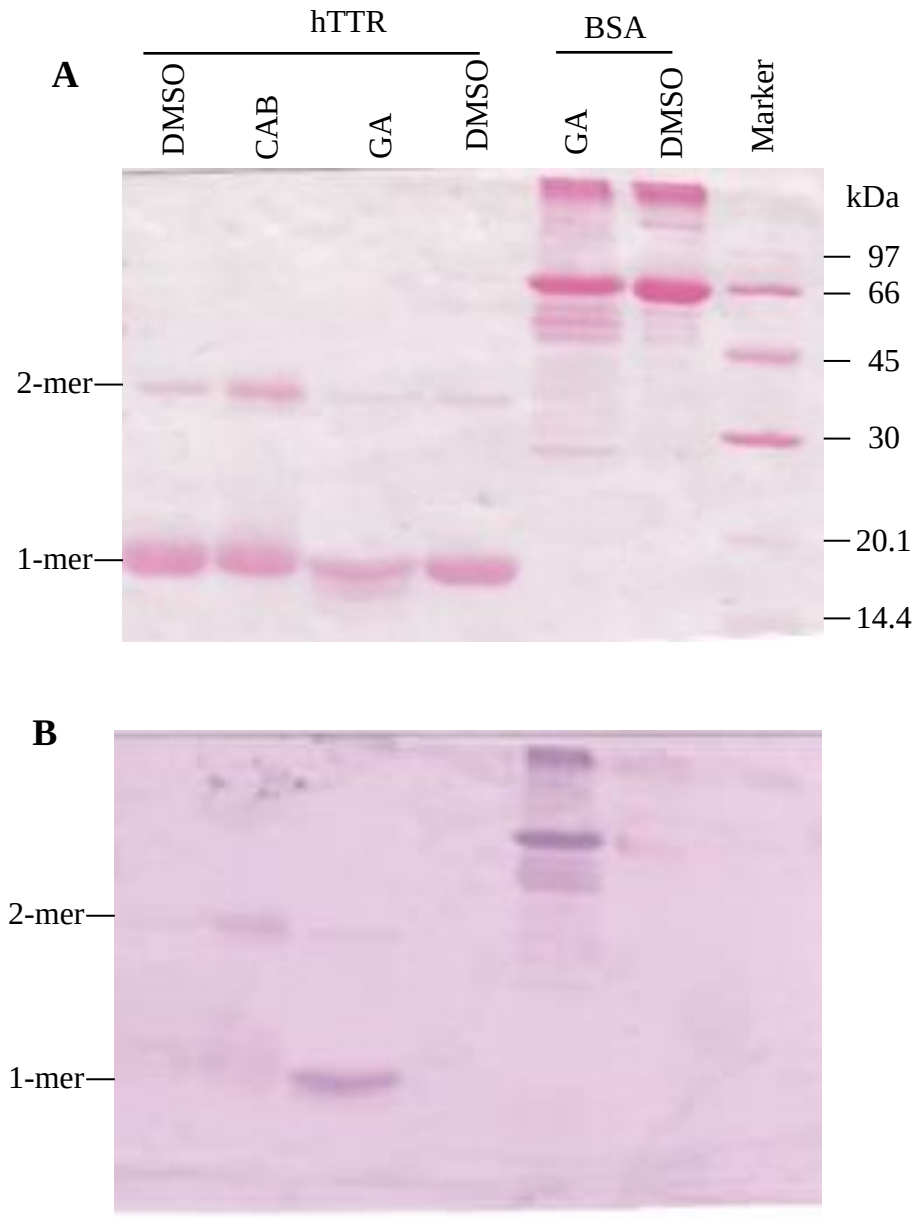

Figure 10. NBT-redox cycling staining to determine CAB binding to TTR (A). Ponceau S staining of hTTR treated or non-treated (vehicle) with bioactives after electroblotting of SDS-PAGE onto the nitrocellulose membrane (Protein: Drug ratio of 1:10). (B). Nitroblue tetrazolium (NBT)/glycinate staining of the membrane above after de-staining of Ponceau S dye. GA (gallic acid)

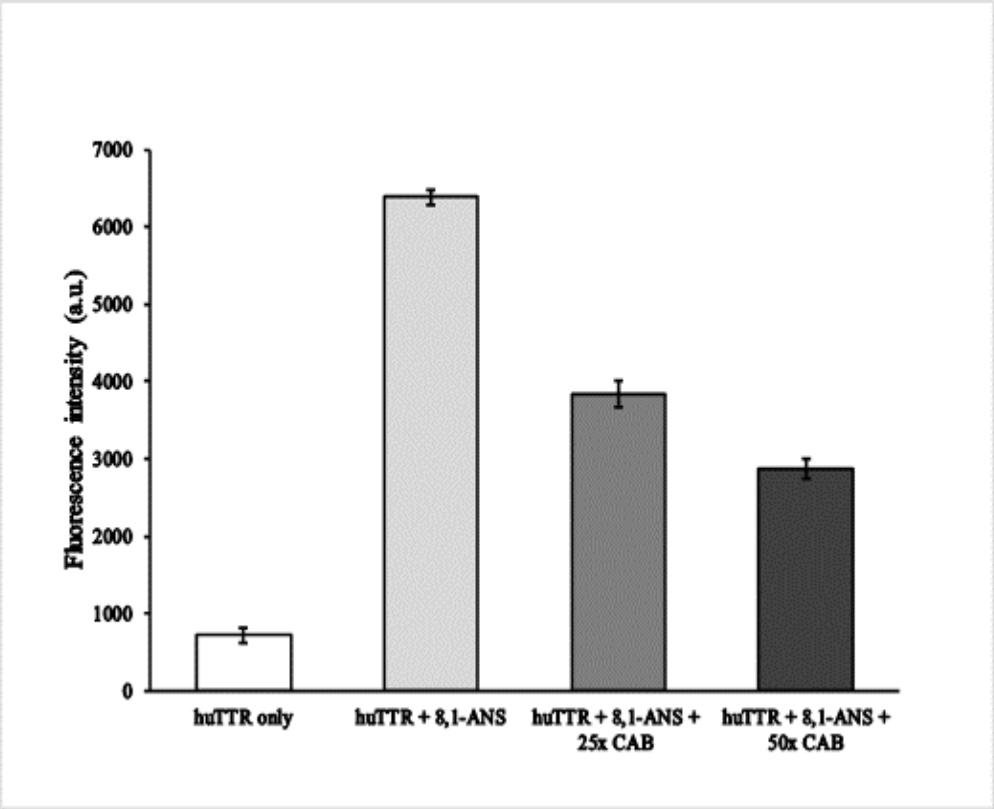

Figure 11. Displacement of bound 8-anilino-1-naphthalene sulfonic acid (ANS) from human TTR by increasing concentrations of CAB. The bar chart columns and error bars are the means standard deviations of triplicates, respectively.

3.5 Chemical characteristics of CAB

An elucidation of the chemical constituents and properties of CAB was determined in order to understand it's biological effects on TTR. The antioxidant activity of CAB was determined by FRAP assay, widely used for determining the capacity of products of natural origin such as plant extracts, fruits, vegetables or supplements to act as reductants by single electron transfers. The higher the FRAP value, the more potent the compound or extract. CAB gave a FRAP value of 284.17 µmol Trolox equivalent per gram of CAB, which is considerably high in comparison to previous reports. Furthermore, the ability of CAB to scavenge free radicals was determined by the DPPH assay. Herein the extent to which the extract can scavenge reactive free radical species deduced from its ability to quench the stable $DPPH^{\cdot}$ by donating hydrogen ions to it. From the DPPH assay, CAB demonstrated an IC_{50} value of 28.53 which can be considered to be moderate when compared to that of common antioxidant standards like Trolox and ascorbic acid. It is widely accepted that several

biological activities including the antioxidant properties of most plant-derived products are attributable to their phenolic content. The total phenolic and flavonoid content of CAB were determined by Folin-Ciocalteu and aluminum chloride colorimetric assays, respectively. As shown in Table 3 below CAB had a high phenolic and flavonoid content, which could be contributing to its protective ability against TTR amyloidogenesis.

Table 2. Chemical characteristics of CAB

Characteristics	CAB
Phenolic content (mg gallic acid/g dry weight)	43.86 ± 0.34
Flavonoid content (mg quercetin/g dry weight)	13.89 ± 0.23
FRAP (µmol Trolox)	284.17 ± 14.21
DPPH [IC_{50}] µg/mL	28.81 ± 0.54

Table 3. HPLC-ESI-QTOF-MS Profile in the negative ion mode of *Centella asiatic* bioactives (CAB)

Peak No.	Retention time	Observed accurate mass (m/z)	Predicted formula	Calculated mass (Da)	Tentative identity of compound
4	2.0	503.1527 $[M-H]^-$	$C_{21}H_{28}O_{14}$	504.1479	Caffeic acid dihexoside
12	15.1	353.0877 $[M-H]^-$	$C_{16}H_{18}O_9$	354.0951	3-*O*-Caffeoylquinic acid
14	17.0	353.088 $[M-H]^-$	$C_{16}H_{18}O_9$	354.0951	5-*O*-Caffeoylquinic acid
21	21.3	693.2790 $[M-H_20-H]^-$	$C_{34}H_{48}O_{16}$	712.2942	Nominilic acid 17-glucoside
22	21.6	477.0685 $[M-H]^-$	$C_{21}H_{18}O_{13}$	478.0747	Quercetin 3-*O*-glucoronide
23	22.4	5151195 $[M-H]^-$	$C_{25}H_{24}O_{12}$	516.1268	3,4-*O*-Dicaffeoylquinic acid
24	22.9	515.1209 $[M-H]^-$	$C_{25}H_{24}O_{12}$	516.1268	3,5-*O*-Dicaffeoylquinic acid
25	23.3	601.1226 $[M-H]^-$	$C_{28}H_{26}O_{15}$	602.1272	3,5-*O*-Dicaffeoyl-4-malonylquinic acid
26	23.6	515.1203 $[M-H]^-$	$C_{25}H_{24}O_{12}$	516.1268	4,5-*O*-Dicaffeoylquinic acid
27	24.0	601.1209 $[M-H]^-$	$C_{28}H_{26}O_{15}$	602.1272	3,5-*O*-Dicaffeoyl-4-malonylquinic acid isomer
28	24.4	601.1228 $[M-H]^-$	$C_{28}H_{26}O_{15}$	602.1272	Eriodictyol 7-(6-galloylglucoside)
29	24.7	1019.5149 $[M+Formate]^-$	$C_{49}H_{79}O_{22}$	1019.5063	Asiaticoside B

30	24.8	1019.5149 [M+Formate]$^-$	$C_{49}H_{79}O_{22}$	1019.5063	Madecassoside
31	25.1	529.1351 [M-H]$^-$	$C_{26}H_{26}O_{12}$	530.1424	3-Caffeoyl-4-feruloylquinic acid
32	25.2	873.4522 [M+Formate-H]$^-$	$C_{43}H_{69}O_{18}$	874.4562	Centellasaponin B
33	25.7	1003.5166 [M+Formate-H]$^-$	$C_{49}H_{79}O_{21}$	1004.5192	Centellasaponin A
34	26.1	957.5088 [M-H]$^-$	$C_{48}H_{78}O_{19}$	958.5137	Asiaticoside
36	27.8	1061.5180 [M-H]$^-$	$C_{51}H_{82}O_{23}$	1062.5247	Avenacoside A
39	29.8	987.5213 [M-H]$^-$	$C_{49}H_{79}O_{20}$	988.5243	Soyasaponin I
40	30.2	571.0881 [M-H_2O-H]$^-$	$C_{30}H_{20}O_{12}$	572.0955	Manniflavanone

Details of the individual bioactive metabolites present in CAB was obtained by qualitative LC-MS screening of the extract (Table 4). It was revealed that CAB had many chlorogenic acids (caffeoylquinic acids) such as 3-O-caffeoylquinic acid, 5-O-caffeoylquinic acid, 3,5-O-Dicaffeoylquinic acid, 3,5-O-dicaffeoyl-4-malonylquinic acid (Irbic acid) as well as triterpenoids such as asiaticoside, madecassoside, centellasaponin B. This was consistent with previous reports that the major bioactive components of C. asiatica aerial parts are the phenolics such as chlorogenic acids and the pentacyclic triterpenoids (Alqahtani et al., 2015; Maulidiani et al., 2014).

Summary

Here, we have demonstrated using a number of cell-free assays that *C. asiatica* extract is capable of modulating TTR amyloidogenesis. CAB prevented hTTR fibril formation and attenuated the quaternary structural alterations required for amyloidogenesis by binding at the thyroxine binding site of the native tetramer and putatively raised the kinetic barrier for dissociation. CAB is replete with antioxidant bioactives which might be responsible for its anti-TTR amyloidogenic activities. Thus, it is expected that with further investigations the potential therapeutic application of this bioactive resource could be harnessed for ameliorating ATTR amyloidosis

CHAPTER 4

Transthyretin amyloidogenesis inhibitory and fibril disrupting activities of *Bacopa monnieri* (L.) Wettst extract

An adaptation from a published journal article (Eze et al., Biomolecules. 2019 Dec 9;9(12)

4.1 Introduction

There is an abundance of circumstantial evidence linking the formation of human transthyretin aggregates and/or amyloid fibrils with the ensuing tissue damages that underlies the clinical manifestations of TTR amyloidosis. Although there is a paucity of direct evidence on how amyloid fibrils alter the physiological microenvironment leading to cytotoxicity, it is widely accepted that dissociation of native tetrameric TTR into amyloid-competent monomers is the most critical and rate-determining step in TTR amyloidogenesis; as such, preventing tetramer dissociation indeed poses a conservative and viable therapeutic strategy. This strategy referred to as kinetic stabilization of native state transthyretin, undergirds the development of the regulatory-approved drug Tafamidis for the treatment of some forms of TTR amyloidosis. Likewise, several NSAIDs have also shown to be effective at stabilizing TTR structure. However, Tafamidis is still limited in its effectiveness against late-stage TTR amyloidosis and there are still concerns surrounding it long-term side complications in patients. NSAIDs, on the other hand is rift with side effects such as GIT disturbance which further exacerbates the malnutrition challenges faced by FAP patients. At the moment, emerging therapeutic options such as Patisiran and Inotersen are showing some promise in providing health benefits to TTR amyloidosis patients (Gertz et al., 2019), but the long-term side effects are yet to be established. Thus, there is a need for sustained research effort towards the identification of safe and yet effective remedies for TTR amyloidosis (see Chapter 1 for detailed review).

In this section, we describe investigations pertaining to the impact of *Bacopa monnieri* extract (BME) on TTR amyloidogenesis and fibril dissociation. Curcumin (Cur), the major phenolic compound in Turmeric (*Curcuma longa*), was used as a positive control in the tetramer stability assays. Human TTR was purified from plasma as previously described, while recombinant L55P TTR was successfully expressed using the Pichia pastoris expression system (Figure 12) and purified by preparative discontinuous native PAGE (Figure 13). The impact of BME on hTTR and L55P TTR amyloidogenesis is described thusly.

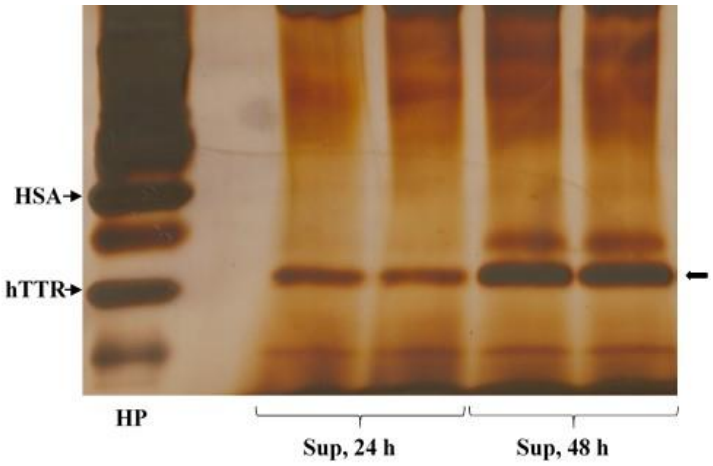

Figure 12 Expression of L55P TTR in *P. pastoris* expression system. Lane 1(HP): pretreated human plasma, Lanes 3 to 6: culture-free *P. pastoris* supernatant (Sup) after incubation in BMMY.

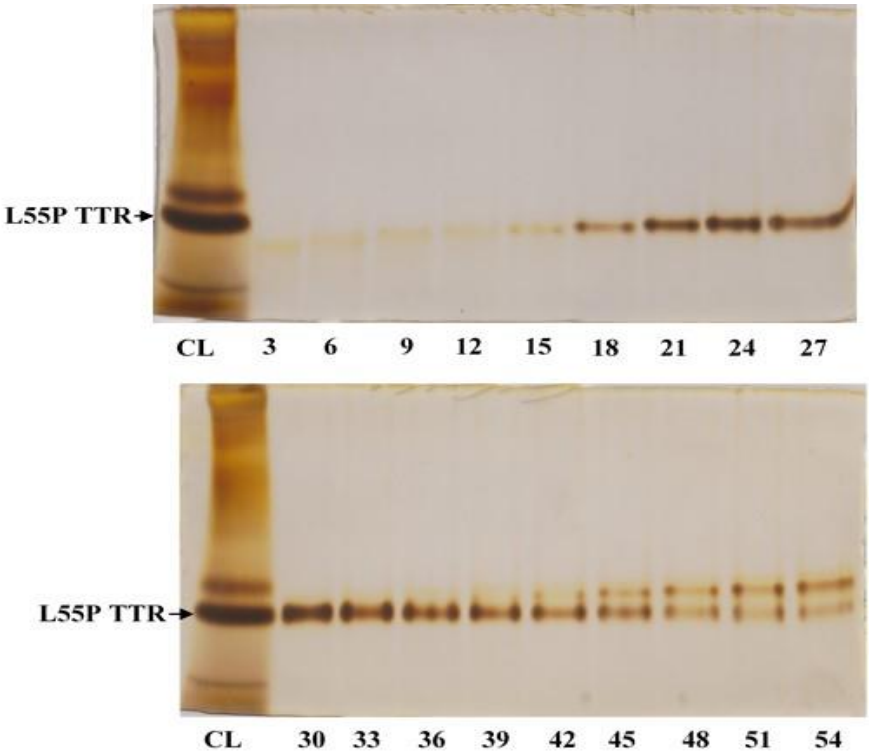

Figure 13 Purification of L55P TTR from concentrated culture-free *P. pastoris* supernatant.

4.2. *Bacopa monnieri* extract attenuated TTR fibril formation

The acid-mediated denaturation/fibril formation assay provides a reliable means for ascertaining the extent of TTR amyloidogenesis *in vitro*. Under mildly acidic conditions of pH 4, TTR tetramers dissociate into non-native monomers capable of self-assembly/misassembly into various amyloidogenic quaternary structural intermediates when present at physiological concentrations and temperature over an extended period (>72 hours). This process can be monitored excellently on SDS-PAGE which shows the native tetramers as dimers whereas the monomers and sometimes, the amyloidogenic quaternary structural intermediates as monomers too (Kelly et al., 1997). Thus, by quantifying the tetramers left at the end of denaturation stress, an estimate of the relative stability of the TTR can be obtained.

As shown in Figure 14, in the absence of BME i.e. DMSO only, the percentage of hTTR tetramers left at the end of acid-mediated denaturation reduced to 56.23 ± 1.08 as opposed to 96.28 ± 1.59 in the presence of BME. The higher amount of tetrameric hTTR gives an indication of the protective effect of BME against acid-mediated tetramer dissociation which is a prerequisite for amyloidogenesis. These results were further supported by findings from the urea-mediated denaturation assay (Figure 15). After hTTR was incubated in 6 M urea for 72 hours, it was revealed that in the presence of BME the percentage of folded hTTR was higher compared to hTTR in the absence of BME (DMSO only). The results for hTTR urea induced dissociation was mirrored when L55P TTR was used (results not included).

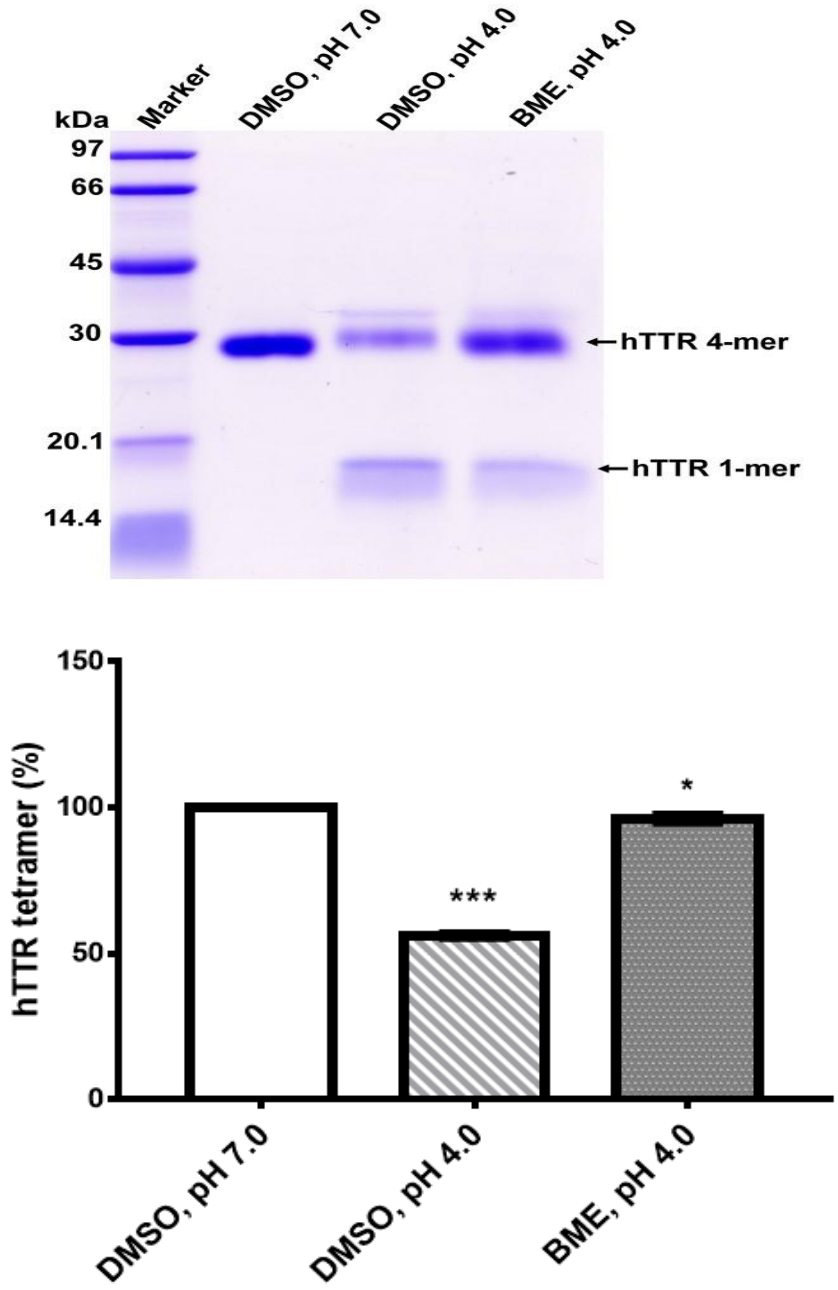

Figure 14 A. Representative Non-reduced SDS-PAGE gel image of hTTR resistance to acid mediated denaturation without (Lane 3) or with (Lane 4) BME. Lane 1; protein molecular weight marker. B. Quantitative analysis of the effect of BME on hTTR tetramer resistance to moderate acidic denaturation conditions. Statistical significance was defined as *P<0.05, **P<0.01 and ***P<0.001. Results are presented as mean ± standard deviation

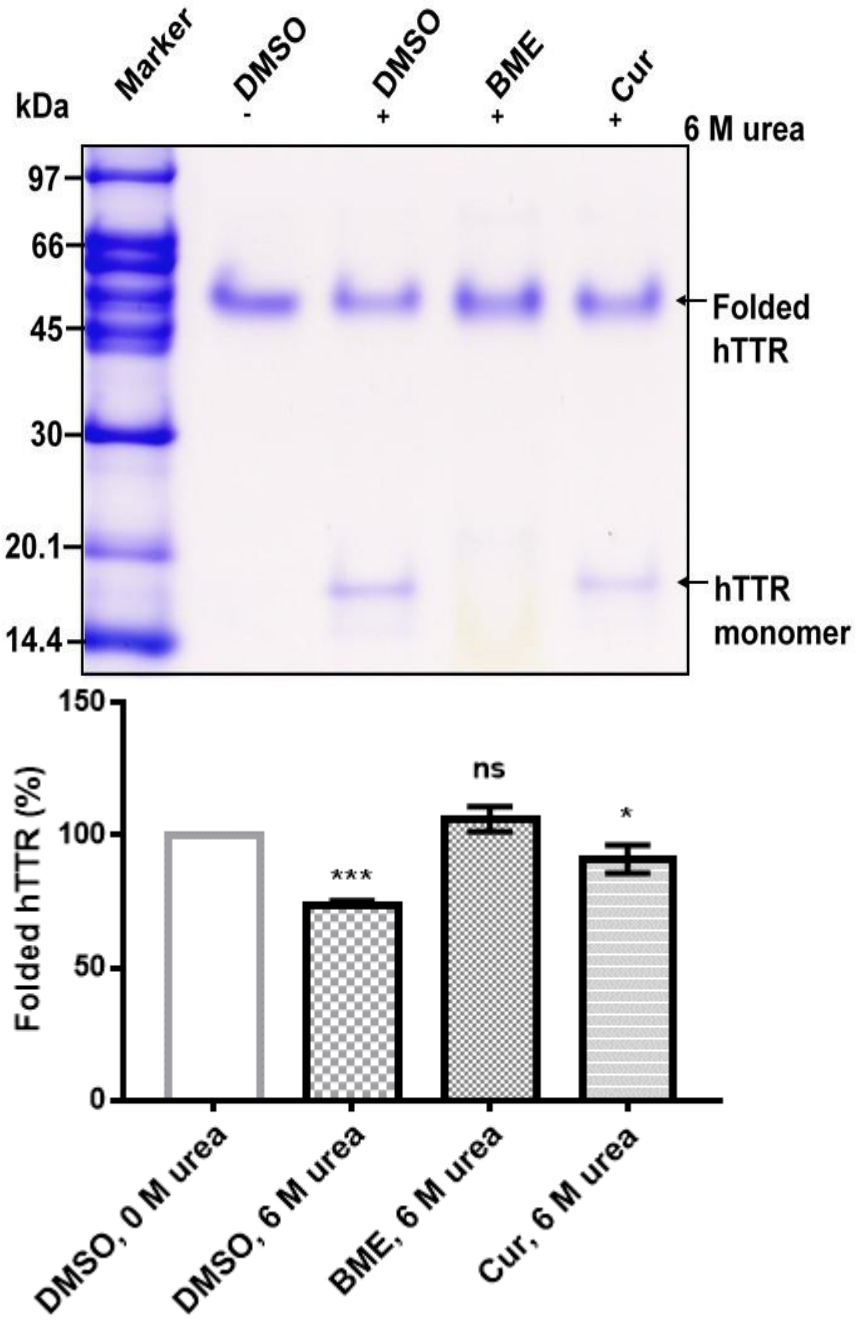

Figure 15 Impact of BME on native TTR dissociation under urea mediated denaturation stress. Percentage of folded hTTR left after 72 hours of incubation in the presence or absence of BME.

Further, the morphological changes associated with TTR with or without BME was determined by transmission electron microscopy (TEM). Electron micrographs

revealed (Figure 16) that in the absence of BME, mature fibrils were formed as well as amorphous oligomers, presumably on the fibrillation pathway (Figure 16A). However, in the presence of BME, no hTTR fibrils were observed nor were there any aggregates (Figure 16B). This seems to suggest that BME inhibited the formation of hTTR fibrils which could be due to the resistance to tetramer dissociation induced by BME as earlier observed.

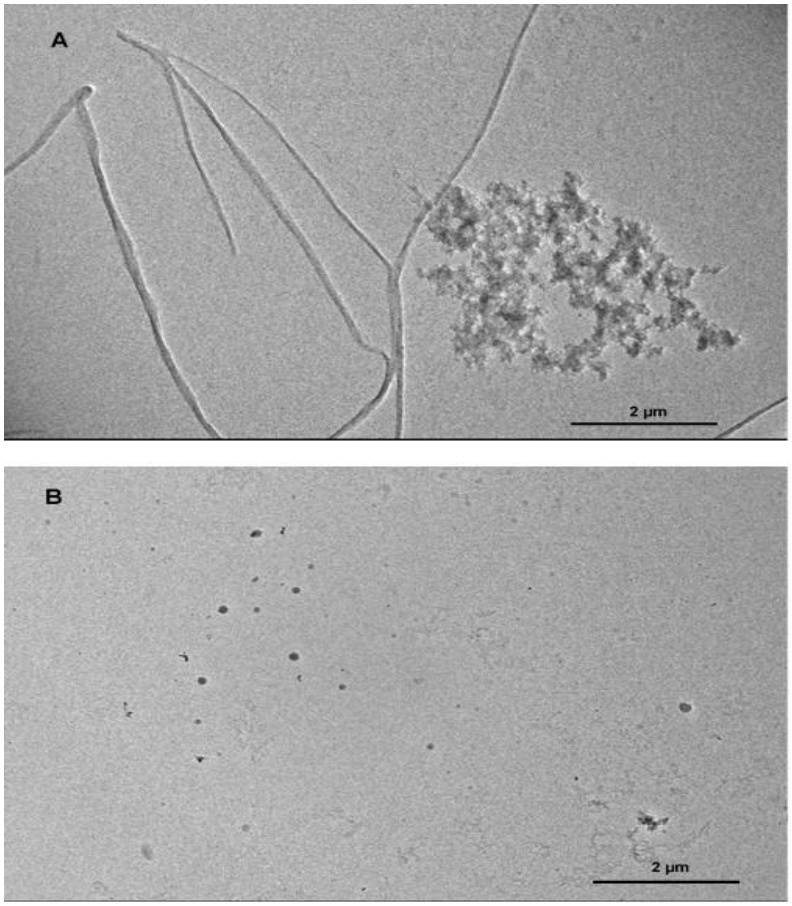

Figure 16 Electron micrographs of hTTR subjected to acid-mediated aggregation assay in the absence (A) or presence (B) of BME after 14 days of incubation at 37 °C.

To determine the quaternary structural changes that is associated with hTTR upon co-incubation the presence or absence of BME after denaturation stress, glutaraldehyde cross-linking assay was performed. The Tricine SDS-PAGE image reveals the profile of the different protein conformations present after denaturation (Figure 17). It can be observed that in acid- and urea-mediated denaturation conditions, in the absence of BME, there was a marked decrease in the intensity of hTTR tetramers Figure 17A, B, Lane 3. Contrariwise, in the presence of BME, the intensity of hTTR tetramer bands were enhanced Figure 17A, B, Lane 4. On

increasing concentrations of BME, there was a general increase in the intensity of the quaternary structural species of native TTR (i.e. tetramer, trimer and monomer) (Figure 18). However, the difference in tetramer band intensity between the various concentrations tested was not significant ($P < 0.05$). This is presumably due to binding saturation of the BME ligands to hTTR at all the concentrations tested. Thus, it can be deduced from these results that the presence of BME preserved the quaternary

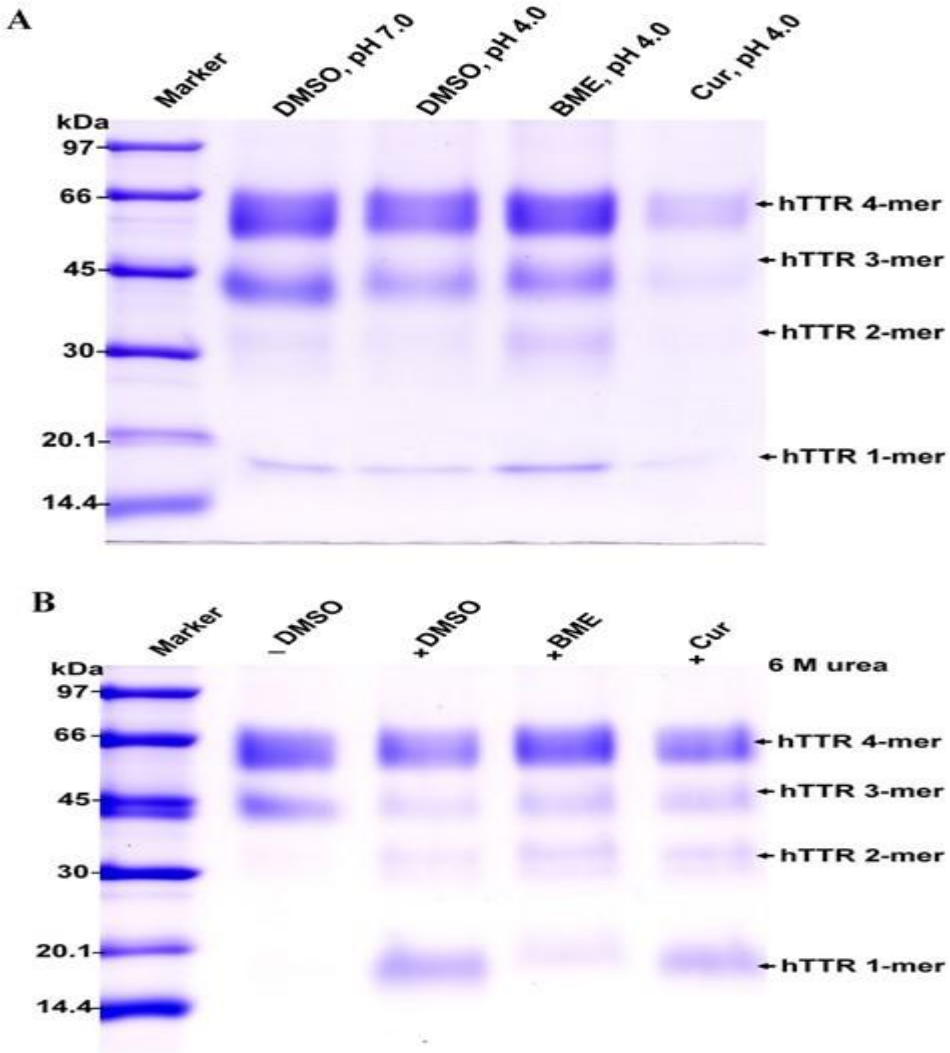

Figure 17 Tricine-SDS-PAGE gel images of glutaraldehyde cross-linked protein samples with or without BME after acid-mediated denaturation (A) and urea-mediated denaturation (B) assays.

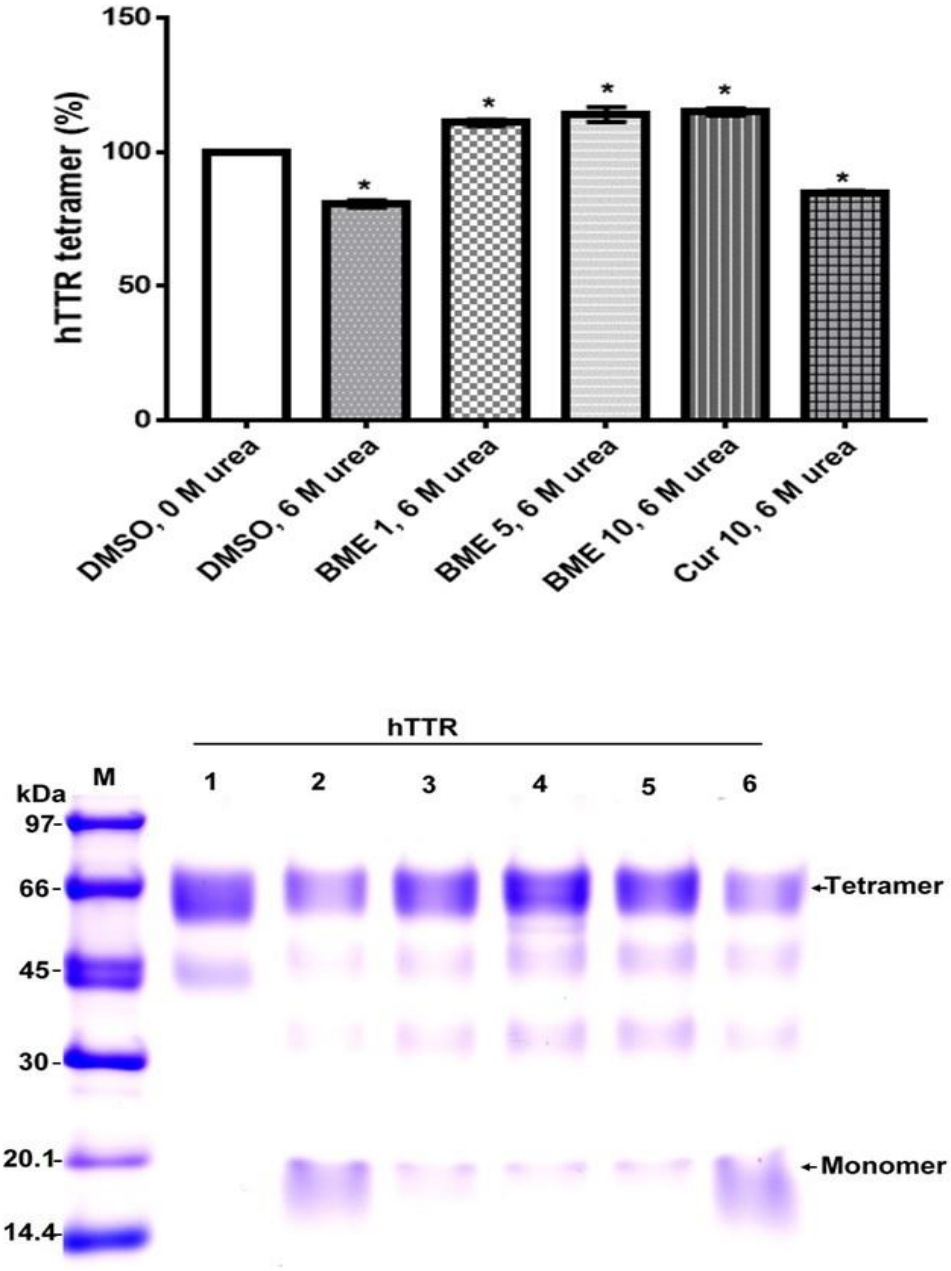

Figure 18 (A) Quantitative analysis of dose-dependent activity of BME on urea-mediated denaturation of hTTR. (B) Representative Tricine-SDS-PAGE gel image of the effect of increasing BME amounts on hTTR tetramer stability. M; molecular weight marker, 1; hTTR in DMSO, without urea, 2; hTTR in DMSO, 6M urea, 3; hTTR in 1 µg/µL BME, 6M urea, 4; hTTR in 5µg/µL BME, 6M urea, 5; hTTR in 10µg/µL BME, 6M urea and 6; 10µg/µL curcumin, 6M urea.

4.3 Impact of BME on hTTR preformed fibrils

Transthyretin preformed fibrils were formed after aging for 14 days under acid-induced denaturation conditions. The formation of mature TTR amyloid fibrils was confirmed by TEM. Fibril disruption assay was performed by further incubation of

the preformed fibrils with or without BME for 24 h at 37 °C. The effect of BME on TTR preformed fibrils was determined by visualizing the protein using TEM (Figure 19). Electron micrograph revealed that in the absence of BME, the mature amyloid fibrils were present after 24 h. In the presence of BME there was no change in the morphology or amount of TTR fibrils compare to when BME was absent. The tricine-SDS-PAGE image reflected similar observations. Thus, it can be surmised that BME did not alter or dis-associate TTR preformed fibrils.

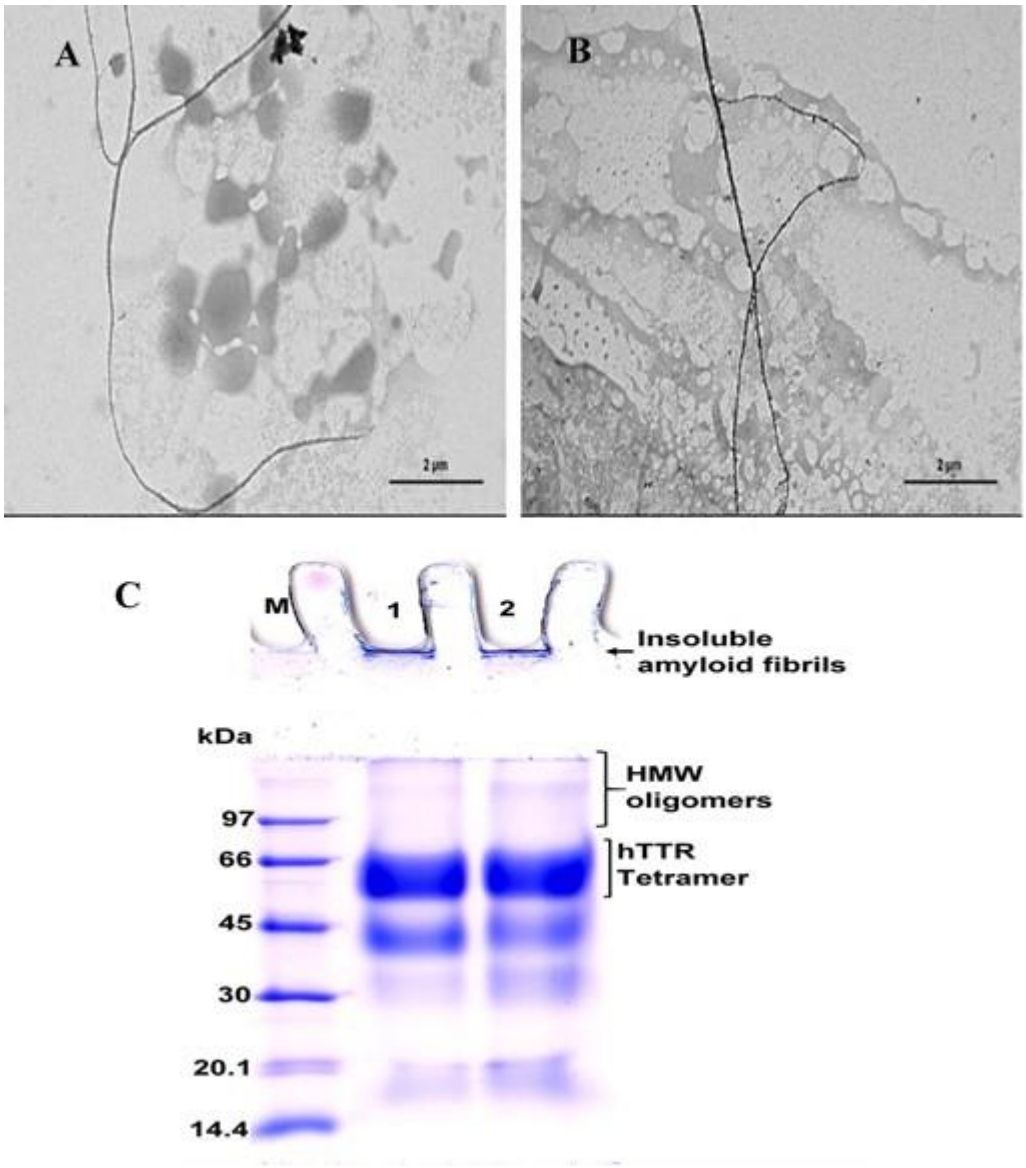

Figure 19 Electron micrographs of pre-formed hTTR amyloid fibrils in the absence (A) or presence of BME (B) after incubation for 24 h. (C) Tricine-SDS-PAGE gel representation of hTTR fibril disruption activity of BME. Lane 1 (M); protein molecular weight marker, Lane 2: hTTR pre-formed fibrils without BME, Lane 3: hTTR pre-formed fibrils with BME

4.4 BME displaces ANS from hTTR TBP

To determine the plausible molecular interactions between TTR and BME, ANS binding displacement assay was performed. Most of the small molecule ligands that had demonstrated kinetic stabilization of native transthyretin were shown to bind at the thyroxine binding pocket of the tetramer. This interaction can be characterized by ANS displacement assay. Figure 20A shows that ANS alone in the aqueous buffer had a very low fluorescence intensity similar to TTR only. However, when ANS was co-incubated with native TTR tetramer, the fluorescence intensity was sharply increased which was suggestive of the binding of ANS to the thyroxine binding pockets (TBP) native TTR. Interestingly, when BME was included, the fluorescence intensity decreased dose-dependently. From this, it can be inferred that BME displaces ANS from and occupies the TBP of TTR.

The nature of the binding interaction of BME presumably at the T4-binding sites of TTR was further explored via NBT-redox cycling assay. Herein, the pre-incubated protein sample with or without BME was resolved on SDS-PAGE followed by electroblotting on nitrocellulose membrane. The membrane was soaked in a solution of NBT dye in potassium glycinate buffer, pH 10. The membrane was washed with ultrapure water and restained with Ponceau S dye. Bovine serum albumin (BSA) and gallic acid (GA) served as positive controls. As shown in Figure 20, in the absence of GA (DMSO only) there was no purple coloration in the BSA lane. However, when BSA was co-incubated with GA, an intense purple band appeared indicative of a strong, SDS-resistant quinoprotein adduct. When hTTR or L55P was co-incubated with BME, neither revealed any purple formazan band. From these results it could be deduced that the binding interactions between BME and TTR weak and certainly noncovalent.

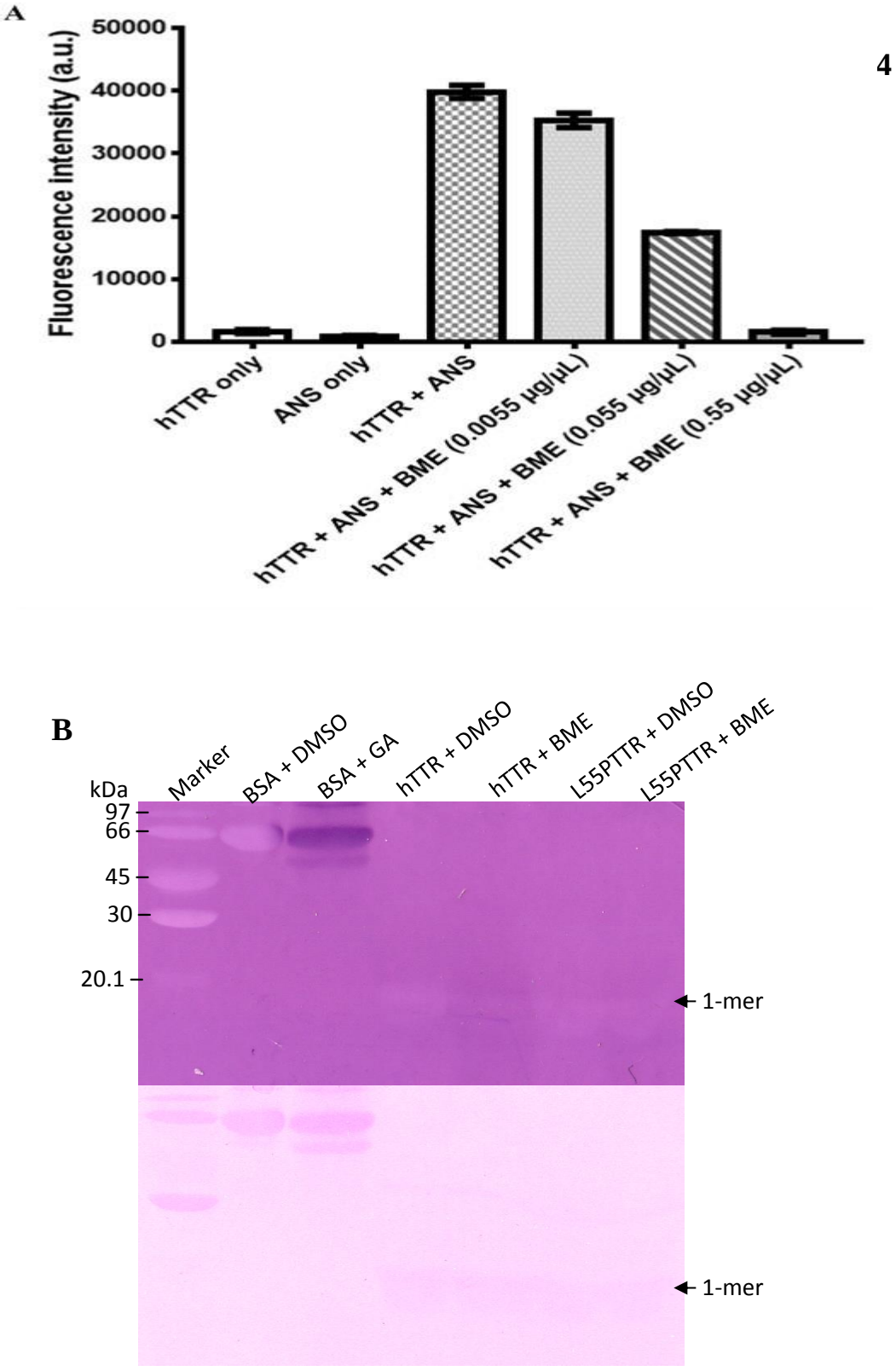

Figure 20. (A) Fluorescence intensities of ANS-TTR without or with increasing concentrations of BME for the determination of inhibitor binding at the T4-binding sites. (B) Nitrocellulose membrane with protein-inhibitor complex after NBT redox-cycling. Upper Membrane was stained with NBT dye (upper), destained and restained with Ponceau S dye (lower).

4.5 Phytochemical properties of BME

Quantitative analysis of the major individual saponins present in BME was determined by reverse-phase HPLC analysis using the pure compounds as standards. The total saponin content was 16.03 % w/w of dried extract made up of Bacopaside I (3.54 % w/w), Bacopaside II (6.68 % w/w), Bacoside A3 (2.22 % w/w), Bacopaside X (3.25 % w/w). These values were remarkably higher than previous reports on similar extracts from the same plant (Łojewski et al., 2016). In addition, BME contained significant amounts of phenolics and flavonoids (Table 5). Plant derived phenolics, especially flavonoids had been associated with antioxidant activities. Thus, the antioxidant and radical scavenging properties of BME were determined by FRAP and DPPH assay, respectively. It was found that BME had a FRAP value of 306.82 µmol Fe (II)/g BME and DPPH IC50 value of 90.84 mg/L. The high FRAP value is indicative of BME potent antioxidant capacity as a reductant while the DPPH value suggests it ability to scavenge free radicals. The detailed LC-MS analysis of the individual phytochemicals found in BME had previously been reported (Nuengchamnong et al., 2016). These antioxidant bioactives might be responsible for the observed anti-amyloidogenic activities of BME.

Table 4. Chemical characteristics of BME

Characteristics	BME
Total saponin content (% w/w of dried extract)	16.03 ± 0.01
Phenolic content (mg gallic acid/g dry weight)	26.45 ± 0.34
Flavonoid content (mg quercetin/g dry weight)	17.6 ± 1.5
FRAP (µmol Trolox)	190 ± 8.39
DPPH [IC_{50}] µg/mL	90.84 ± 0.44

Summary

It can be surmised that in addition to its reported anti-amyloidogenic activities on Alzheimer's and Parkinson disease models, *B. monnieri* extract is capable of inhibiting transthyretin amyloidogenesis in vitro. Through weak, non-covalent binding interactions at the thyroxine-binding sites of the homotetramer, BME enabled the resistance of the protein against acid- and urea-mediated dissociation into monomers – the initial and rate determining step for amyloidogenesis. Thus, BME contained bioactives that could have health-promoting implications for TTR amyloidosis.

CHAPTER 5

Discussion

Native transthyretin is regarded as one of the most intriguing proteins recognized to date because of its multi-functional roles. Besides its established functions as transporter of thyroxine and vitamin A with the assistance of retinol binding protein, transthyretin, inter-alia, has been noted to potentially participate in neuroprotection by sequestering beta amyloid peptide, involved in the pathogenesis of Alzheimer's disease (Li et al., 2013). Under certain conditions this otherwise remarkably stable protein unfolds, mis-aggregates and accumulates as toxic deposits in several organs leading to many amyloid diseases such as familial amyloid polyneuropathy, familial amyloid cardiomyopathy, central nervous system selective amyloidosis or senile systemic amyloidosis (Kelly et al., 1997). For the past several decades, orthotopic liver transplantation was the major therapeutic intervention, however, due to the invasive nature, associated complications amidst other limitations, there had been a significant push for safer, effective pharmacologic interventions with less discomfort to the patients who are often fragile at the point of diagnosis. It is against this backdrop that sustained research effort towards the identification alternative therapeutic agents is indeed warranted (Johnson et al., 2012).

Tetrameric human TTR is a dimer of dimers whose stability is a net effect the stabilizing and destabilizing intermolecular forces present. The stabilizing forces include the inter-strand and monomer-monomer hydrogen bonds as well as many noncovalent interactions. The destabilizing forces are perhaps typified by the repulsive electrostatic interactions originating from the epsilon amino group of lysine 15 in one dimer such as A-B and its symmetrical counterpart, C-D located at the interface of these two dimers. The repulsive charges help to compromise the tetramer at this juncture potentially leading to a scission (Foss et al., 2005; Hammarström et al., 2001). The dimer-dimer interface also creates a hydrophobic channel which bears two funnel-shape tyrosine binding pockets. As early as 1994, it was recognized that binding of thyroxine to these TBP reduced the tendency of the native protein to dissociate and consequently, prevents it from adopting the amyloid compatible monomeric structure. However, T4 and its analogues could not be adopted

therapeutically for ATTR amyloidosis because of its hormonal activities. Nevertheless, it served as a proof-of concept for the development of the therapeutic strategy referred to as kinetic stabilization. Herein, small molecules kinetic stabilizers, are designed to bind to the thyroxine binding channel of the tetramer with the intention of stabilizing the native protein over its dissociative amyloidogenic intermediates. The regulatory-approved drug Tafamidis, is a first-in-kind kinetic stabilizer with demonstrated health benefits to patients. While the drug is well tolerated in patients, the long-term consequences and extremely high cost are obvious sources of concern (Johnson et al., 2012). Recently, bioactive from natural sources have been generating a lot of attraction not only as potential sources for pharmacological scaffolds, but also as alternative treatments in stand-alone, supplements or as part of combination regiments (Chaudhary et al., 2019). The abundance of small molecule bioactives in plants also increases their appeal as sources of kinetic stabilizers. In this work, two plants *Centella asiatica* and *Bacopa monnieri* were investigated for their abilities to modulate transthyretin amyloidosis *in vitro*. Our findings suggest that *C. asiatica* bioactives (CAB) and *B. monnieri* extract (BME) were able to stabilize and thus prevent tetrameric transthyretin from dissociating to monomers by binding to the thyroxine binding sites of the protein. The biological activities of these plant extracts could be attributable to the richness of their phytochemical content, predominantly phenolics and triterpenoid saponins. Thus, *C. asiatica* and *B. monnieri* could be considered for further investigations towards the therapeutic development of TTR amyloidosis remedies.

Under normal physiological circumstances, native tetrameric TTR is remarkably stable, a fact that has been attributed to its rich beta-sheet content. The four identical monomers making up the quaternary structure of native TTR are each composed of 127 amino acids arranged as eight β-strands A to H, and a short α-helix. Two monomers fold on edge to produce an extended dimer of 16 β-strand held together by hydrogen bonds. Association between two dimers, mostly hydrophobic in character forms the tetrameric structure with a hydrophobic channel running across the dimer-dimer interface. This hydrophobic channel accommodates two funnel-shaped binding sites for thyroxine (T4), the natural ligand for TTR (Blake et al., 1978). Often the T4-binding sites of TTR in circulation (> 99 %) are not occupied by

T4 creating room for ligand binding by small molecules which could alter the conformation and properties of the tetramer (Purkey et al., 2001).

The binding of small molecule ligands to the T4 binding sites of TTR often improves the intramolecular interactions across the two dimers with the consequent enhancement of the kinetic barrier for dissociation. However, this does not always translate to kinetic stabilization of the tetramer. Our results demonstrate that CAB and BME reduced the dissociation of folded TTR, and in particular, TTR tetramers to constituent monomers. These findings were buttressed by the glutaraldehyde chemical cross-linking assay which established that extract treated TTR solutions had higher resistance to dissociation induced by urea or mild acidic stress. The resultant higher proportion of tetramers in the presence as opposed to be absence of extracts after denaturation could be interpreted as an indication of protein kinetic stability conferred by the plant bioactives (Florio et al., 2015; Yokoyama et al., 2014).

Detailed qualitative LC-MS profiling of both plant extracts revealed the presence of numerous secondary metabolites, some of which had earlier been reported for their anti-amyloidogenic activity. For instance, quercetin known to be an effective kinetic stabilizer, was identified in both extract as well as apigenin. In addition to several phenolics, triterpenoid saponins such as asiaticoside and madecassoside were present in CAB. In BME, the bacoside triterpenoid psuedojujubogenins and jujubogenins were identified (Ferreira et al., 2011; Florio et al., 2015; Maulidiani et al., 2014; Nuengchamnong et al., 2016). Triterpenoids as a class are interesting because very few reports had noted their ability to inhibit amyloidogenesis, especially as kinetic stabilizers. Thus, their presence in these extracts as main phytoconstituents and putative bioactivities suggests the possibility of their structures serving as novel scaffolds for the structure design of more effective TTR stabilizers.

Given that TTR amyloidogenesis is triggered by tetramer dissociation, in addition to the fact that both extracts inhibited the unravelling of TTR tetramer into monomers, it was therefore prudent to ascertain whether the tetramer stabilizing effects of the extracts were translated downstream of the amyloidogenesis pathway such as in fibril formation. Under mildly acidic conditions at physiological temperature, when TTR was aged for 14 days without CAB or BME, amorphous aggregates and mature TTR amyloid fibrils were generated. This was consistent with

previous reports that acidification enabled the dissociation and conformational changes needed for the formation of TTR amyloid species *in vitro*. This had earlier been postulated as a reflection of the lysosomal acidic conditions which putatively could modulate TTR fibrillation *in vivo* (Kelly et al., 1997). In the presence of CAB, the formation of TTR amyloid fibrils was mitigated. Formation of amorphous aggregates was however unimpeded. Similar to CAB, BME was able to attenuate the formation of mature TTR amyloid fibrils. BME was also able to prevent the formation of TTR aggregate from the dissociation of folded normal TTR. In the past, it has been reported that several plant-derived bioactives especially phenolics inhibited the dissociation and fibrillation of TTR as shown by both extracts. It has also been reported that some plant phenolics such as EGCG binds to TTR and promotes their aggregation into "off-pathway" oligomers which are non-cytotoxic. It is plausible that the same is applicable to the interaction of CAB and TTR. On the other hand, bioactives such as honeybee propolis and curcumin from Turmeric were shown to inhibit fibril formation in similar manner to BME (Ferreira et al., 2011; Yokoyama et al., 2014).

With the exception of EGCG and a few compounds binding at a separate and unique site on TTR tetramer, most natural inhibitors of TTR fibrillation bind to the T4 binding sites (Ortore et al., 2016). Data from the NBT redox-cycling assay established that CAB binds to TTR tetramer and monomer, though to a lesser extent. The binding interactions between CAB and TTR was strong and SDS-resistant, suggestive of covalent-type interactions. On the other hand, the NBT redox-cycling results for BME and TTR was indicative of a non-covalent and transient binding interactions which was non-stable under SDS-PAGE-NBT assay (Popovych et al., 2012). Probing further into the extract-TTR interactions using the small fluorescent probe ANS, it was deduced that CAB and BME bound at the T4-binding sites of the homotetramer. To make sure the observed effects of the extracts were due to binding to transthyretin rather than fluorescence quenching of the probe by the extracts, a counter experiment was performed using bovine serum albumin (BSA) instead of TTR. BSA has a hydrophobic groove to which ANS binds with a resultant increase in fluorescence. When the extracts were added into a solution of BSA and ANS, there was no change in the fluorescence intensity. Thus, it is plausible that by filling the T4-binding

pockets of TTR, these bioactives enhance the intramolecular interactions between the two dimers on either side of the hydrophobic channel with a consequent increase in their kinetic stability (Pullakhandam et al., 2009). Also, it is possible that these plant extracts contained anions capable of shielding epsilon amino groups of lysine 15 and its symmetrical equivalent Lysine 15' across the crystallographic Z-axis responsible for contributing towards tetramer dissociation by virtue of their electrostatic repulsion (Hammarström et al., 2001). Although the precise mode of interaction between the bioactives and TTR as well as the involvement of Lysine 15 residues is entirely speculative, these results echoed similar patterns previously reported for the stabilizing activities of small molecule ligands from natural products on TTR amyloidogenesis (Popovych et al., 2012). Likewise, it worth mentioning that both extracts demonstrated antioxidant activities just like previously reported anti-amyloidogenic bioactive compounds. How the antioxidant property of the bioactives directly contribute to the anti-amyloidogenic properties of the extracts is yet to be investigated, but important clues might be found in fact that age-related oxidative modifications and loss of albumin antioxidant function promote transthyretin amyloidogenesis antioxidant molecules such as Carvedilol and TUDCA resist the deposition of toxic TTR aggregates (Kugimiya et al., 2011; Macedo et al., 2010, 2008; Zhao et al., 2013). As such, compounds capable of modulating TTR microenvironment by reducing the oxidant potential, could mitigate the tendency of the protein to enter the amyloid pathway. It is expected that insights from the investigations presented herein provides a rationale for further exploration of these plant extracts as potential therapeutic candidates for ameliorating TTR amyloidosis.

CHAPTER 6

Conclusions

The transthyretin amyloidosis is a group of progressive, devastating and often fatal diseases. It is characterized by the systemic deposition and accumulation of abnormal TTR aggregates in organs leading to deterioration and dysfunction. For several decades, orthotopic liver transplantation was the only disease modifying remedy and only for a few types of hereditary ATTR amyloidosis forms. Recent breakthroughs in scientific investigations had culminated in the development of three regulatory-approved therapeutic agents namely, Tafamidis, and the recently FDA-approved gene therapies Inotersen and Patisiran (Adams et al., 2019; Gertz et al., 2019) The rarity of treatment options necessitates continued research effort aimed towards expansion of the array of safe, effective, available and less-expensive therapeutic alternatives

C. asiatica and *B. monnieri* are popular nervine with a long history of use in Ayurveda for improving cognition, reducing stress, ameliorating mental retardation and as adaptogens. They are widely cultivated in Asia and several parts of the tropics where they are consumed as spices, vegetable, herbal supplements or remedies. Previous reports have demonstrated several pharmacologic and biologic activities emanating from these extracts, attributable to triterpene saponins and phenolics – the major bioactive ingredients in these plants. The resurgence of demand for natural products over synthetic their counterparts, poor performance of synthetic agents against complex multifactorial degenerative diseases and the general safety profile of *C. asiatica* and *B. monnieri* increase their appeal as candidates for therapeutic investigation against TTR amyloidosis (for review, see Chapter 1).

Here, it has been demonstrated that *C. asiatica* and *B. monnieri* extracts possessed the ability to modulate TTR amyloidogenesis in vitro by virtue of binding at the thyroxine-binding pockets of the homotetramer and consequently stabilizing the protein against dissociation into monomers. The extracts also prevented the formation of TTR fibrils, albeit, only *B. monnieri* was able to abrogate the entire amyloidogenic pathway. Given their reported good safety profile, neuroprotective effects and the evidence presented here for its protection against TTR amyloidogenic propensity, it will be worthwhile to further explore these plant extracts as potential therapeutic agents against TTR amyloidogenesis. Also, it has been reported that TTR plays a potential neuroprotective role against Alzheimer's disease, one which is directly related to its stability (Alemi et al., 2017). The tetramer stabilizing effects of *C. asiatica* and *B. monnieri* suggest that they might by extension exert neuroprotective activities on Alzheimer's disease. It is expected that further research efforts centered on these botanicals will fully maximize their potential as prospective neuroprotective agents for ameliorating amyloidoses.

REFERNCES

Ackermann, E.J., Guo, S., Booten, S., Alvarado, L., Benson, M., Hughes, S., Monia, B.P., 2012. Clinical development of an antisense therapy for the treatment of transthyretin-associated polyneuropathy. Amyloid 19 Suppl 1, 43–44. https://doi.org/10.3109/13506129.2012.673140

Adams, D., Koike, H., Slama, M., Coelho, T., 2019. Hereditary transthyretin amyloidosis: a model of medical progress for a fatal disease. Nature Reviews Neurology 15, 387–404. https://doi.org/10.1038/s41582-019-0210-4

Adams, D., Théaudin, M., Cauquil, C., Algalarrondo, V., Slama, M., 2014. FAP neuropathy and emerging treatments. Curr Neurol Neurosci Rep 14, 435. https://doi.org/10.1007/s11910-013-0435-3

Alemi, M., Silva, S.C., Santana, I., Cardoso, I., 2017. Transthyretin stability is critical in assisting beta amyloid clearance- Relevance of transthyretin stabilization in Alzheimer's disease. CNS Neurosci Ther 23, 605–619. https://doi.org/10.1111/cns.12707

Alqahtani, A., Tongkao-on, W., Li, K.M., Razmovski-Naumovski, V., Chan, K., Li, G.Q., 2015. Seasonal Variation of Triterpenes and Phenolic Compounds in Australian Centella asiatica (L.) Urb. Phytochem Anal 26, 436–443. https://doi.org/10.1002/pca.2578

Ando, Y., Terazaki, H., Nakamura, M., Ando, E., Haraoka, K., Yamashita, T., Ueda, M., Okabe, H., Sasaki, Y., Tanihara, H., Uchino, M., Inomata, Y., 2004. A different amyloid formation mechanism: de novo oculoleptomeningeal amyloid deposits after liver transplantation. Transplantation 77, 345–349. https://doi.org/10.1097/01.TP.0000111516.60013.E6

Bartalena, L., Robbins, J., 1992. Variations in thyroid hormone transport proteins and their clinical implications. Thyroid 2, 237–245. https://doi.org/10.1089/thy.1992.2.237

Baures, P.W., Oza, V.B., Peterson, S.A., Kelly, J.W., 1999. Synthesis and evaluation of inhibitors of transthyretin amyloid formation based on the non-steroidal anti-inflammatory drug, flufenamic acid. Bioorg. Med. Chem. 7, 1339–1347. https://doi.org/10.1016/s0968-0896(99)00066-8

Bendeck, M.P., Conte, M., Zhang, M., Nili, N., Strauss, B.H., Farwell, S.M., 2002. Doxycycline modulates smooth muscle cell growth, migration, and matrix remodeling after arterial injury. Am. J. Pathol. 160, 1089–1095. https://doi.org/10.1016/S0002-9440(10)64929-2

Benson, M.D., Buxbaum, J.N., Eisenberg, D.S., Merlini, G., Saraiva, M.J.M., Sekijima, Y., Sipe, J.D., Westermark, P., 2018. Amyloid nomenclature 2018: recommendations by the International Society of Amyloidosis (ISA) nomenclature committee. Amyloid 25, 215–219. https://doi.org/10.1080/13506129.2018.1549825

Benson, M.D., Kincaid, J.C., 2007. The molecular biology and clinical features of amyloid neuropathy. Muscle Nerve 36, 411–423. https://doi.org/10.1002/mus.20821

Benson, M.D., Smith, R.A., Hung, G., Kluve-Beckerman, B., Showalter, A.D., Sloop, K.W., Monia, B.P., 2010. Suppression of choroid plexus transthyretin levels by antisense oligonucleotide treatment. Amyloid 17, 43–49. https://doi.org/10.3109/13506129.2010.483121

Berk, J.L., Suhr, O.B., Obici, L., Sekijima, Y., Zeldenrust, S.R., Yamashita, T., Heneghan, M.A., Gorevic, P.D., Litchy, W.J., Wiesman, J.F., Nordh, E., Corato, M., Lozza, A., Cortese, A., Robinson-Papp, J., Colton, T., Rybin, D.V., Bisbee, A.B., Ando, Y., Ikeda, S., Seldin, D.C., Merlini, G., Skinner, M., Kelly, J.W., Dyck, P.J., Diflunisal Trial Consortium, 2013. Repurposing diflunisal for familial amyloid polyneuropathy: a randomized clinical trial. JAMA 310, 2658–2667. https://doi.org/10.1001/jama.2013.283815

Blake, C.C., Geisow, M.J., Oatley, S.J., Rérat, B., Rérat, C., 1978. Structure of prealbumin: secondary, tertiary and quaternary interactions determined by Fourier refinement at 1.8 A. J. Mol. Biol. 121, 339–356. https://doi.org/10.1016/0022-2836(78)90368-6

Blancas-Mejía, L.M., Ramirez-Alvarado, M., 2013. Systemic amyloidoses. Annu. Rev. Biochem. 82, 745–774. https://doi.org/10.1146/annurev-biochem-072611-130030

Bulawa, C.E., Connelly, S., Devit, M., Wang, L., Weigel, C., Fleming, J.A., Packman, J., Powers, E.T., Wiseman, R.L., Foss, T.R., Wilson, I.A., Kelly, J.W., Labaudinière, R., 2012. Tafamidis, a potent and selective transthyretin kinetic stabilizer that inhibits the amyloid cascade. Proc. Natl. Acad. Sci. U.S.A. 109, 9629–9634. https://doi.org/10.1073/pnas.1121005109

Cardoso, I., Saraiva, M.J., 2006. Doxycycline disrupts transthyretin amyloid: evidence from studies in a FAP transgenic mice model. FASEB J. 20, 234–239. https://doi.org/10.1096/fj.05-4509com

Chaudhary, N., Sasaki, R., Shuto, T., Watanabe, M., Kawahara, T., Suico, M.A., Yokoyama, T., Mizuguchi, M., Kai, H., Devkota, H.P., 2019. Transthyretin Amyloid Fibril Disrupting Activities of Extracts and Fractions from Juglans mandshurica Maxim. var. cordiformis (Makino) Kitam. Molecules 24. https://doi.org/10.3390/molecules24030500

Cheng, C.L., Guo, J.S., Luk, J., Koo, M.W.L., 2004. The healing effects of Centella extract and asiaticoside on acetic acid induced gastric ulcers in rats. Life Sci. 74, 2237–2249. https://doi.org/10.1016/j.lfs.2003.09.055

Chomchalow, N., 2013. Curing Incurable Alzheimer's Disease with Medicinal Plants. AU Journal of Technology 16.

Coelho, T., Maia, L.F., Martins da Silva, A., Waddington Cruz, M., Planté-Bordeneuve, V., Lozeron, P., Suhr, O.B., Campistol, J.M., Conceição, I.M., Schmidt, H.H.-J., Trigo, P., Kelly, J.W., Labaudinière, R., Chan, J., Packman, J., Wilson, A., Grogan, D.R., 2012. Tafamidis for transthyretin familial amyloid polyneuropathy: a randomized, controlled trial. Neurology 79, 785–792. https://doi.org/10.1212/WNL.0b013e3182661eb1

Cohen, A.S., Calkins, E., 1959. Electron microscopic observations on a fibrous component in amyloid of diverse origins. Nature 183, 1202–1203. https://doi.org/10.1038/1831202a0

Costa, P.P., Figueira, A.S., Bravo, F.R., 1978. Amyloid fibril protein related to prealbumin in familial amyloidotic polyneuropathy. Proc. Natl. Acad. Sci. U.S.A. 75, 4499–4503. https://doi.org/10.1073/pnas.75.9.4499

Costa, R., Ferreira-da-Silva, F., Saraiva, M.J., Cardoso, I., 2008. Transthyretin protects against A-beta peptide toxicity by proteolytic cleavage of the peptide:

a mechanism sensitive to the Kunitz protease inhibitor. PLoS ONE 3, e2899. https://doi.org/10.1371/journal.pone.0002899

Dhanasekaran, M., Holcomb, L.A., Hitt, A.R., Tharakan, B., Porter, J.W., Young, K.A., Manyam, B.V., 2009. Centella asiatica extract selectively decreases amyloid beta levels in hippocampus of Alzheimer's disease animal model. Phytother Res 23, 14–19. https://doi.org/10.1002/ptr.2405

Dogan, A., 2015. Classification of Amyloidosis by Mass Spectrometry-Based Proteomics, in: Picken, M.M., Herrera, G.A., Dogan, A. (Eds.), Amyloid and Related Disorders: Surgical Pathology and Clinical Correlations, Current Clinical Pathology. Springer International Publishing, Cham, pp. 311–322. https://doi.org/10.1007/978-3-319-19294-9_23

Eisele, Y.S., Monteiro, C., Fearns, C., Encalada, S.E., Wiseman, R.L., Powers, E.T., Kelly, J.W., 2015. Targeting protein aggregation for the treatment of degenerative diseases. Nat Rev Drug Discov 14, 759–780. https://doi.org/10.1038/nrd4593

Ericzon, B.-G., Lundgren, E., Suhr, O.B., 2009. Liver Transplantation for Transthyretin Amyloidosis, in: Richardson, S.J., Cody, V. (Eds.), Recent Advances in Transthyretin Evolution, Structure and Biological Functions. Springer, Berlin, Heidelberg, pp. 239–260. https://doi.org/10.1007/978-3-642-00646-3_15

Ernst, O., Zor, T., 2010. Linearization of the Bradford Protein Assay. J Vis Exp. https://doi.org/10.3791/1918

Ferreira, N., Saraiva, M.J., Almeida, M.R., 2012. Epigallocatechin-3-gallate as a potential therapeutic drug for TTR-related amyloidosis: "in vivo" evidence from FAP mice models. PLoS ONE 7, e29933. https://doi.org/10.1371/journal.pone.0029933

Ferreira, N., Saraiva, M.J., Almeida, M.R., 2011. Natural polyphenols inhibit different steps of the process of transthyretin (TTR) amyloid fibril formation. FEBS Lett. 585, 2424–2430. https://doi.org/10.1016/j.febslet.2011.06.030

Florio, P., Folli, C., Cianci, M., Del Rio, D., Zanotti, G., Berni, R., 2015. Transthyretin Binding Heterogeneity and Anti-amyloidogenic Activity of Natural Polyphenols and Their Metabolites. J. Biol. Chem. 290, 29769–29780. https://doi.org/10.1074/jbc.M115.690172

Fong, V.-H., Vieira, A., 2013. Transthyretin aggregates induce production of reactive nitrogen species. Neurodegener Dis 11, 42–48. https://doi.org/10.1159/000338153

Fong, V.H., Vieira, A., 2013. Pro-oxidative effects of aggregated transthyretin in human Schwannoma cells. Neurotoxicology 39, 109–113. https://doi.org/10.1016/j.neuro.2013.08.013

Foss, T.R., Wiseman, R.L., Kelly, J.W., 2005. The pathway by which the tetrameric protein transthyretin dissociates. Biochemistry 44, 15525–15533. https://doi.org/10.1021/bi051608t

Gertz, M.A., Mauermann, M.L., Grogan, M., Coelho, T., 2019. Advances in the treatment of hereditary transthyretin amyloidosis: A review. Brain Behav 9. https://doi.org/10.1002/brb3.1371

Gray, N.E., Sampath, H., Zweig, J.A., Quinn, J.F., Soumyanath, A., 2015. Centella asiatica Attenuates Amyloid-β-Induced Oxidative Stress and Mitochondrial

Dysfunction. J. Alzheimers Dis. 45, 933–946. https://doi.org/10.3233/JAD-142217

Greenwald, J., Riek, R., 2010. Biology of amyloid: structure, function, and regulation. Structure 18, 1244–1260. https://doi.org/10.1016/j.str.2010.08.009

Gutteridge, A., Thornton, J., 2005. Conformational changes observed in enzyme crystal structures upon substrate binding. J. Mol. Biol. 346, 21–28. https://doi.org/10.1016/j.jmb.2004.11.013

Hammarström, P., Jiang, X., Deechongkit, S., Kelly, J.W., 2001. Anion shielding of electrostatic repulsions in transthyretin modulates stability and amyloidosis: insight into the chaotrope unfolding dichotomy. Biochemistry 40, 11453–11459. https://doi.org/10.1021/bi010673+

Hammarström, P., Jiang, X., Hurshman, A.R., Powers, E.T., Kelly, J.W., 2002. Sequence-dependent denaturation energetics: A major determinant in amyloid disease diversity. Proc. Natl. Acad. Sci. U.S.A. 99 Suppl 4, 16427–16432. https://doi.org/10.1073/pnas.202495199

Hammarström, P., Wiseman, R.L., Powers, E.T., Kelly, J.W., 2003. Prevention of transthyretin amyloid disease by changing protein misfolding energetics. Science 299, 713–716. https://doi.org/10.1126/science.1079589

Hirohata, M., Hasegawa, K., Tsutsumi-Yasuhara, S., Ohhashi, Y., Ookoshi, T., Ono, K., Yamada, M., Naiki, H., 2007. The anti-amyloidogenic effect is exerted against Alzheimer's beta-amyloid fibrils in vitro by preferential and reversible binding of flavonoids to the amyloid fibril structure. Biochemistry 46, 1888–1899. https://doi.org/10.1021/bi061540x

Hou, X., Parkington, H.C., Coleman, H.A., Mechler, A., Martin, L.L., Aguilar, M.-I., Small, D.H., 2007. Transthyretin oligomers induce calcium influx via voltage-gated calcium channels. J. Neurochem. 100, 446–457. https://doi.org/10.1111/j.1471-4159.2006.04210.x

Jacobson, D.R., McFarlin, D.E., Kane, I., Buxbaum, J.N., 1992. Transthyretin Pro55, a variant associated with early-onset, aggressive, diffuse amyloidosis with cardiac and neurologic involvement. Hum. Genet. 89, 353–356. https://doi.org/10.1007/bf00220559

Jiang, X., Smith, C.S., Petrassi, H.M., Hammarström, P., White, J.T., Sacchettini, J.C., Kelly, J.W., 2001. An engineered transthyretin monomer that is nonamyloidogenic, unless it is partially denatured. Biochemistry 40, 11442–11452. https://doi.org/10.1021/bi011194d

Johnson, S.M., Connelly, S., Fearns, C., Powers, E.T., Kelly, J.W., 2012. The Transthyretin Amyloidoses: From Delineating the Molecular Mechanism of Aggregation Linked to Pathology to a Regulatory Agency Approved Drug. J Mol Biol 421, 185–203. https://doi.org/10.1016/j.jmb.2011.12.060

Kawaji, T., Ando, Y., Hara, R., Tanihara, H., 2010. Novel therapy for transthyretin-related ocular amyloidosis: a pilot study of retinal laser photocoagulation. Ophthalmology 117, 552–555. https://doi.org/10.1016/j.ophtha.2009.07.042

Kelly, J.W., Colon, W., Lai, Z., Lashuel, H.A., McCulloch, J., McCutchen, S.L., Miroy, G.J., Peterson, S.A., 1997. Transthyretin quaternary and tertiary structural changes facilitate misassembly into amyloid. Adv. Protein Chem. 50, 161–181. https://doi.org/10.1016/s0065-3233(08)60321-6

Kelly, J.W., Lansbury, P.T., 1994. A chemical approach to elucidate tin mechanism of transthyretin and β-protein amyloid fibril formation. Amyloid 1, 186–205. https://doi.org/10.3109/13506129409148451

Kugimiya, T., Jono, H., Saito, S., Maruyama, T., Kadowaki, D., Misumi, Y., Hoshii, Y., Tasaki, M., Su, Y., Ueda, M., Obayashi, K., Shono, M., Otagiri, M., Ando, Y., 2011. Loss of functional albumin triggers acceleration of transthyretin amyloid fibril formation in familial amyloidotic polyneuropathy. Laboratory Investigation 91, 1219–1228. https://doi.org/10.1038/labinvest.2011.71

Kulkarni, R., Girish, K.J., Kumar, A., 2012. Nootropic herbs (Medhya Rasayana) in Ayurveda: An update. Pharmacogn Rev 6, 147–153. https://doi.org/10.4103/0973-7847.99949

Li, X., Zhang, X., Ladiwala, A.R.A., Du, D., Yadav, J.K., Tessier, P.M., Wright, P.E., Kelly, J.W., Buxbaum, J.N., 2013. Mechanisms of Transthyretin Inhibition of β-Amyloid Aggregation In Vitro. J Neurosci 33, 19423–19433. https://doi.org/10.1523/JNEUROSCI.2561-13.2013

Limpeanchob, N., Jaipan, S., Rattanakaruna, S., Phrompittayarat, W., Ingkaninan, K., 2008. Neuroprotective effect of Bacopa monnieri on beta-amyloid-induced cell death in primary cortical culture. J Ethnopharmacol 120, 112–117. https://doi.org/10.1016/j.jep.2008.07.039

Łojewski, M., Pomierny, B., Muszyńska, B., Krzyżanowska, W., Budziszewska, B., Szewczyk, A., 2016. Protective Effects of Bacopa Monnieri on Hydrogen Peroxide and Staurosporine: Induced Damage of Human Neuroblastoma SH-SY5Y Cells. Planta Med. 82, 205–210. https://doi.org/10.1055/s-0035-1558166

Macedo, B., Batista, A.R., Ferreira, N., Almeida, M.R., Saraiva, M.J., 2008. Anti-apoptotic treatment reduces transthyretin deposition in a transgenic mouse model of Familial Amyloidotic Polyneuropathy. Biochimica et Biophysica Acta (BBA) - Molecular Basis of Disease 1782, 517–522. https://doi.org/10.1016/j.bbadis.2008.05.005

Macedo, B., Magalhães, J., Batista, A.R., Saraiva, M.J., 2010. Carvedilol treatment reduces transthyretin deposition in a familial amyloidotic polyneuropathy mouse model. Pharmacol. Res. 62, 514–522. https://doi.org/10.1016/j.phrs.2010.08.001

Maquart, F.X., Bellon, G., Gillery, P., Wegrowski, Y., Borel, J.P., 1990. Stimulation of collagen synthesis in fibroblast cultures by a triterpene extracted from Centella asiatica. Connect. Tissue Res. 24, 107–120. https://doi.org/10.3109/03008209009152427

Maulidiani, Abas, F., Khatib, A., Shaari, K., Lajis, N.H., 2014. Chemical characterization and antioxidant activity of three medicinal Apiaceae species. Industrial Crops and Products 55, 238–247. https://doi.org/10.1016/j.indcrop.2014.02.013

Monaco, H.L., Rizzi, M., Coda, A., 1995. Structure of a complex of two plasma proteins: transthyretin and retinol-binding protein. Science 268, 1039–1041. https://doi.org/10.1126/science.7754382

Murakami, T., Ohsawa, Y., Zhenghua, L., Yamamura, K.-I., Sunada, Y., 2010. The transthyretin gene is expressed in Schwann cells of peripheral nerves. Brain Res. 1348, 222–225. https://doi.org/10.1016/j.brainres.2010.06.017

Naiki, H., Hasegawa, K., Ono, K., Yamada, M., 2010. [Search for antiamyloidogenic compounds based on a nucleation-dependent polymerization model]. Yakugaku Zasshi 130, 503–509. https://doi.org/10.1248/yakushi.130.503

Nathan, P.J., Clarke, J., Lloyd, J., Hutchison, C.W., Downey, L., Stough, C., 2001. The acute effects of an extract of Bacopa monniera (Brahmi) on cognitive function in healthy normal subjects. Hum Psychopharmacol 16, 345–351. https://doi.org/10.1002/hup.306

Nuengchamnong, N., Sookying, S., Ingkaninan, K., 2016. LC-ESI-QTOF-MS based screening and identification of isomeric jujubogenin and pseudojujubogenin aglycones in Bacopa monnieri extract. J Pharm Biomed Anal 129, 121–134. https://doi.org/10.1016/j.jpba.2016.06.052

Ortore, G., Orlandini, E., Braca, A., Ciccone, L., Rossello, A., Martinelli, A., Nencetti, S., 2016. Targeting Different Transthyretin Binding Sites with Unusual Natural Compounds. ChemMedChem 11, 1865–1874. https://doi.org/10.1002/cmdc.201600092

Pinto, M., Blasi, D., Nieto, J., Arsequell, G., Valencia, G., Planas, A., Quintana, J., Centeno, N.B., 2011. Ligand-binding properties of human transthyretin. Amyloid 18 Suppl 1, 51–54. https://doi.org/10.3109/13506129.2011.574354018

Popovych, N., Brender, J.R., Soong, R., Vivekanandan, S., Hartman, K., Basrur, V., Macdonald, P.M., Ramamoorthy, A., 2012. Site Specific Interaction of the Polyphenol EGCG with the SEVI Amyloid Precursor Peptide PAP(248–286). J Phys Chem B 116, 3650–3658. https://doi.org/10.1021/jp2121577

Powers, E.T., Morimoto, R.I., Dillin, A., Kelly, J.W., Balch, W.E., 2009. Biological and chemical approaches to diseases of proteostasis deficiency. Annu. Rev. Biochem. 78, 959–991. https://doi.org/10.1146/annurev.biochem.052308.114844

Prapunpoj, P., Leelawatwattana, L., 2009. Evolutionary changes to transthyretin: structure-function relationships. FEBS J. 276, 5330–5341. https://doi.org/10.1111/j.1742-4658.2009.07243.x

Pullakhandam, R., Srinivas, P.N.B.S., Nair, M.K., Reddy, G.B., 2009. Binding and stabilization of transthyretin by curcumin. Arch. Biochem. Biophys. 485, 115–119. https://doi.org/10.1016/j.abb.2009.02.013

Purkey, H.E., Dorrell, M.I., Kelly, J.W., 2001. Evaluating the binding selectivity of transthyretin amyloid fibril inhibitors in blood plasma. Proc. Natl. Acad. Sci. U.S.A. 98, 5566–5571. https://doi.org/10.1073/pnas.091431798

Redondo, C., Damas, A.M., Olofsson, A., Lundgren, E., Saraiva, M.J., 2000. Search for intermediate structures in transthyretin fibrillogenesis: soluble tetrameric Tyr78Phe TTR expresses a specific epitope present only in amyloid fibrils. J. Mol. Biol. 304, 461–470. https://doi.org/10.1006/jmbi.2000.4220

Refai, E., Dekki, N., Yang, S.-N., Imreh, G., Cabrera, O., Yu, L., Yang, G., Norgren, S., Rössner, S.M., Inverardi, L., Ricordi, C., Olivecrona, G., Andersson, M., Jörnvall, H., Berggren, P.-O., Juntti-Berggren, L., 2005. Transthyretin constitutes a functional component in pancreatic beta-cell stimulus-secretion coupling. Proc. Natl. Acad. Sci. U.S.A. 102, 17020–17025. https://doi.org/10.1073/pnas.0503219102

Reixach, N., Adamski-Werner, S.L., Kelly, J.W., Koziol, J., Buxbaum, J.N., 2006. Cell based screening of inhibitors of transthyretin aggregation. Biochem. Biophys. Res. Commun. 348, 889–897. https://doi.org/10.1016/j.bbrc.2006.07.109

Reixach, N., Deechongkit, S., Jiang, X., Kelly, J.W., Buxbaum, J.N., 2004. Tissue damage in the amyloidoses: Transthyretin monomers and nonnative oligomers are the major cytotoxic species in tissue culture. Proc. Natl. Acad. Sci. U.S.A. 101, 2817–2822. https://doi.org/10.1073/pnas.0400062101

Rios, X., Gómez-Vallejo, V., Martín, A., Cossío, U., Morcillo, M.Á., Alemi, M., Cardoso, I., Quintana, J., Jiménez-Barbero, J., Cotrina, E.Y., Valencia, G., Arsequell, G., Llop, J., 2019. Radiochemical examination of transthyretin (TTR) brain penetration assisted by iododiflunisal, a TTR tetramer stabilizer and a new candidate drug for AD. Sci Rep 9, 13672. https://doi.org/10.1038/s41598-019-50071-w

Russo, A., Borrelli, F., 2005. Bacopa monniera, a reputed nootropic plant: an overview. Phytomedicine 12, 305–317. https://doi.org/10.1016/j.phymed.2003.12.008

Sant'anna, R.O., Braga, C.A., Polikarpov, I., Ventura, S., Lima, L.M.T.R., Foguel, D., 2013. Inhibition of human transthyretin aggregation by non-steroidal anti-inflammatory compounds: a structural and thermodynamic analysis. Int J Mol Sci 14, 5284–5311. https://doi.org/10.3390/ijms14035284

Schwarzman, A.L., Gregori, L., Vitek, M.P., Lyubski, S., Strittmatter, W.J., Enghilde, J.J., Bhasin, R., Silverman, J., Weisgraber, K.H., Coyle, P.K., 1994. Transthyretin sequesters amyloid beta protein and prevents amyloid formation. Proc. Natl. Acad. Sci. U.S.A. 91, 8368–8372. https://doi.org/10.1073/pnas.91.18.8368

Schwarzman, A.L., Tsiper, M., Wente, H., Wang, A., Vitek, M.P., Vasiliev, V., Goldgaber, D., 2004. Amyloidogenic and anti-amyloidogenic properties of recombinant transthyretin variants. Amyloid 11, 1–9. https://doi.org/10.1080/13506120410001667458

Sekijima, Y., 2014. Recent progress in the understanding and treatment of transthyretin amyloidosis. J Clin Pharm Ther 39, 225–233. https://doi.org/10.1111/jcpt.12145

Singh, R.H., Narsimhamurthy, K., Singh, G., 2008. Neuronutrient impact of Ayurvedic Rasayana therapy in brain aging. Biogerontology 9, 369–374. https://doi.org/10.1007/s10522-008-9185-z

Sipe, J.D., Benson, M.D., Buxbaum, J.N., Ikeda, S., Merlini, G., Saraiva, M.J.M., Westermark, P., 2014. Nomenclature 2014: Amyloid fibril proteins and clinical classification of the amyloidosis. Amyloid 21, 221–224. https://doi.org/10.3109/13506129.2014.964858

Sivaramakrishna, C., Rao, C.V., Trimurtulu, G., Vanisree, M., Subbaraju, G.V., 2005. Triterpenoid glycosides from Bacopa monnieri. Phytochemistry 66, 2719–2728. https://doi.org/10.1016/j.phytochem.2005.09.016

Skinner, M., Shirahama, T., Cohen, A.S., Deal, C.L., 1982. The association of amyloid P-component (AP) with the amyloid fibril: an updated method for amyloid fibril protein isolation. Prep. Biochem. 12, 461–476. https://doi.org/10.1080/10826068208070597

Sousa, M.M., Cardoso, I., Fernandes, R., Guimarães, A., Saraiva, M.J., 2001. Deposition of transthyretin in early stages of familial amyloidotic polyneuropathy: evidence for toxicity of nonfibrillar aggregates. Am. J. Pathol. 159, 1993–2000. https://doi.org/10.1016/s0002-9440(10)63050-7

Sousa, M.M., Norden, A.G., Jacobsen, C., Willnow, T.E., Christensen, E.I., Thakker, R.V., Verroust, P.J., Moestrup, S.K., Saraiva, M.J., 2000. Evidence for the role of megalin in renal uptake of transthyretin. J. Biol. Chem. 275, 38176–38181. https://doi.org/10.1074/jbc.M002886200

Sousa, M.M., Saraiva, M.J., 2003. Neurodegeneration in familial amyloid polyneuropathy: from pathology to molecular signaling. Prog. Neurobiol. 71, 385–400. https://doi.org/10.1016/j.pneurobio.2003.11.002

Stough, C., Lloyd, J., Clarke, J., Downey, L.A., Hutchison, C.W., Rodgers, T., Nathan, P.J., 2001. The chronic effects of an extract of Bacopa monniera (Brahmi) on cognitive function in healthy human subjects. Psychopharmacology (Berl.) 156, 481–484. https://doi.org/10.1007/s002130100815

Ueda, M., Ando, Y., 2014. Recent advances in transthyretin amyloidosis therapy. Transl Neurodegener 3, 19. https://doi.org/10.1186/2047-9158-3-19

Vrana, J.A., Gamez, J.D., Madden, B.J., Theis, J.D., Bergen, H.R., Dogan, A., 2009. Classification of amyloidosis by laser microdissection and mass spectrometry-based proteomic analysis in clinical biopsy specimens. Blood 114, 4957–4959. https://doi.org/10.1182/blood-2009-07-230722

Westermark, G.T., Westermark, P., 2008. Transthyretin and amyloid in the islets of Langerhans in type-2 diabetes. Exp Diabetes Res 2008, 429274. https://doi.org/10.1155/2008/429274

Yokoyama, T., Kosaka, Y., Mizuguchi, M., 2014. Inhibitory activities of propolis and its promising component, caffeic acid phenethyl ester, against amyloidogenesis of human transthyretin. J. Med. Chem. 57, 8928–8935. https://doi.org/10.1021/jm500997m

Zhao, L., Buxbaum, J.N., Reixach, N., 2013. Age-related oxidative modifications of transthyretin modulate its amyloidogenicity. Biochemistry 52, 1913–1926. https://doi.org/10.1021/bi301313b

biomolecules

MDPI

Article

Structural Stabilization of Human Transthyretin by *Centella asiatica* (L.) Urban Extract: Implications for TTR Amyloidosis

Fredrick Nwude Eze, Ladda Leelawatwattana and Porntip Prapunpoj *

Department of Biochemistry, Faculty of Science, Prince of Songkla University, Hat Yai, Songkhla 90112, Thailand; fredrickeze@rocketmail.com (F.N.E.); ladda.l@psu.ac.th (L.L.)

* Correspondence: porntip.p@psu.ac.th; Tel.: +66-74-288275

Received: 4 February 2019; Accepted: 21 March 2019; Published: 29 March 2019

Abstract: Transthyretin is responsible for a series of highly progressive, degenerative, debilitating, and incurable protein misfolding disorders known as transthyretin (TTR) amyloidosis. Since dissociation of the homotetrameric protein to its monomers is crucial in its amyloidogenesis, stabilizing the native tetramer from dissociating using small-molecule ligands has proven a viable therapeutic strategy. The objective of this study was to determine the potential role of the medicinal herb *Centella asiatica* on human transthyretin (huTTR) amyloidogenesis. Thus, we investigated the stability of huTTR with or without a hydrophilic fraction of *C. asiatica* (CAB) against acid/urea-mediated denaturation. We also determined the influence of CAB on huTTR fibrillation using transmission electron microscopy. The potential binding interactions between CAB and huTTR was ascertained by nitroblue tetrazolium redox-cycling and 8-anilino-1-naphthalene sulfonic acid displacement assays. Additionally, the chemical profile of CAB was determined by liquid chromatography quadruple time-of-flight mass spectrometry (HPLC-QTOF-MS). Our results strongly suggest that CAB bound to and preserved the quaternary structure of huTTR in vitro. CAB also prevented transthyretin fibrillation, although aggregate formation was unmitigated. These effects could be attributable to the presence of phenolics and terpenoids in CAB. Our findings suggest that *C. asiatica* contains pharmaceutically relevant bioactive compounds which could be exploited for therapeutic development against TTR amyloidosis.

Keywords: transthyretin; TTR amyloidosis; protein misfolding; neuroprotection; *Centella asiatica*; antioxidants; triterpenoids; phenolics; HPLC-MS

1. Introduction

Misfolding and/or aggregation of proteins is at the heart of the etiopathogenesis of a group of debilitating disorders referred to as amyloidosis [1]. Many of these diseases such as Parkinson's disease, Huntington's, Alzheimer's, and transthyretin (TTR) amyloidosis are still incurable. As a result, a lot of investigative effort is focused on developing effective, safe, and reliable therapeutic agents.

In humans, TTR amyloidosis is a group of proteinopathies triggered by partial unfolding, misfolding, aggregation, and accumulation of TTR into a spectrum of cytotoxic aggregates [2]. Under normal physiological circumstances, TTR is a homotetrameric protein that transports thyroid hormones and retinol A via its interaction with a holo-retinol-binding protein [3]. In mature adults, a late-onset acquired TTR amyloidosis also known as senile systemic amyloidosis (SSA) is caused by the accumulation of wild-type in organs. SSA affects at least 25% of octogenarians, accounts for more than 10% of heart failure with preserved fraction [4], and is associated with the development of congestive heart failure [5,6]. Accumulation of variant TTR precipitates familial TTR amyloidosis, such as familial amyloidosis cardiomyopathy (TTR-FAC) [5], familial amyloidotic polyneuropathy (TTR-FAP), and

central nervous system selective amyloidosis (CNSA) [7]. Onset for familial TTR amyloidosis could occur within the second decade of life depending on the TTR mutant involved. TTR amyloidosis can be very progressive and debilitating with mortality within the first 10 to 15 years of onset [8]. Orthotopic liver transplantation, with several limitations including highly invasive, unsuitability of patients, lack of donors, etc., is still the primary form of disease-modifying therapy for most TTR-FAP patients. Recently, the disease-modifying drug, Tafamidis, was approved for treating TTR-FAP [9]. However, in a just-concluded long-term study, it was observed that the slow progression of neuropathy in TTR-FAP patients could not be prevented by Tafamidis [10]. Thus, it is pertinent to search for safe, more effective, and less invasive therapeutic alternatives.

Although the current understanding of the molecular pathophysiology underlying TTR amyloidosis is still incomplete, it is widely regarded that tetramer dissociation into monomers is the initial and consequential step in its amyloidogenesis [11,12]. Thus, preventing tetramer dissociation by enhancing its kinetic stability has been proposed as an effective therapeutic strategy [8]. The kinetic stabilization strategy involves the use of small-molecule ligands to prevent conformational excursions of the native tetramer by binding to its thyroxine (T4)-binding sites [8]. Kinetic stabilization of TTR tetramers formed the rational basis for the development of the TTR-FAP drug, Tafamidis [13].

Native wild-type TTR, while significantly stable under normal physiological conditions [14], is susceptible to oxidative modifications, which could alter its conformation and stability [15]. The role of protein oxidation was noted in the increased amyloidogenicity of nitric oxide-modified TTR but not in unmodified TTR [15]. Also, age-associated oxidation of TTR reportedly impacts the onset of senile systemic amyloidosis [16]. Furthermore, while prefibrillar and mature TTR amyloid fibrils were not or less cytotoxic, all forms of oxidized native TTR were shown to be cytotoxic [2,16]. This backdrop highlights the role of oxidative damage in TTR amyloidogenesis and prompted the notion that, in addition to kinetic stabilizers, antioxidant treatment could be considered as an alternative/supplement therapy. Interestingly, most of the natural bioactives that have been reported to stabilize TTR such as quercetin, epigallocatechin gallate (EGCG), gallic acid, curcumin, and propolis extract are also potent antioxidants [17,18].

In addition, it has been noted that the protective effect exerted by antioxidants in chronic and neurodegenerative diseases in vivo is derived mainly from the additive, synergistic, and complementary effects of the several bioactive constituents present in the phytocomplex, such as plant extracts, fruits, and vegetables, rather than individual phytocomponents [19]. The antioxidant activity of medicinal plant extracts was also found to strongly correlate with their ability to limit the assembly of beta-amyloid, which is central to Alzheimer's disease pathology [20]. For a multifactorial disease with a complex pathology such as TTR amyloidosis, plant extracts or products could provide potential multi-target therapeutic agents.

Centella asiatica is a small, succulent, and herbaceous plant popular in several parts of the world for its medicinal and culinary value. It is indigenous to the tropical and subtropical regions of Asia, Africa, and the southern parts of the USA. In Thailand, it is known locally as Bua-bok and is used for making a very popular herbal drink, Nam Bai Bua Bok. The fresh aerial parts are eaten with rice and are part of many local food recipes. In folk medicine, *C. asiatica* is a popular nervine and adaptogen. It is used for wound healing, treatment of neurological disorders, and promoting general wellbeing [21]. The major bioactive components of *C. asiatica* are a group of pentacyclic triterpenoids known as centellosides. In addition, *C. asiatica* is richly endowed with phenolics and flavonoids [22]. *C. asiatica* reportedly has many pharmacological and biological effects including antioxidant, anti-inflammatory, inhibition of β amyloid peptide aggregation and toxicity, and anti-α-synuclein aggregation [23,24]. Despite these reports, currently, there is no data on its potential pharmacological effect on TTR amyloidogenesis. Together with its rich phytochemical and good safety profile, we decided to investigate the potential role of *C. asiatica* in the modulation huTTR amyloidogenesis.

Thus, we examined the impact of a hydrophilic fraction of *C. asiatica* (CAB) on native huTTR structural stability and fibril formation using urea/acid-mediated denaturation assays, and transmission

electron microscopy, respectively. We also determined the plausible binding interactions of CAB-huTTR complex and the chemical properties CAB. The present results provide relevant insight into the neuroprotective potential of *C. asiatica*, specifically, with regards to TTR amyloidosis.

2. Materials and Methods

2.1. Purification of huTTR from Plasma

Human TTR from plasma was isolated in a two-step protocol which consisted of a decrease in albumin burden and followed by preparative discontinuous native-PAGE as previously described [25,26]. The eluting fractions were monitored for the presence of huTTR by 10% native-PAGE. Protein bands were detected by silver staining. Fractions containing only huTTR were pooled, concentrated, and checked for purity by SDS-PAGE with Coomassie blue R-250 staining. The concentration of purified huTTR was determined by the Bradford assay [27] and stored at −20 °C.

2.2. Preparation of CAB

C. asiatica was obtained locally in Hat Yai city, Southern Thailand. The identity of the whole plant specimen was authenticated by Associate Professor Dr. Kitichate Sridith, Curator-in-Chief of the National Herbarium at Prince of Songkla University, Hat Yai, Thailand. A specimen was deposited in the herbarium with voucher number F.N.1 (PSU). Plant aerial parts were repeatedly washed with tap water followed by reverse osmosis water. The plant sample was air-dried for 12 h to reduce moisture content and then oven-dried at 60 °C for another 12 h. Dried *C. asiatica* was ground into a fine powder and stored in an opaque container at −20 °C for extraction within 24 h.

C. asiatica powder (450 g) was extracted with 2 L of cold acetone/methanol/water (2:2:1 *v*/*v*/*v*) containing 0.5% glacial acetic acid for 2 h as previously reported [28]. The plant mixture was filtered through a Buchner funnel overlaid with filter paper (Whatman No. 1) using a vacuum pump. The filtrate was concentrated to one-third of its original volume by a rotary evaporator at a temperature of 40 °C. Thereafter, the filtrate was defatted by partitioning in an equal volume of n-hexane twice, using a separatory funnel. The lower phase was further partitioned in dichloromethane twice to remove chlorophyll, waxes, and other less polar components. The upper hydrophilic phase in the separatory funnel was collected and residual organic solvents were removed under vacuum by speed-vac to remove residual organic solvents, and then lyophilized to a hygroscopic powder. This powder obtained from the hydrophilic fraction of *C. asiatica* was hereafter referred to as CAB (*C. asiatica* bioactives). CAB was aliquoted into opaque vials and stored at −20 °C. The scheme for CAB preparation is shown in Figure S2.

2.3. Nitroblue Tetrazolium (NBT) Redox-Cycling Assay

The binding of CAB to huTTR was determined by NBT staining which distinguishes quinone-modified from unmodified proteins [29]. Human TTR (2.1 μg/μL) in 50 mM Tris-HCl pH 7.5 was incubated in the presence of CAB or gallic acid (GA), or DMSO (vehicle), at 10× the molar equivalent of human TTR concentration. The samples were mixed with sample buffer containing 4% SDS and immediately boiled for 10 min prior to separation by SDS-PAGE (15% resolving gel). The gel was electrotransferred onto a nitrocellulose membrane. After transfer, the membrane was stained with Ponceau S dye (0.1% Ponceau S in 5% acetic acid) for 1 h to confirm blotting. Subsequently, the membrane was washed with distilled water, Tris-buffered saline with Tween 20 (TBS-T) and rinsed with Milli-Q water to remove the Ponceau S stain. Then, it was re-stained with glycinate/NBT solution (10 mg NBT tablet in 14 mL of 2 M potassium glycinate buffer, pH 10) for 45 min to identify proteins that interacted with phenolics or related compounds.

2.4. Determination of the Stability of huTTR in the Presence of CAB

TTR tetramer dissociation into monomeric subunits is quite slow under normal physiological pH. However, dissociation of TTR tetramer and subsequent misfolding of monomers is significantly increased in vitro under conditions of high urea concentration or mild acidity [14]. Resistance to urea-induced or acid-induced dissociation of TTR tetramer to monomers provides insight into the stability of native TTR against the partial denaturation of monomers required for amyloidogenesis. This is because tetramer dissociation precedes monomer unfolding and misfolding [30]. Purified huTTR in 50 mM Tris-HCl buffer pH 7.5 was dialyzed against 10 mM sodium phosphate buffer containing 100 mM KCl and 1 mM ethylenediamine tetraacetic acid (EDTA), pH 7.4 (GF buffer) for 24 h with 3 buffer changes prior to stability assays as follows.

2.4.1. Against Urea-Mediated Denaturation

The influence of CAB on huTTR stability against urea-mediated dissociation was evaluated as previously described [31]. In brief, huTTR (1 µg) in a GF buffer, pH 7.4 was supplemented with CAB (100× molar equivalents with respect to huTTR) dissolved in GF buffer containing DMSO, 50:50 *v*/*v* (GMSO) or GMSO only, and incubated for 2 h at 37 °C. Denaturation was triggered by adding urea (in GF buffer containing 1 mM 1,4-Dithiothreitol, pH 7.4) into the protein complex to a final concentration of 7 M and subsequently incubating for 96 h at ~6 °C in the dark. Folded huTTR (i.e., tetramers, trimers, and dimers) that remained after the denaturation was determined by 14% Tricine SDS-PAGE. The running buffer contained 0.025% SDS and the sample loading buffer 0.2% SDS. It has been suggested that these detergent concentrations are enough to prevent monomer reassociation, but too low to trigger tetramer dissociation [32]. Resolved proteins were identified by staining with Coomassie brilliant blue R-250 dye (0.1%) solution. Bands representing folded huTTR on the gel were quantified by densitometry using gel documentation on LabWorks 4.0 software (UVP Ltd., Cambridge, UK). The relative percentage of folded huTTR that remained after denaturation was calculated as an indication of native huTTR stability.

2.4.2. Against Acid-Mediated Denaturation

The effect of CAB on the stability of huTTR under mildly acidic conditions was performed as described previously [33]. Briefly, huTTR (0.5 µg/uL) in a GF buffer, pH 7.4 was supplemented with or without 100× molar excess of CAB followed by incubation for 2 h at 37 °C. Tetramer dissociation was initiated by reducing the pH of the reaction mixture to 4.0 by adding an equal volume of acetate/acetic acid buffer containing 100 mM KCl, 1 mM EDTA, and 2 mM dithiothreitol (DTT), pH 4.0. Thereafter, the protein complex was incubated at 37 °C for 14 days in the dark and under aseptic condition. Glutaraldehyde cross-linking assay was performed to determine the amount and quaternary structure of huTTR that remained after 14 days of denaturation stress. Briefly, glutaraldehyde was added to the protein complex to a final concentration of 2.5%, and the assay mixture was incubated for 4 min at room temperature. Cross-linking was terminated by the addition of $NaBH_4$ (7% in 0.1 M NaOH) at an equal volume to glutaraldehyde. Then, the mixture was mixed with 4x loading buffer containing 8% SDS and 5% beta-mercaptoethanol and boiled for 10 min prior to analysis by 10% Tricine SDS-PAGE. The separated protein bands were visualized by Coomassie blue staining. The intensity of the tetrameric form of huTTR was quantified by densitometry using gel documentation. The stability of huTTR was inferred from the relative percentage of tetramer that remained after denaturation.

2.5. Determination of 8,1-ANS Binding Displacement from huTTR by CAB

Fluorophore, 8-anilino-1-naphthalene sulfonic acid (8,1-ANS), reportedly binds at the T4-binding site of native huTTR in solution [34]. Thus, its displacement by small-molecule ligands is often used to probe for ligand binding to the T4-binding site of TTR tetramer [33]. To perform 8,1-ANS binding-displacement assay, huTTR (0.055 µg/µL) was incubated in the presence or absence of 8,1-ANS,

(10 μM) for 10 min, followed by the addition of CAB at 25× and 50× molar equivalents with respect to human TTR. To measure fluorescence, protein samples were excited at 385/40 and emission was collected at 480/20 using a Synergy HT (Bio-Tek Instruments, Winooski, VT, USA) microplate reader.

2.6. Determination of the Influence of CAB on huTTR Fibrillation by Transmission Electron Microscopy (TEM)

TEM was used to study the impact of CAB on huTTR fibril formation as previously described [35]. Human TTR (1 μg/μL) in a GF buffer was supplemented with or without CAB (20× molar equivalents with respect to huTTR). The mixture was subsequently incubated for 2 h at 37 °C to facilitate binding. Fibril formation was initiated by reducing pH to 4.0, via the addition of an equal volume of acetate buffer (pH, 4.0) to the mixture, and followed by incubation at 37 °C for 7 days. The extent of aggregate and fibril formation was ascertained by TEM of the TTR mixtures. In brief, aliquots of the TTR mixtures were diluted with Milli-Q water (1:20, *v*/*v*). A drop (~10 μL) of the solution was applied onto a 400-mesh formvar-coated copper grid for 1 min. Excess sample was removed with a wedge of filter paper. The grid was immediately rinsed with a drop of Milli-Q water, dried, and negatively stained with 2% uranyl acetate in 70% methanol for 2 min. Excess stain was blotted out and the grid was thoroughly air-dried. TEM images were obtained with a JEM-2010 (JEOL Ltd., Akishima, Tokyo, Japan) electron microscope, running at 160 KV.

2.7. Determination of CAB Antioxidant Properties

2.7.1. DPPH (1,1-Diphenyl-2-picrylhydrazyl) Radical Scavenging Activity

CAB was tested for its scavenging effect on DPPH radical following the method as described [36]. CAB was prepared in 50% aqueous methanol while Trolox (purchased from Aldrich Chemical Company, Steinheim, Germany) was prepared in distilled water and served as an antioxidant standard. CAB or Trolox solution (10 μL) was diluted with methanol (140 μL), and then DPPH solution in methanol (150 μL, 0.1 mM) was added. The reaction mixture in which CAB was replaced with aqueous methanol and Trolox was replaced with distilled water were included as controls. Blank probes contained methanol (290 μL) and 10 μL of CAB or Trolox. Blank probes for controls contained only methanol (300 μL). Sample and control reactions were incubated for 30 min before reading absorbance at 515 nm. After blank correction, DPPH radical scavenging activity (%) was obtained from the equation:

$$\text{inhibition (\%)} = (\text{absorbance of control} - \text{absorbance of sample})/\text{absorbance of sample} \times 100 \quad (1)$$

A curve was plotted for inhibition versus concentration. The antioxidant activity of CAB and Trolox was obtained from the curve and expressed as the concentration that scavenged the DPPH radical by 50% (IC_{50}) in a mean ± standard deviation of triplicates determination.

2.7.2. Ferric Reducing Antioxidant Power (FRAP)

The reducing power of CAB was determined by FRAP assay as described by [37]. FRAP solution containing 300 mM acetate buffer pH 3.6, 10 mM TPTZ 2,4,6-Tri(2-pyridyl)-s-triazine (TPTZ) solution, and 20 mM $FeCl_3.6H_2O$ solution (10:1:1, *v*/*v*/*v*) was prepared and incubated for 30 min at 37 °C. CAB solution was prepared by diluting the powder with 50% aqueous methanol. Trolox (up to 600 μmol/L) was included as the antioxidant standard for calibration. The assay was performed in a 96-well plate. Aliquots (10 μL) of CAB solution or Trolox solution were mixed with FRAP solution (200 μL) and incubated for 30 min at 37 °C. Then, absorbance was monitored at 650 nm. CAB antioxidant activity was expressed as a micromole of Trolox equivalents per gram of CAB. The higher the FRAP value, the stronger the reducing potential.

2.8. Determination of the Chemical Composition of CAB

2.8.1. Total Phenolic Content

The phenolic content in CAB was determined using the Folin–Ciocalteu assay with slight modification [38]. CAB solution (10 µg/µL) and gallic acid (GA; 1 µg/µL) in DMSO/methanol (10:90, *v*/*v*) were prepared in which the latter was used as a standard. Aliquot (100 µL) of CAB solution, blank or standard solution (from 0 to 80 µg), was added into test tubes. Then, 200 µL of Folin–Ciocalteu reagent (10%) was added and vortexed. After 5 min of incubation, 800 µL of Na_2CO_3 (700 mM) was added and vortexed. The assay mixture was incubated in the dark at room temperature for 2 h. Then, 200 µL of the blue mixture formed was transferred into a 96-well microplate and absorbance was measured at 765 nm, using a Synergy HT microplate reader (Bio-Tek Instruments, Winooski, VT, US). A plot of the amount of gallic acid (µg) versus absorbance at 765 nm was prepared and used to obtain the total phenolic content of the CAB. Linearity for the gallic acid standard curve for determining phenolic content was obtained between 0 and 20 µg. Data obtained from quadruplicates were reported as mean ± standard error of the mean and expressed in milligrams of gallic acid equivalent per gram of CAB.

2.8.2. Total Flavonoid Content

Total flavonoid content of CAB was determined by the aluminum chloride colorimetric assay with slight modifications as previously described [39]. CAB solution (10 µg/µL) was prepared in 50% aqueous methanol, and quercetin standard (1 µg/µL) was prepared in 100% methanol. CAB or quercetin solution (30 µL) was diluted with 160 µL of methanol and subsequently mixed with 10% aluminum chloride (30 µL) and 1 M sodium acetate (30 µL) in a total volume of 1100 µL of the assay. The mixture was vortexed and subsequently incubated in the dark for 30 min. Absorbance was read at 415 nm. Sample and standard solutions were prepared in quadruplicates. The calibration curve of the absorbance versus concentration of quercetin standard was plotted and used to calculate total flavonoid content of which was expressed as the mean ± standard error in milligrams of quercetin equivalents per gram of CAB.

2.8.3. Thin-Layer Chromatography (TLC) Profile of CAB

To determine the major phytoconstituents present in CAB, TLC was conducted on aluminum-backed silica gel 60 NH_2 F_{254S} TLC plates (Merck Millipore, Darmstadt Germany). CAB was reconstituted in methanol/water/acetic acid (100:10:4, *v*/*v*/*v*) and 5 µL (~300 µg) of CAB solution was spotted on a TLC plate, and the plate was transferred to a glass jar lined with filter paper and saturated for 30 min with developing solvent containing water/acetic acid/formic acid/ethyl acetate (5:1:1:17, *v*/*v*/*v*/*v*). The separation was terminated after the solvent front had migrated about 8 cm from the origin, and the plate was dried up in a fume hood to remove any residual solvent. One plate was stained with *p*-Anisaldehyde-sulfuric acid reagent, another was dipped into 3% ferric chloride reagent, and the third was sprayed with 2% $AlCl_3$ in methanol after saturation with ammonia solution. All plates were observed under visible light and ultraviolet light (254 and 366 nm) before and after derivatization, respectively.

2.8.4. High-Performance Liquid Chromatography-Mass Spectrometry (HPLC-MS) Fingerprint of CAB

LC-MS analysis of CAB was performed as previously described [40]. The sample was resuspended in methanol and filtered through a 0.22 µm nylon membrane. Separation of analyte was performed with a Poroshell 120 EC-C18 column (4.6 × 150 mm, 2.7 µm), Agilent Technologies. The solvent system consisted of water (as eluent A) and acetonitrile (as eluent B). Both eluents contained formic acid (0.1% *v*/*v*). The flow rate was maintained at 0.3 mL/min. The gradient employed for the separation was as follows: 0% B, 0–5 min; then increased linearly to 80% B, 5–50 min; maintained at 80% B, 50–53 min; then returned to 0% B, 53–55 min; and finally, re-equilibrated in 0% B, 55–60 min. The stream of separated components was channeled into a micrOTOF-QII™ESI-Qq-TOF mass spectrometer (Bruker

Daltonics, Bremen, Germany) equipped with an electrospray ionization source. Ions were detected in the negative mode within a mass range of 50–1500 Da. Parameters set for mass spectra acquisition included a capillary voltage of 3500 V, nebulizer pressure of 2.0 Bar, drying gas of 8.0 L/min, and drying temperature of 180 °C. Sodium formate solution (10 mM) was used as a calibration standard to ensure that the mass/charge ratios recorded by the instrument were indeed accurate. Data acquisition was performed on Bruker Compass DataAnalysis 4.0 software (Bruker Daltonics, Bremen, Germany). Tentative identity of compounds was established by comparing the accurate mass measurements obtained with previously identified compounds in *C. asiatica* reported in literature and online databases including METLIN and ChemSpider.

2.9. Statistical Analysis

Data of the huTTR stability assays were presented as the mean ± standard error of the mean (SEM). The percentages of folded huTTR or tetramers preincubated with or without CAB that remained after denaturation stress were compared using ANOVA followed by the Tukey–Kramer test. Differences were considered statistically significant at $p < 0.05$.

3. Results

3.1. CAB Directly Binds to huTTR

To determine whether CAB binds directly to huTTR purified from human plasma (Figure S1), we used nitroblue tetrazolium (NBT) redox-cycling staining [35]. Some natural product components, especially phenolics and related compounds, reportedly auto-oxidize into quinones which can interact with nucleophilic centers in protein such as the sulfhydryl group of a cysteine residue [41]. Under alkaline pH conditions (for example, in the presence of NBT/potassium-glycinate solution, pH 10), such quinoprotein adducts formed undergo redox cycling with glycine accompanied by a concomitant reduction of NBT into a visible blue-purple formazan color on the membrane [29]. This color formation indicates interaction between the bioactives and protein.

As shown in Figure 1a, Ponceau S staining revealed the presence of huTTR monomers and dimers based on their positions on the membrane. TTR tetramer normally migrates as an apparent dimer under non-reduced and non-boiled SDS-PAGE. [42,43]. The membrane was later distained of Ponceau S. Upon subjecting the membrane to NBT/glycinate staining, purple huTTR bands were detected in the lanes containing CAB, whereas no color reaction was observed in the absence of CAB (DMSO only) (Figure 1a). In the presence of gallic acid (positive control), the NBT stain produced a bright formazan color corresponding to the band position of the huTTR monomer. However, in the presence of CAB, the formazan color was present at the position representing huTTR dimers and monomers (although, quite faintly) (Figure 1a). The presence of the formazan color in the lane of CAB-associated huTTR indicated direct binding interactions. The higher intensity of the formazan color associated with the dimeric band suggested CAB binding preference for quaternary over tertiary huTTR forms, and that the CAB–huTTR complex formed is quite stable under reduced SDS-PAGE conditions.

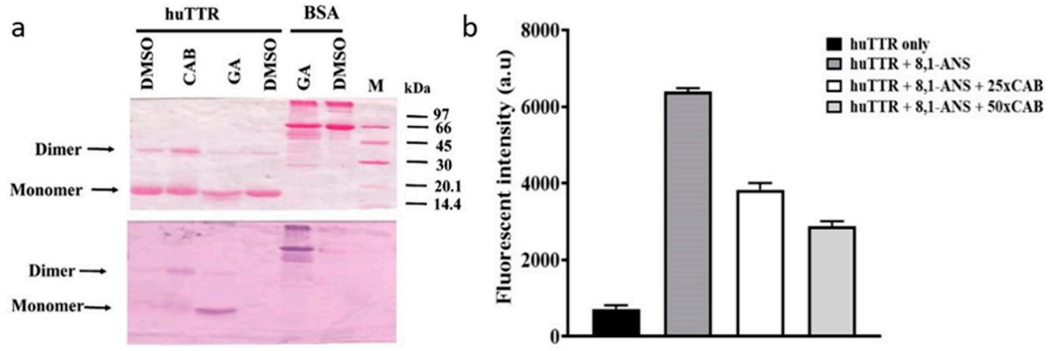

Figure 1. (**a**) Ponceau S staining of human transthyretin (huTTR) treated or non-treated (vehicle) with bioactives after electroblotting of SDS-PAGE onto the nitrocellulose membrane (above). Protein: Drug ratio of 1:10. Nitroblue tetrazolium (NBT)/glycinate staining of the membrane above after de-staining Ponceau S (below). (**b**) Displacement of bound 8-anilino-1-naphthalene sulfonic acid from huTTR by increasing concentrations of *Centella asiatica* (CAB). The bar chart columns and error bars represent the means of triplicates and standard deviations, respectively.

3.2. CAB Binds to the T4-Binding Sites of huTTR

To further understand the binding interactions between huTTR and CAB, 1,8-ANS binding displacement assay was performed. The fluorescent dye, 8,1-ANS is very sensitive to its surrounding chemical environment [44]. In aqueous environments, it produces a weak fluorescence; however, the fluorescent quantum yield increases significantly with a blue shift in the emission maxima when the surrounding becomes less polar [44]. ANS binds to the T4-binding sites of TTR tetramers with a corresponding increase in the magnitude of fluorescent quantum yield and a blue shift from 515 nm to about 465 nm [34]. Given the hydrophobic nature of the T4-binding pockets, the increase in fluorescence due to 8,1-ANS binding makes sense. Thus, several studies have utilized the displacement of 8,1-ANS from the T4-binding site as a probe to determine the binding of small-molecule ligands to the T4-binding pockets of tetrameric TTR [18,33]. In addition, the ANS fluorescence could serve as an indicator for the stability and compactness of the TTR core [45]. In this study, the binding of ANS to huTTR increased the quantum yield (Figure 1b). The addition of CAB reduced the fluorescent intensity dose-dependently, which suggests the displacement of 8,1-ANS from the T4-binding site of huTTR tetramers (Figure 1b). These results suggest the binding of CAB at the T4-binding sites of huTTR tetramers.

3.3. CAB Increases huTTR Structural Stability

To determine the impact of CAB on huTTR kinetic stability in vitro, urea-mediated denaturation assay was performed. HuTTR was preincubated with or without CAB, and subjected to denaturation by 7 M urea (final concentration). The intensity of folded huTTR was higher in the presence of CAB than in its absence (Figure 2a). The percentage of folded CAB-associated huTTR that resisted urea-mediated dissociation was 89.65 ± 4.6%. In contrast, the percentage of folded huTTR in the absence of CAB was lower, 58.87 ± 4.37% (Figure 2b). These results demonstrated that CAB improved the stability of huTTR tetramer against the denaturation stress.

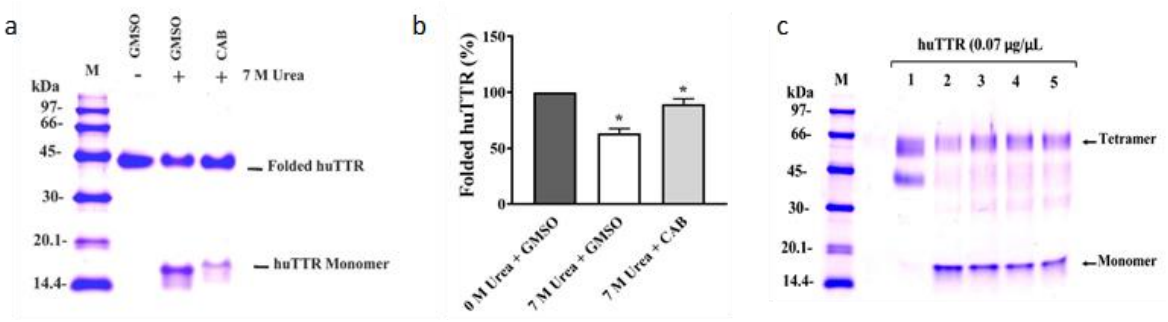

Figure 2. (**a**) Resistance to urea-mediated denaturation of huTTR in the presence and absence of *Centella asiatica* bioactive (CAB) components. HuTTR (0.07 μg/μL) was incubated in the presence of CAB (6.67 μg/μL) dissolve in GMSO or in the presence of GMSO only. (**b**) Bar chart represents the means of huTTR with and without CAB (protein: CAB mass ratio 1:100) and with their standard errors. * values are significantly different at $p < 0.05$. (**c**) Tricine SDS-PAGE gel (10%) of huTTR with increasing concentrations of CAB subjected to urea-denaturation stress and cross-linked with glutaraldehyde. M: Protein molecular weight marker; 1: 0 M urea + GMSO only; 2: 7 M urea + GMSO only; 3: 7 M urea + CAB (3.33 μg/μL); 4: 7 M urea + CAB (6.66 μg/μL); 5: 7 M urea + CAB (13.33 μg/μL).

To further understand the potential role of CAB on huTTR amyloidogenesis, we examined the quaternary structural changes in CAB-associated huTTR under urea denaturation by glutaraldehyde cross-linking assay. Human TTR was preincubated without or with varying concentrations of CAB and subjected to denaturation stress. Tricine SDS-PAGE of glutaraldehyde cross-linked huTTR samples revealed protein bands of ~60 kDa and ~16 kDa, corresponding to huTTR tetramers and monomers, respectively (Figure 2c). It is noteworthy that while the intensity of the monomeric band diminished as the amount of CAB increased, the intensity of huTTR tetrameric band increased correspondingly (Figure 2c). These findings indicated that CAB increased the quaternary structural stability of huTTR concentration-dependently.

In vitro, TTR rapidly dissociates when subjected to mildly acidic conditions. This facilitates its auto-aggregation [11,46]. In order to understand the impact of CAB on the stability of huTTR under conditions which promote amyloidogenesis, acid-mediated denaturation assay was performed. After subjecting huTTR samples to denaturation stress, the percentage of huTTR tetramers in the presence of CAB was higher than in the absence (Figure 3). In the presence of CAB, the percentage of huTTR tetramers that remained was 68.32 ± 0.81% as opposed to 30.24 ± 0.78% in its absence. These results indicated that CAB enhanced the quaternary structural stability of huTTR and confirmed the findings from the urea-mediated denaturation assay.

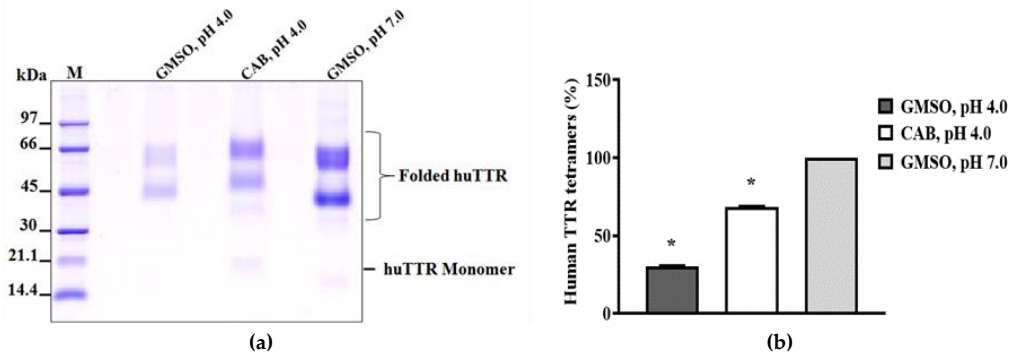

Figure 3. The resistance of human transthyretin in the absence or presence of CAB against acid-mediated denaturation. HuTTR (0.5 µg/µL) was incubated with or without CAB (50 µg/µL) and subjected to acidic denaturation conditions for 2 weeks. (**a**) The image represents the resolved protein mixtures on 10% Tricine SDS-PAGE gels after cross-linking with glutaraldehyde. M: Protein molecular weight marker; 1: huTTR with GMSO only, pH 4.0; 2: huTTR with CAB, pH 4.0; 3: huTTR with GMSO only, pH 7.0. (**b**) Bar chart represents the extent of huTTR stability, derived from the percentage of tetramers (%) left after denaturation. * values are significantly different at $p < 0.05$.

3.4. CAB Prevents huTTR Fibril Formation

The influence of CAB on huTTR fibrillation was determined by examining the morphology of the protein using transmission electron microscopy (TEM). Based on the electron micrographs, no huTTR mature fibril was formed in the presence of CAB; however, the formation of aggregate was not impeded (Figure 4b). Conversely, in the absence of CAB, not only did huTTR transform into aggregate, but also produced mature fibrils (Figure 4c,d). These findings suggested that CAB prevented the formation of mature huTTR fibrils under moderately acidic conditions in vitro. The electron micrograph of CAB incubated alone under similar conditions is shown in Figure S4.

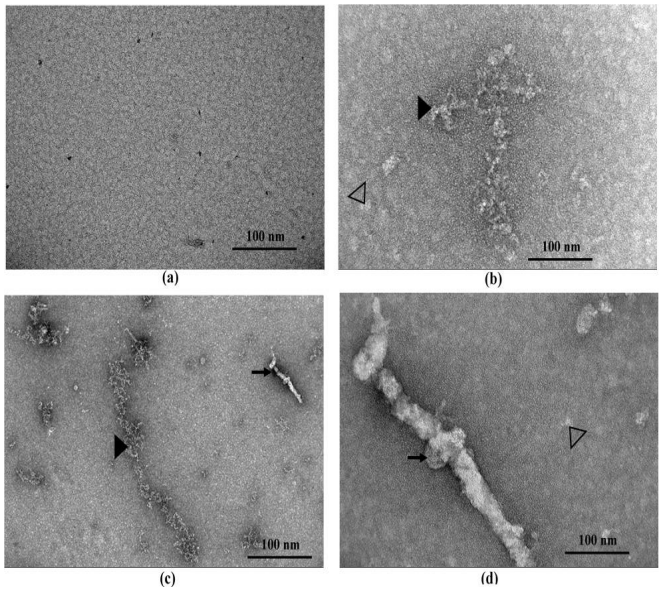

Figure 4. The TEM micrograph of huTTR incubated in the presence or absence of CAB. (**a**) Human transthyretin (TTR) in GF buffer, pH 7.4 supplemented with GMSO and incubated at −20 °C. (**b**) Human TTR supplemented CAB, final pH 4.0 and incubated at 37 °C for 7 days. (**c**) Human TTR supplemented with GMSO, pH 4.0 and incubated at 37 °C for 7 days. (**d**) Same image as (**c**) but with higher magnification. Arrows represent mature fibrils, filled arrow-heads large amorphous aggregates, and not-filled arrow-heads oligomers.

3.5. Antioxidant Activity of CAB

To determine the antioxidant activity of CAB, DPPH radical scavenging and FRAP assays were performed. The DPPH assay measures the ability of component(s) to quench the DPPH radical by transferring H to it. From the DPPH assay, CAB and the antioxidant standard displayed IC_{50} values of 28.53 and 2.81 µg/mL, respectively. While the radical-scavenging effect of CAB was lower than that of the standard, the abilities of both substances to remove the free radical were of the same magnitude. The FRAP assay showed that the reducing potential of CAB was 284.17 µmol Trolox equivalents per gram of CAB which is considered high [47]. These results demonstrated that CAB possessed potent antioxidant capacity.

3.6. Chemical Characterization of CAB

3.6.1. Total Phenolic and Flavonoid Contents

The antioxidant activities of many fruits and plants have been largely attributed to the presence of phenolics and flavonoids [48]. In this report, Folin–Ciocalteu and aluminum chloride colorimetric assays were used to determine the total phenolic and flavonoid contents of CAB, respectively. The content of phenolics in CAB was 43.86 ± 0.34 mg of gallic acid equivalent per gram, while the flavonoids content was 13.89 ± 0.23 mg of quercetin equivalents per gram of CAB.

3.6.2. TLC Profile of CAB

Phytochemical analysis to determine the major chemical profile of CAB was performed by thin layer chromatography on an aminopropyl-modified silica gel TLC plate. After derivatization with *p*-Anisaldehyde-sulfuric acid reagent, emergence of pink, purple, and yellow bands were observed under white light, indicating the presence of terpenoids and phenolics (Figure S3d). The emergence of bands that quenched the fluorescence indicator on the TLC plate under ultraviolet light at 254 nm (Figure S3b), suggested the presence of phenolics. Likewise, the appearance of bright yellow colored bands under white light, after the TLC plate was saturated with ammonia solution and sprayed with 2% methanolic $AlCl_3$, (Figure S3c) was typical of phenolic acids and flavonoids [49].

3.6.3. HPLC-QTOF-MS Analysis of CAB

HPLC-QTOF-MS was used to determine the chemical profile of CAB. The base peak chromatogram (negative ion mode) is revealed in Figure 5. The tentative identity of the major peaks obtained, retention times, accurate masses, and predicted molecular formulae are presented in Table 1. Identification of compounds was accomplished by comparing the accurate masses obtained with those of previously reported compounds present in *C. asiatica* found in the literature [40,50] and in online databases including METLIN and ChemSpider. Eight caffeoylquinic acids (chlorogenic acids) were identified including 3-*O*-caffeoylquinic acid, 5-*O*-caffeoylquinic acid, 3,4-*O*-dicaffeoylquinic acid, 3,5-*O*-dicaffeoylquinic acid, 3,5-*O*-dicaffeoyl-4-malonylquinic, 3-caffeoyl-4-feruloylquinic acid, and 4,5-*O*-dicaffeoylquinic acid (Table 1). In addition, seven pentacyclic triterpenoids were present including asiaticoside B, madecassoside, centellasaponin B, centellasaponin A, asiaticoside, avenacoside A, and soyasaponin I. The flavonoids quercetin 3-*O*-glucuronide and eriodictyol 7-(6-galloylglucoside) were also identified (Table 1). Thus, the prevalent chemical groups in CAB were chlorogenic acids and pentacyclic triterpenoids. The chemical composition of CAB was similar to those previously reported for *C. asiatica* [22,40,50].

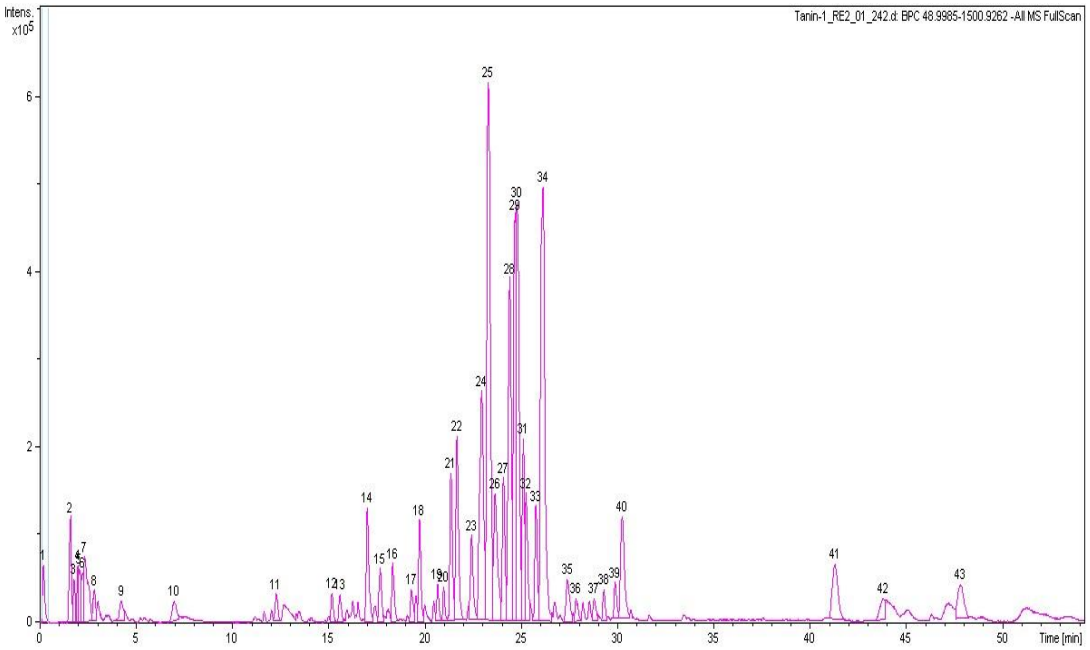

Figure 5. Base peak chromatogram of compounds in CAB obtained using HPLC-QTOF-MS in the negative mode.

Table 1. Profile of major bioactives detected in CAB by HPLC-QTOF-MS.

Peak No.	Retention Time	Observed Accurate Mass (*m*/*z*)	Predicted Formula	Calculated Mass (Da)	Tentative Identity of Compound
4	2.0	503.1527 [M − H]$^-$	$C_{21}H_{28}O_{14}$	504.1479	Caffeic acid dihexoside
12	15.1	353.0877 [M − H]$^-$	$C_{16}H_{18}O_9$	354.0951	3-*O*-Caffeoylquinic acid
14	17.0	353.088 [M − H]$^-$	$C_{16}H_{18}O_9$	354.0951	5-*O*-Caffeoylquinic acid
21	21.3	693.2790 [M − H_2O − H]$^-$	$C_{34}H_{48}O_{16}$	712.2942	Nominilic acid 17-glucoside
22	21.6	477.0685 [M − H]$^-$	$C_{21}H_{18}O_{13}$	478.0747	Quercetin 3-*O*-glucoronide
23	22.4	5151195 [M − H]$^-$	$C_{25}H_{24}O_{12}$	516.1268	3,4-*O*-Dicaffeoylquinic acid
24	22.9	515.1209 [M − H]$^-$	$C_{25}H_{24}O_{12}$	516.1268	3,5-*O*-Dicaffeoylquinic acid
25	23.3	601.1226 [M − H]$^-$	$C_{28}H_{26}O_{15}$	602.1272	3,5-*O*-Dicaffeoyl-4-malonylquinic acid
26	23.6	515.1203 [M − H]$^-$	$C_{25}H_{24}O_{12}$	516.1268	4,5-*O*-Dicaffeoylquinic acid
27	24.0	601.1209 [M − H]$^-$	$C_{28}H_{26}O_{15}$	602.1272	3,5-*O*-Dicaffeoyl-4-malonylquinic acid isomer
28	24.4	601.1228 [M − H]$^-$	$C_{28}H_{26}O_{15}$	602.1272	Eriodictyol 7-(6-galloylglucoside)
29	24.7	1019.5149 [M + Formate]$^-$	$C_{49}H_{79}O_{22}$	1019.5063	Asiaticoside B
30	24.8	1019.5149 [M + Formate]$^-$	$C_{49}H_{79}O_{22}$	1019.5063	Madecassoside
31	25.1	529.1351 [M − H]$^-$	$C_{26}H_{26}O_{12}$	530.1424	3-Caffeoyl-4-feruloylquinic acid
32	25.2	873.4522 [M + Formate − H]$^-$	$C_{43}H_{69}O_{18}$	874.4562	Centellasaponin B
33	25.7	1003.5166 [M + Formate − H]$^-$	$C_{49}H_{79}O_{21}$	1004.5192	Centellasaponin A
34	26.1	957.5088 [M − H]$^-$	$C_{48}H_{78}O_{19}$	958.5137	Asiaticoside
36	27.8	1061.5180 [M − H]$^-$	$C_{51}H_{82}O_{23}$	1062.5247	Avenacoside A
39	29.8	987.5213 [M − H]$^-$	$C_{49}H_{79}O_{20}$	988.5243	Soyasaponin I
40	30.2	571.0881 [M − H_2O − H]$^-$	$C_{30}H_{20}O_{12}$	572.0955	Manniflavanone

4. Discussion

In this study, we demonstrated that the bioactive compounds in CAB modulated huTTR amyloidogenesis by binding to the T4-binding sites of the tetramer. This enhanced the quaternary structural stability of huTTR against denaturation stresses. In addition, CAB prevented the fibrillation of huTTR under acid-induced aggregation conditions and demonstrated potent antioxidant activity.

Biophysical evidence has shown that dissociation of TTR tetramer is the initial and most critical step in TTR amyloidogenesis [8,11,12,51–53]. Thus, it is reasoned that enhancing TTR tetramer kinetic stability would make for an effective therapeutic strategy. Kinetic stabilization of native TTR tetramers can be accomplished by small-molecule ligands binding to the T4-binding sites of tetrameric TTR, which

elevates the kinetic barrier for its dissociation [8]. Since TTR amyloidogenesis is a concentration-driven process, by enhancing tetramer stability, the process is depleted of required amyloidogenic-competent monomers [54].

Natural products such as curcumin and propolis are now receiving more attention as potential kinetic stabilizers [18,55]. Commercial bee propolis (brand name: Bio30) extract, rich in caffeoyl acid phenethyl ester, reportedly stabilized the tetramers and inhibited transthyretin amyloidogenesis in vitro [18]. Our data demonstrated that CAB preserved the quaternary structural stability of huTTR, as reflected by the resistance of CAB-associated huTTR against urea- and acid-mediated denaturation conditions (Figures 2 and 3). These results concurred with previous findings of increased TTR structural stability by natural products [18,35,55,56]. This often involves, as earlier noted, binding of the small-molecule ligands at the T4-binding sites of the homotetramers [17]. The two T4-binding sites are situated in a particularly weak dimer–dimer interface. Electrostatic repulsion by side chains of symmetric residues (e.g., Lys 15, Lys15′) located at the surface of this hydrophobic pocket contributes significantly to the decrease in tetramer stability [53]. Since more than 99.5% of the T4-binding sites of TTR tetramers in serum are unoccupied under normal physiological conditions [57], an opportunity is created for small-ligand binding. Binding of small-molecule ligands at the T4-binding sites within the hydrophobic channel increase interactions and serve as tithers between the two dimers, and as potential anion shields that reduce the effects of electrostatic repulsion between the dimers. Consequently, the conformational stability of the tetramer is enhanced [53,56]. Thus, the increase in huTTR stability in this study could be attributed to the binding of CAB as small ligands at T4-binding sites of the tetramers as revealed by the ANS-binding displacement assay (Figure 1b). The increased ANS fluorescence (Figure 1b) is also indicative of the compactness of tetramers and integrity of the protein inner core [45] upon CAB binding. This was further supported by the preference of CAB binding to folded huTTR as revealed by the NBT assay (Figure 1a). CAB is phenol-rich. It is plausible that the phenolic components present in CAB form quinoprotein adducts with huTTR via Schiff base addition involving the Lys15, Lys15′ residues within the T4-binding sites [58,59]. Details of the molecular interactions between CAB and huTTR could constitute a future investigation.

CAB also binds (albeit, weakly) to huTTR monomers as indicated by the faint formazan color in the NBT redox-cycling assay (Figure 1a). Non-native monomers are the precursors for TTR aggregation and fibril formation [30,51]. The binding of CAB to huTTR monomers could partly explain the inhibition of huTTR amyloid fibril formation under conditions of mild acidity (Figure 4). Previously, it was reported that the aqueous extract of *C. asiatica* completely prevented the formation of amyloid-beta aggregates from monomers, and disintegrated preformed fibrils [23]. While our data showed that CAB prevented the formation of mature huTTR amyloid fibrils, the formation of aggregates was unabated (Figure 4b). This could be because huTTR oligomers, after being modified by CAB could no longer proceed in the amyloid cascade, (i.e., form mature fibrils). While such aggregates could be innocuous as previously demonstrated [60] in some natural phenolic products, it is yet to be investigated in CAB. The LC-MS data (Table 1) revealed that the major group of compounds in CAB are triterpenoids and phenolics. The ability of CAB to modulate TTR amyloidogenesis and fibril formation could be partly explained by the aromatic rings present in these compounds, and the formation of noncovalent interactions between them and amino acid residues of the β-sheet-rich core of the amyloidogenic protein [18,23,61].

Pro-oxidation is a feature in the pathophysiology of many neurodegenerative diseases including TTR amyloidogenesis [15,16]. Cytotoxic TTR comes in various conformations including amyloidogenic monomers, small soluble aggregates, and oxidatively-modified tetramers [16]. Upon interaction with cells, amyloidogenic TTR reduces cell viability and induces the release of reactive species [62]. Oxidatively modified TTR reportedly influences amyloidogenicity and age of onset in senile systemic amyloidosis [16]. In addition, a decrease in serum albumin antioxidant capacity was reported to accelerate TTR amyloid deposition in FAP patients [63]. Contrariwise, administration of a potent antioxidant, carvedilol, decreased TTR deposition, and oxidative and ER stresses in a FAP animal model [64]. All this underscores the importance of pro-oxidants in the promotion of antioxidants in

amelioration of TTR amyloidosis. Our data indicated that CAB possessed potent radical scavenging activity and reduction ability as demonstrated by IC_{50} and FRAP values 28.53 μg/mL and 284.17 μmol Trolox equivalents per gram of CAB, respectively. Compared with the previous reports on 44 plant extracts [47,65], CAB possessed excellent antioxidant capacity which could be attributed to its high phenolic and flavonoid content [48,66] (Pittella et al., 2009). Thus, the mitigation of huTTR amyloidogenesis by CAB could partly be attributed to its phenolic content [35,60,61] and antioxidative ability [20,64,67]. In addition, CAB as an antioxidant could potentially enhance oxidative balance by quenching reactive species and thus, reducing their deleterious effects on not only, huTTR, but also lipids, genetic materials, and aggregated-TTR-induced oxidative stress [48,64].

A potential drawback of this study is the possibility that a single compound or group of compounds might be responsible for the observed bioactivity of CAB. However, it has been widely reported that the bioactivity exerted by phytochemicals in natural products such as plant extract is mainly due to the additive, synergistic, and complementary effects of many rather than any individual phytoconstituent [19] (Liu, 2003). Also, CAB as a phytocomplex, rather than an isolated phytochemical, could make for a better multitarget agent for a complex multifactorial disorder such as TTR amyloidosis.

In this report, we have provided strong evidence that the hydrophilic fraction of *C. asiatica* contains potentially useful bioactives or lead compounds that could ameliorate TTR amyloidosis. Since TTR stability is vital in beta-amyloid clearance [68], CAB could also be relevant in Alzheimer's disease therapy. Prior, evidence had been presented for the neuroprotective and cognitive enhancement action of *C. asiatica* extracts [69,70]. In addition, *C. asiatica* bioactives were shown to be neuritogenic [71], synaptogenic [70], and anxiolytic [72]. Moreover, previous studies indicated that *C. asiatica* extracts decreased oxidative damage [73], increased cyclic AMP response element binding protein (CREB) phosphorylation, modulated the extracellular signal-regulated kinases (ERK) and protein kinase B signaling pathways [69,71] and was anti-inflammatory [74], which suggests a wide spectrum of biological activities. However, pertaining to the anti-TTR amyloidogenic activity of CAB, further studies are still required in order to elucidate the potency and safety in cell and animal models of the disease.

5. Conclusions

Based on the mechanistic studies presented herein, we determined that CAB might be a potential candidate or source material for future therapeutic development for TTR amyloidosis and/or related neurodegenerative diseases.

Supplementary Materials: The following are available online at http://www.mdpi.com/2218-273X/9/4/128/s1. Figure S1: Purification of huTTR from plasma Figure S2: Preparation of CAB from *C. asiatica*; Figure S3: Thin layer chromatography profile of CAB; Figure S4: TEM image of CAB alone.

Author Contributions: F.N.E. planned and conducted experiments, analyzed, and organized the data, generated figures, interpreted the results, and wrote the manuscript. L.L. assisted in planning the experiments, co-administrated the project, and reviewed the manuscript. P.P. conceptualized the idea, administrated the project, supervised the study, planned the experiments, co-interpreted, and reviewed the manuscript.

Acknowledgments: This research was supported by the National Research Council of Thailand, Prince of Songkla University and the Excellent Biochemistry Program Fund of Prince of Songkla University, Thailand. F.N.E. is a recipient of scholarship for his PhD research from Thailand's Education Hub for ASEAN Countries (TEH-AC 055/2014) and the Graduate School of Prince of Songkla University, Thailand.

Conflicts of Interest: The authors declare no conflict of interest. The funders had no role in the design of the study; in the collection, analyses, or interpretation of data; in the writing of the manuscript, or in the decision to publish the results.

References

1. Sipe, J.D.; Benson, M.D.; Buxbaum, J.N.; Ikeda, S.; Merlini, G.; Saraiva, M.J.M.; Westermark, P. Amyloid fibril proteins and amyloidosis: Chemical identification and clinical classification International Society of Amyloidosis 2016 Nomenclature Guidelines. *Amyloid* **2016**, *23*, 209–213. [CrossRef]

2. Reixach, N.; Deechongkit, S.; Jiang, X.; Kelly, J.W.; Buxbaum, J.N. Tissue damage in the amyloidoses: Transthyretin monomers and nonnative oligomers are the major cytotoxic species in tissue culture. *Proc. Natl. Acad. Sci. USA* **2004**, *101*, 2817–2822. [CrossRef] [PubMed]
3. Kopelman, M.; Cogan, U.; Mokady, S.; Shinitzky, M. The interaction between retinol-binding proteins and prealbumins studied by fluorescence polarization. *Biochim. Biophys. Acta (BBA)-Protein Struct.* **1976**, *439*, 449–460. [CrossRef]
4. González-López, E.; Gallego-Delgado, M.; Guzzo-Merello, G.; de Haro-Del Moral, F.J.; Cobo-Marcos, M.; Robles, C.; Bornstein, B.; Salas, C.; Lara-Pezzi, E.; Alonso-Pulpon, L.; et al. Wild-type transthyretin amyloidosis as a cause of heart failure with preserved ejection fraction. *Eur. Heart J.* **2015**, *36*, 2585–2594. [CrossRef] [PubMed]
5. Cornwell, G.G.; Murdoch, W.L.; Kyle, R.A.; Westermark, P.; Pitkänen, P. Frequency and distribution of senile cardiovascular amyloid: A clinicopathologic correlation. *Am. J. Med.* **1983**, *75*, 618–623. [CrossRef]
6. Westermark, P.; Sletten, K.; Johansson, B.; Cornwell, G.G. Fibril in senile systemic amyloidosis is derived from normal transthyretin. *Proc. Natl. Acad. Sci. USA* **1990**, *87*, 2843–2845. [CrossRef]
7. Kelly, J.W. Alternative conformations of amyloidogenic proteins govern their behavior. *Curr. Opin. Struct. Biol.* **1996**, *6*, 11–17. [CrossRef]
8. Johnson, S.M.; Wiseman, R.L.; Sekijima, Y.; Green, N.S.; Adamski-Werner, S.L.; Kelly, J.W. Native state kinetic stabilization as a strategy to ameliorate protein misfolding diseases: A focus on the transthyretin amyloidoses. *Acc. Chem. Res.* **2005**, *38*, 911–921. [CrossRef]
9. Schmidt, H.H.-J. Tafamidis for the treatment of transthyretin-associated familial amyloid polyneuropathy. *Expert Opin. Orphan Drugs* **2013**, *1*, 837–845. [CrossRef]
10. Planté-Bordeneuve, V.; Gorram, F.; Salhi, H.; Nordine, T.; Ayache, S.S.; Le Corvoisier, P.; Azoulay, D.; Feray, C.; Damy, T.; Lefaucheur, J.-P. Long-term treatment of transthyretin familial amyloid polyneuropathy with tafamidis: A clinical and neurophysiological study. *J. Neurol.* **2017**, *264*, 268–276. [CrossRef]
11. Lai, Z.; Colón, W.; Kelly, J.W. The acid-mediated denaturation pathway of transthyretin yields a conformational intermediate that can self-assemble into amyloid. *Biochemistry* **1996**, *35*, 6470–6482. [CrossRef] [PubMed]
12. Jiang, X.; Smith, C.S.; Petrassi, H.M.; Hammarström, P.; White, J.T.; Sacchettini, J.C.; Kelly, J.W. An Engineered Transthyretin Monomer that Is Nonamyloidogenic, Unless It Is Partially Denatured. *Biochemistry* **2001**, *40*, 11442–11452. [CrossRef]
13. Obici, L.; Merlini, G. An overview of drugs currently under investigation for the treatment of transthyretin-related hereditary amyloidosis. *Expert Opin. Investig. Drugs* **2014**, *23*, 1239–1251. [CrossRef]
14. Lashuel, H.A.; Wurth, C.; Woo, L.; Kelly, J.W. The most pathogenic transthyretin variant, L55P, forms amyloid fibrils under acidic conditions and protofilaments under physiological conditions. *Biochemistry* **1999**, *38*, 13560–13573. [CrossRef]
15. Saito, S.; Ando, Y.; Nakamura, M.; Ueda, M.; Kim, J.; Ishima, Y.; Akaike, T.; Otagiri, M. Effect of nitric oxide in amyloid fibril formation on transthyretin-related amyloidosis. *Biochemistry* **2005**, *44*, 11122–11129. [CrossRef]
16. Zhao, L.; Buxbaum, J.N.; Reixach, N. Age-related oxidative modifications of transthyretin modulate its amyloidogenicity. *Biochemistry* **2013**, *52*, 1913–1926. [CrossRef] [PubMed]
17. Ortore, G.; Orlandini, E.; Braca, A.; Ciccone, L.; Rossello, A.; Martinelli, A.; Nencetti, S. Targeting Different Transthyretin Binding Sites with Unusual Natural Compounds. *ChemMedChem* **2016**, *11*, 1865–1874. [CrossRef] [PubMed]
18. Yokoyama, T.; Kosaka, Y.; Mizuguchi, M. Inhibitory activities of propolis and its promising component, caffeic acid phenethyl ester, against amyloidogenesis of human transthyretin. *J. Med. Chem.* **2014**, *57*, 8928–8935. [CrossRef] [PubMed]
19. Liu, R.H. Health benefits of fruit and vegetables are from additive and synergistic combinations of phytochemicals. *Am. J. Clin. Nutr.* **2003**, *78*, 517S–520S. [CrossRef] [PubMed]
20. Lee, J.-E.; Kim, M.-S.; Park, S.-Y. Effect of natural antioxidants on the aggregation and disaggregation of beta-amyloid. *Trop. J. Pharm. Res.* **2017**, *16*, 2629–2635. [CrossRef]
21. Gohil, K.J.; Patel, J.A.; Gajjar, A.K. Pharmacological Review on Centella asiatica: A Potential Herbal Cure-all. *Indian J. Pharm. Sci.* **2010**, *72*, 546–556. [CrossRef]
22. Alqahtani, A.; Tongkao-on, W.; Li, K.M.; Razmovski-Naumovski, V.; Chan, K.; Li, G.Q. Seasonal Variation of Triterpenes and Phenolic Compounds in Australian *Centella asiatica* (L.) Urb. *Phytochem. Anal.* **2015**, *26*, 436–443. [CrossRef]

23. Berrocal, R.; Vasudevaraju, P.; Indi, S.S.; Sambasiva Rao, K.R.S.; Rao, K.S. In vitro evidence that an aqueous extract of Centella asiatica modulates α-synuclein aggregation dynamics. *J. Alzheimers Dis.* **2014**, *39*, 457–465. [CrossRef]
24. Gray, N.E.; Morré, J.; Kelley, J.; Maier, C.S.; Stevens, J.F.; Quinn, J.F.; Soumyanath, A. Caffeoylquinic acids in Centella asiatica protect against β-amyloid toxicity. *J. Alzheimers Dis.* **2014**, *40*, 359–373. [CrossRef]
25. Prapunpoj, P.; Leelawatwatana, L.; Schreiber, G.; Richardson, S.J. Change in structure of the N-terminal region of transthyretin produces change in affinity of transthyretin to T4 and T3. *FEBS J.* **2006**, *273*, 4013–4023. [CrossRef]
26. Leelawatwattana, L.; Praphanphoj, V.; Prapunpoj, P. Effect of the N-terminal sequence on the binding affinity of transthyretin for human retinol-binding protein. *FEBS J.* **2011**, *278*, 3337–3347. [CrossRef]
27. Ernst, O.; Zor, T. Linearization of the Bradford Protein Assay. *J. Vis. Exp.* **2010**, 38. [CrossRef]
28. Hellström, J.K.; Mattila, P.H. HPLC determination of extractable and unextractable proanthocyanidins in plant materials. *J. Agric. Food Chem.* **2008**, *56*, 7617–7624. [CrossRef]
29. Paz, M.A.; Flückiger, R.; Boak, A.; Kagan, H.M.; Gallop, P.M. Specific detection of quinoproteins by redox-cycling staining. *J. Biol. Chem.* **1991**, *266*, 689–692.
30. Quintas, A.; Saraiva, M.J.M.; Brito, R.M.M. The Tetrameric Protein Transthyretin Dissociates to a Non-native Monomer in Solution a novel model for amyloidogenesis. *J. Biol. Chem.* **1999**, *274*, 32943–32949. [CrossRef]
31. Mu, Y.; Jin, S.; Shen, J.; Sugano, A.; Takaoka, Y.; Qiang, L.; Imbimbo, B.P.; Yamamura, K.; Li, Z. CHF5074 (CSP-1103) stabilizes human transthyretin in mice humanized at the transthyretin and retinol-binding protein loci. *FEBS Lett.* **2015**, *589*, 849–856. [CrossRef]
32. Nilsson, L.; Larsson, A.; Begum, A.; Iakovleva, I.; Carlsson, M.; Brännström, K.; Sauer-Eriksson, A.E.; Olofsson, A. Modifications of the 7-Hydroxyl Group of the Transthyretin Ligand Luteolin Provide Mechanistic Insights into Its Binding Properties and High Plasma Specificity. *PLoS ONE* **2016**, *11*, e0153112. [CrossRef]
33. Pullakhandam, R.; Srinivas, P.N.B.S.; Nair, M.K.; Reddy, G.B. Binding and stabilization of transthyretin by curcumin. *Arch. Biochem. Biophys.* **2009**, *485*, 115–119. [CrossRef]
34. Cheng, S.Y.; Pages, R.A.; Saroff, H.A.; Edelhoch, H.; Robbins, J. Analysis of thyroid hormone binding to human serum prealbumin by 8-anilinonaphthalene-1-sulfonate fluorescence. *Biochemistry* **1977**, *16*, 3707–3713. [CrossRef]
35. Ferreira, N.; Pereira-Henriques, A.; Almeida, M.R. Transthyretin chemical chaperoning by flavonoids: Structure-activity insights towards the design of potent amyloidosis inhibitors. *Biochem. Biophys. Rep.* **2015**, *3*, 123–133. [CrossRef]
36. Lesjak, M.; Beara, I.; Simin, N.; Pintać, D.; Majkić, T.; Bekvalac, K.; Orčić, D.; Mimica-Dukić, N. Antioxidant and anti-inflammatory activities of quercetin and its derivatives. *J. Funct. Foods* **2018**, *40*, 68–75. [CrossRef]
37. Benzie, I.F.; Strain, J.J. The ferric reducing ability of plasma (FRAP) as a measure of "antioxidant power": The FRAP assay. *Anal. Biochem.* **1996**, *239*, 70–76. [CrossRef]
38. Ainsworth, E.A.; Gillespie, K.M. Estimation of total phenolic content and other oxidation substrates in plant tissues using Folin-Ciocalteu reagent. *Nat. Protoc.* **2007**, *2*, 875–877. [CrossRef]
39. Pintać, D.; Majkić, T.; Torović, L.; Orčić, D.; Beara, I.; Simin, N.; Mimica–Dukić, N.; Lesjak, M. Solvent selection for efficient extraction of bioactive compounds from grape pomace. *Ind. Crops Prod.* **2018**, *111*, 379–390. [CrossRef]
40. Long, H.S.; Stander, M.A.; Van Wyk, B.-E. Notes on the occurrence and significance of triterpenoids (asiaticoside and related compounds) and caffeoylquinic acids in Centella species. *S. Afr. J. Bot.* **2012**, *82*, 53–59. [CrossRef]
41. Iwamoto, N.; Sumi, D.; Ishii, T.; Uchida, K.; Cho, A.K.; Froines, J.R.; Kumagai, Y. Chemical knockdown of protein-tyrosine phosphatase 1B by 1,2-naphthoquinone through covalent modification causes persistent transactivation of epidermal growth factor receptor. *J. Biol. Chem.* **2007**, *282*, 33396–33404. [CrossRef]
42. McCutchen, S.L.; Kelly, J.W. Intermolecular disulfide linkages are not required for transthyretin amyloid fibril formation in vitro. *Biochem. Biophys. Res. Commun.* **1993**, *197*, 415–421. [CrossRef]
43. Schneider, F.; Hammarström, P.; Kelly, J.W. Transthyretin slowly exchanges subunits under physiological conditions: A convenient chromatographic method to study subunit exchange in oligomeric proteins. *Protein Sci.* **2001**, *10*, 1606–1613. [CrossRef]
44. Miranker, A.D.; Dobson, C.M. Collapse and cooperativity in protein folding. *Curr. Opin. Struct. Biol.* **1996**, *6*, 31–42. [CrossRef]

45. Yang, D.T.; Joshi, G.; Cho, P.Y.; Johnson, J.A.; Murphy, R.M. Transthyretin as both a sensor and a scavenger of β-amyloid oligomers. *Biochemistry* **2013**, *52*, 2849–2861. [CrossRef]
46. Lashuel, H.A.; Lai, Z.; Kelly, J.W. Characterization of the transthyretin acid denaturation pathways by analytical ultracentrifugation: Implications for wild-type, V30M, and L55P amyloid fibril formation. *Biochemistry* **1998**, *37*, 17851–17864. [CrossRef]
47. Fernandes, R.P.P.; Trindade, M.A.; Tonin, F.G.; Lima, C.G.; Pugine, S.M.P.; Munekata, P.E.S.; Lorenzo, J.M.; de Melo, M.P. Evaluation of antioxidant capacity of 13 plant extracts by three different methods: Cluster analyses applied for selection of the natural extracts with higher antioxidant capacity to replace synthetic antioxidant in lamb burgers. *J. Food Sci. Technol.* **2016**, *53*, 451–460. [CrossRef]
48. Scalbert, A.; Johnson, I.T.; Saltmarsh, M. Polyphenols: Antioxidants and beyond. *Am. J. Clin. Nutr.* **2005**, *81*, 215S–217S. [CrossRef]
49. Wagner, H.; Bladt, S. Saponin Drugs. In *Plant Drug Analysis: A Thin Layer Chromatography Atlas*, 2nd ed.; Springer: Berlin/Heidelberg, Germany, 1996.
50. Maulidiani; Abas, F.; Khatib, A.; Shaari, K.; Lajis, N.H. Chemical characterization and antioxidant activity of three medicinal Apiaceae species. *Ind. Crops Prod.* **2014**, *55*, 238–247. [CrossRef]
51. Colon, W.; Kelly, J.W. Partial denaturation of transthyretin is sufficient for amyloid fibril formation in vitro. *Biochemistry* **1992**, *31*, 8654–8660. [CrossRef]
52. Kelly, J.W.; Colon, W.; Lai, Z.; Lashuel, H.A.; McCulloch, J.; McCutchen, S.L.; Miroy, G.J.; Peterson, S.A. Transthyretin quaternary and tertiary structural changes facilitate misassembly into amyloid. *Adv. Protein Chem.* **1997**, *50*, 161–181.
53. Hammarström, P.; Jiang, X.; Deechongkit, S.; Kelly, J.W. Anion shielding of electrostatic repulsions in transthyretin modulates stability and amyloidosis: Insight into the chaotrope unfolding dichotomy. *Biochemistry* **2001**, *40*, 11453–11459. [CrossRef]
54. Sekijima, Y.; Kelly, J.W.; Ikeda, S. Pathogenesis of and therapeutic strategies to ameliorate the transthyretin amyloidoses. *Curr. Pharm. Des.* **2008**, *14*, 3219–3230. [CrossRef]
55. Ferreira, N.; Gonçalves, N.P.; Saraiva, M.J.; Almeida, M.R. Curcumin: A multi-target disease-modifying agent for late-stage transthyretin amyloidosis. *Sci. Rep.* **2016**, *6*, 26623. [CrossRef]
56. Florio, P.; Folli, C.; Cianci, M.; Del Rio, D.; Zanotti, G.; Berni, R. Transthyretin Binding Heterogeneity and Anti-amyloidogenic Activity of Natural Polyphenols and Their Metabolites. *J. Biol. Chem.* **2015**, *290*, 29769–29780. [CrossRef]
57. Hamilton, J.A.; Benson, M.D. Transthyretin: A review from a structural perspective. *Cell. Mol. Life Sci.* **2001**, *58*, 1491–1521. [CrossRef]
58. Ishii, T.; Mori, T.; Tanaka, T.; Mizuno, D.; Yamaji, R.; Kumazawa, S.; Nakayama, T.; Akagawa, M. Covalent modification of proteins by green tea polyphenol (-)-epigallocatechin-3-gallate through autoxidation. *Free Radic. Biol. Med.* **2008**, *45*, 1384–1394. [CrossRef]
59. Tomar, D.; Khan, T.; Singh, R.R.; Mishra, S.; Gupta, S.; Surolia, A.; Salunke, D.M. Crystallographic Study of Novel Transthyretin Ligands Exhibiting Negative-Cooperativity between Two Thyroxine Binding Sites. *PLoS ONE* **2012**, *7*, e43522. [CrossRef]
60. Ferreira, N.; Saraiva, M.J.; Almeida, M.R. Natural polyphenols inhibit different steps of the process of transthyretin (TTR) amyloid fibril formation. *FEBS Lett.* **2011**, *585*, 2424–2430. [CrossRef]
61. Lakey-Beitia, J.; Berrocal, R.; Rao, K.S.; Durant, A.A. Polyphenols as therapeutic molecules in Alzheimer's disease through modulating amyloid pathways. *Mol. Neurobiol.* **2015**, *51*, 466–479. [CrossRef]
62. Manral, P.; Reixach, N. Amyloidogenic and non-amyloidogenic transthyretin variants interact differently with human cardiomyocytes: Insights into early events of non-fibrillar tissue damage. *Biosci. Rep.* **2015**, *35*, e00172. [CrossRef]
63. Kugimiya, T.; Jono, H.; Saito, S.; Maruyama, T.; Kadowaki, D.; Misumi, Y.; Hoshii, Y.; Tasaki, M.; Su, Y.; Ueda, M.; et al. Loss of functional albumin triggers acceleration of transthyretin amyloid fibril formation in familial amyloidotic polyneuropathy. *Lab. Investig.* **2011**, *91*, 1219–1228. [CrossRef]
64. Macedo, B.; Magalhães, J.; Batista, A.R.; Saraiva, M.J. Carvedilol treatment reduces transthyretin deposition in a familial amyloidotic polyneuropathy mouse model. *Pharmacol. Res.* **2010**, *62*, 514–522. [CrossRef]
65. Mustafa, R.A.; Abdul Hamid, A.; Mohamed, S.; Bakar, F.A. Total phenolic compounds, flavonoids, and radical scavenging activity of 21 selected tropical plants. *J. Food Sci.* **2010**, *75*, C28–C35. [CrossRef]

66. Pittella, F.; Dutra, R.C.; Junior, D.D.; Lopes, M.T.P.; Barbosa, N.R. Antioxidant and Cytotoxic Activities of *Centella asiatica* (L) Urb. *Int. J. Mol. Sci.* **2009**, *10*, 3713–3721. [CrossRef]
67. Guo, J.; Jono, H.; Kugimiya, T.; Saito, S.; Maruyama, T.; Misumi, Y.; Hoshii, Y.; Su, Y.; Shono, M.; Ueda, M.; et al. Antioxidative effect of albumin on amyloid fibril formation in transthyretin-related amyloidosis. *Amyloid* **2011**, *18* (Suppl. 1), 17–18. [CrossRef]
68. Alemi, M.; Silva, S.C.; Santana, I.; Cardoso, I. Transthyretin stability is critical in assisting beta amyloid clearance- Relevance of transthyretin stabilization in Alzheimer's disease. *CNS Neurosci. Ther.* **2017**, *23*, 605–619. [CrossRef]
69. Xu, Y.; Cao, Z.; Khan, I.; Luo, Y. Gotu Kola (Centella Asiatica) extract enhances phosphorylation of cyclic AMP response element binding protein in neuroblastoma cells expressing amyloid beta peptide. *J. Alzheimers Dis.* **2008**, *13*, 341–349. [CrossRef]
70. Gray, N.E.; Harris, C.J.; Quinn, J.F.; Soumyanath, A. Centella asiatica modulates antioxidant and mitochondrial pathways and improves cognitive function in mice. *J. Ethnopharmacol.* **2016**, *180*, 78–86. [CrossRef]
71. Wanakhachornkrai, O.; Pongrakhananon, V.; Chunhacha, P.; Wanasuntronwong, A.; Vattanajun, A.; Tantisira, B.; Chanvorachote, P.; Tantisira, M.H. Neuritogenic effect of standardized extract of Centella asiatica ECa233 on human neuroblastoma cells. *BMC Complement. Altern. Med.* **2013**, *13*, 204. [CrossRef]
72. Chanana, P.; Kumar, A. Possible Involvement of Nitric Oxide Modulatory Mechanisms in the Neuroprotective Effect of Centella asiatica Against Sleep Deprivation Induced Anxiety Like Behaviour, Oxidative Damage and Neuroinflammation. *Phytother. Res.* **2016**, *30*, 671–680. [CrossRef]
73. Kumari, S.; Deori, M.; Elancheran, R.; Kotoky, J.; Devi, R. In vitro and In vivo Antioxidant, Anti-hyperlipidemic Properties and Chemical Characterization of *Centella asiatica* (L.) Extract. *Front. Pharmacol.* **2016**, *7*, 400. [CrossRef]
74. Ramesh, B.N.; Girish, T.K.; Raghavendra, R.H.; Naidu, K.A.; Rao, U.J.S.P.; Rao, K.S. Comparative study on anti-oxidant and anti-inflammatory activities of Caesalpinia crista and Centella asiatica leaf extracts. *J. Pharm. Bioallied Sci.* **2014**, *6*, 86–91.

biomolecules

MDPI

Article

Transthyretin Anti-Amyloidogenic and Fibril Disrupting Activities of *Bacopa monnieri* (L.) Wettst (Brahmi) Extract

Fredrick Nwude Eze [1], Kornkanok Ingkaninan [2] and Porntip Prapunpoj [1,*]

[1] Department of Biochemistry, Faculty of Science, Prince of Songkla University, Hat Yai, Songkhla 90112, Thailand; fredrickeze@rocketmail.com

[2] Department of Pharmaceutical Chemistry and Pharmacognosy, Faculty of Pharmaceutical Sciences and Center of Excellence for Innovation in Chemistry, Naresuan University, Phitsanulok 65000, Thailand; kornkanoki@nu.ac.th

* Correspondence: porntip.p@psu.ac.th; Tel.: +66-74-288-275

Received: 10 November 2019; Accepted: 6 December 2019; Published: 9 December 2019

Abstract: The homotetrameric plasma protein transthyretin (TTR), is responsible for a series of debilitating and often fatal disorders in humans known as transthyretin amyloidosis. Currently, there is no cure for TTR amyloidosis and treatment options are rare. Thus, the identification and development of effective and safe therapeutic agents remain a research imperative. The objective of this study was to determine the effectiveness of *Bacopa monnieri* extract (BME) in the modulation of TTR amyloidogenesis and disruption of preformed fibrils. Using aggregation assays and transmission electron microscopy, it was found that BME abrogated the formation of human TTR aggregates and mature fibrils but did not dis-aggregate pre-formed fibrils. Through acid-mediated and urea-mediated denaturation assays, it was revealed that BME mitigated the dissociation of folded human TTR and L55P TTR into monomers. ANS binding and glutaraldehyde cross-linking assays showed that BME binds at the thyroxine-binding site and possibly enhanced the quaternary structural stability of native TTR. Together, our results suggest that BME bioactives prevented the formation of TTR fibrils by attenuating the disassembly of tetramers into monomers. These findings open up the possibility of further exploration of BME as a potential resource of valuable anti-TTR amyloidosis therapeutic ingredients.

Keywords: antioxidants; amyloidosis; *Bacopa monnieri*; bioactive compounds; degenerative diseases; fibrillation; transthyretin

1. Introduction

Transthyretin (TTR) is one of the most abundant plasma proteins and is involved in the transport of thyroxine and vitamin A [1,2]. In the cerebrospinal fluid, this 55 kDa homotetrameric protein synthesized in the choroid plexus is the main transporter of thyroxine (T4). Recent evidence seems to suggest a neuroprotective role of TTR in Alzheimer's disease. However, TTR in its pathological form, amyloid transthyretin (ATTR), is responsible for a spectrum of progressive, debilitating, life-altering neurodegenerative diseases known as ATTR amyloidosis which originated from the misfolding, mis-aggregation and systemic deposition of ATTR in several organs. ATTR amyloidosis is a severe clinical disorder leading to death in many cases within seven to ten years after the onset of clinical manifestations [1]. At the moment there is no cure for the disease and effective therapeutic interventions are very limited. Thus, there is a pressing need for investigations targeted toward the identification or development of safe and effective therapeutic interventions.

Native wild-type TTR is fairly stable under physiological conditions but possesses an intrinsic propensity to dissociate into its monomeric form. This propensity is enhanced by single point mutations in the TTR gene leading to variant TTR with altered and often reduced quaternary structural stability. At the moment, there are over 130 variant forms of TTR, most of which are amyloidogenic. Systemic deposition of aggregated variant TTR as amyloid fibrils in various organs of the body constitutes the pathological hallmark of hereditary variant transthyretin (ATTRv) amyloidosis, such as the formally known familial amyloidotic polyneuropathy (FAP) and familial amyloidotic cardiomyopathy (FAC). Deposition of wild-type transthyretin leads to wild-type transthyretin (ATTRwt) amyloidosis or the erstwhile senile systemic amyloidosis. ATTRwt amyloidosis is a leading cause of death in the elderly often involving heart failure [3]. While the complete picture of the molecular mechanisms underlying the transition of normal soluble functional transthyretin into its pathological counterpart is still emerging, the prevailing hypothesis is that the initial and most important step is the dissociation of the native tetramer into monomers [1]. Thus, investigations involving the identification and development of small-molecule ligands that prevented tetramer dissociation, also known as kinetic stabilizers, were considered a viable therapeutic strategy [4]. The recent development of kinetic stabilizers, such as Tafamidis and diflunisal, in addition to TTR gene silencers, including Inotersen and Patisiran, has provided patients with some positive treatment outcomes. However, limitations involving the long-term consequences and failure to prevent neurologic impairment in patients remain major sources of concern [5]. The investigations into safe and effective alternative therapeutic agents for preventing TTR amyloidogenesis and/or disrupting the preformed fibrils (amyloid disrupters), therefore, are still required. Recently, natural products from plants have been receiving increasing attention for their anti-amyloid activities as well as alternative beneficial effects, such as antioxidants, anti-inflammatory, and metal-chelating properties [6–8].

Bacopa monnieri (L.) Wettst also commonly known as Brahmi, Prom-mi, or water hyssop, is a small, perennial herb commonly found in the marshy areas of Asia and many tropical and subtropical regions around the world. *B. monnieri* is a member of the family Plantaginaceae for which there are about 100 species under the same genus. Three species of the plant are common in Thailand viz., *B. floribunda* (R. Br.) Wettst (local name: Phak sam Ian), *B. caroliniana* (Walter) B. L. Rob (local name: Lam pailin), and *B. monnieri* (L.) Wettst (local name: Prom mi). *B. monnieri* is the most common of the three due to its prevalent use in Thai traditional medicine for alleviating cognitive impairment and enhancing intelligence [9]. For thousands of years, Brahmi was widely used in Ayurveda, the Indian traditional system of medicine for treating several neurological disorders and for improving overall well-being [10]. Several pharmacological investigations have demonstrated the antioxidant [11], anti-inflammatory [12], and neuroprotective effects on disorders, such as Alzheimer's disease, Parkinson's disease, and brain injury [13]. However, its impact on ATTR amyloidosis has yet to be investigated. Given its reportedly good safety profile [14] and abundance of bioactive metabolites [15], the objective of the present study was thus to determine the effect of *Bacopa monnieri* extract (BME) on transthyretin amyloidogenesis and fibril disruption. Knowledge from this investigation could provide insights pertaining to the therapeutic potential of BME against ATTR amyloidosis.

2. Materials and Methods

2.1. Expression and Purification of Recombinant L55P TTR

Recombinant L55P TTR was produced in *Pichia pastoris* expression system as described earlier [16]. L55P TTR was purified from the concentrated culture supernatant using preparative discontinuous native-PAGE. Silver staining was used to determine fractions containing only L55P TTR, which were subsequently pooled and concentrated by ultrafiltration. Concentration of the purified L55P TTR was determined by Bradford assay using bovine serum albumin as standard. Pure L55P TTR was stored at −20 °C until use.

2.2. Purification of Human TTR from Plasma

Human plasma was pretreated by reduction of albumin via adsorption in a Cibacron blue 3GA (Sigma-Aldrich, St. Louis, MO, USA) column. The unbound faction was concentrated by ultrafiltration. Human TTR was purified from the concentrated, pretreated human plasma by preparative discontinuous native-PAGE using BIO-RAD Model 491 Prep Cell system (BIO-RAD, Hercules, CA, USA) as described previously [17].

2.3. Plant Material Collection and Preparation of B. monnieri Extract (BME)

Fresh Brahmi was obtained from Naresuan University. Whole plant specimen was identified and authenticated by Dr. Pranee Nangngam with voucher specimen (Saesong004) deposited at the Herbarium of the Department of Biology, Faculty of Science, Naresuan University, Thailand. Brahmi aerial parts of about 10 cm was washed and dried for 24 h at 50 °C in a hot air oven. The dried plant material was then blended into powder. Brahmi powder was extracted as earlier reported [15]. Briefly, pre-soaked plant material was extracted with 95 % ethanol (solid solvent ratio of 1:6 *w*/*v*) by sonicating for 10 min. The residue was further extracted two more times. The ethanolic extracts were combined, filtered and evaporated to obtain *Bacopa monnieri* or Brahmi extract (BME).

2.4. Chemical Characterization of Brahmi Extract

2.4.1. RP-HPLC Quantitative Analysis

It has been widely reported that saponins constitute the major bioactive components in *B. monnieri*, thus the saponin content of Brahmi was quantified using reverse-phase high-performance liquid chromatography as previously reported [18]. Five individual saponins standards, including Bacoside A3, Bacopaside I, Bacopaside II, Bacopaside X, and Bacopopasaposin C were used. Total saponin content was obtained as the sum of the individual saponin and expressed as the percentage weight of the dried extract.

2.4.2. Total Phenolic Content

The content of phenolic compounds in BME was determined by Folin–Ciocalteu as previously described [19]. BME or gallic acid (standard) was solubilized in DMSO: methanol (10:90 *v*/*v*). One hundred microliters of BME, standard or blank was added into test tube followed by freshly prepared 10 % Folin–Ciocalteu reagent (200 µL). For the blank, 200 µL of distilled water was added in place of Folin–Ciocalteu reagent. Five minutes later, 700 mM sodium carbonate solution (800 µL) was added to develop a blue mixture. The solutions were incubated in the dark for 2 h at room temperature. Absorbance was read at 765 nm and a standard curve was plotted from gallic acid (0–0.05 mg). Total phenolic content of BME was obtained from the standard curve and expressed as mg gallic acid equivalent per gram of Brahmi extract dry weight.

2.4.3. Total Flavonoid Content

Content of flavonoid compounds was determined by aluminum chloride colorimetric assay as previously described [19]. One hundred and eighty microliters of BME, quercetin (standard) or blank solubilized in DMSO: methanol (1:5 *v*/*v*) was introduced to test tubes. Methanolic aluminum chloride 10% *w*/*v* (30 µL) was added into the solution. Methanol was added to the blank instead of $AlCl_3$. Subsequently, 1 M sodium acetate (30 µL) and distilled water (850 µL) were added to the mixture and vortexed. Due to the deep coloration of the extract, a blank for the extract was prepared containing all the components but with methanol instead of methanolic $AlCl_3$ solution. The sample, standard and blank solutions were incubated in the dark at room temperature for 30 min. Absorbance was recorded at 415 nm. A standard curve was plotted from quercetin (0–0.05 mg). The total flavonoid content of

Brahmi extract was derived from the standard curve and expressed as mg quercetin equivalent per gram of Brahmi extract dry weight.

2.4.4. Ferric Reducing Antioxidant Power (FRAP) Assay

The antioxidant capacity of Brahmi extract was obtained using FRAP assay as described by Benzie and Strain [20] with slight modifications. Freshly prepared FRAP solution (300 mM acetate buffer pH 3.6, 10 mM 2,4,6-Tris(2-pyridyl)-s-triazine) solution, 20 mM $FeCl_3 \cdot 6H_2O$) was warmed for 30 min at 37 °C in the dark. BME was solubilized in 50% DMSO while ferrous sulfate (0–2 mM) was prepared as standard for calibration. BME or ferrous sulfate solution (10 µL) was added in a 96-well microplate followed by FRAP solution (200 µL). The mixture was incubated at 37 °C for 30 min in the dark. Absorbance was read at a wavelength of 593 nm. FRAP values were obtained from a calibration curve prepared using ferrous sulfate and expressed as mmol ferrous equivalent per gram of Brahmi extract dry weight.

2.4.5. DPPH Radical Scavenging Assay

The anti-radical activity of BME was determined by DPPH assay as described by Lesjak et al. [21]. Ten microliters of plant extract solution (8.33–166.67 mg/L) was added into the wells of a 96-well microtiter plate. Methanol (140 µL) followed by 0.1 mM DPPH (150 µL) in methanol were added to the extract. Methanol without the extract served as control while corresponding blank probes contained 10 µL of extract and 290 µL of methanol. After 30 min of incubation, absorbance was read at 515 nm and the DPPH radical scavenging effect of BME was expressed as IC_{50}, i.e., the extract concentration that inhibited DPPH radical formation by 50%.

2.5. Transthyretin Tetramer Stabilization Assays

2.5.1. Urea-Mediated Denaturation Assay

The effect of BME on human TTR or L55P TTR tetramer stability was determined using urea-mediated denaturation assay. The protein was pre-incubated with BME, curcumin or DMSO (solvent) for 4 h at 37 °C in the dark. Urea solution was added to the protein solution (at a final concentration of 6 M) to initiate dissociation of the tetramers. Protein solution was incubated at 4 °C in the dark for 72 h. Thereafter, the amount of folded L55P TTR (i.e., dimers, trimmers, and tetramers) left was obtained by resolving the protein solution on 10% Tricine SDS-PAGE gel followed by densitometric analysis on LabWorks 4.0 software (UVP Ltd., Cambridge, UK) of the Coomassie brilliant blue R-250, stained protein bands on the gels.

2.5.2. Acid-Mediated Denaturation Assay

Human TTR solution with or without BME was pre-incubated for 4 h to enable binding interactions. Thereafter, protein solutions were subjected to denaturation by addition of acetate buffer, pH 4.0 and incubated at 37 °C in the dark for 14 days. To determine the extent of denaturation, protein solutions were solubilized in SDS sample loading buffer without β-mercaptoethanol (i.e., 0.05 M Tris-HCl, pH 6.8, 10% glycerol, 2% SDS, and 0.1% bromophenol blue dye). Protein samples (without boiling) were resolved on 12% polyacrylamide gel containing 0.1% SDS and separated bands were detected with Coomassie brilliant blue R-250 staining. In principle, under this SDS-PAGE condition, tetrameric transthyretin will be observed as SDS-resistant dimers on the gel [22]. The fraction of human TTR tetramers left after subjection to mild acid denaturation stress was quantified from the gel band intensities via densitometric analysis using gel documentation.

2.6. Transthyretin pH-Induced Fibril Formation and Disruption Assays

The effect of BME on human TTR aggregation and fibril formation was determined by pre-incubating human TTR for 4 h with or without BME at 37 °C. Thereafter, the pH was adjusted to 4.0 with 200 mM acetate buffer, pH 4.0. Aggregation of human TTR was enabled by aging the protein complex for 14 days in the dark at 37 °C under aseptic conditions. The extent of protein aggregation and fibrillation were determined by transmission electron microscopy (TEM). For TEM analysis, a drop of protein solution was spotted unto a formvar-coated copper grid for 3 min. Excess fluid was carefully blotted with a filter paper wedge. The grid was then rinsed with a drop of Milli-Q water (Millipore, Billerica, MA, USA) followed by staining with 2% uranyl acetate in 70% methanol for 2 min. The grid was further rinsed with a drop of Milli-Q, excess fluid blotted away and dried at ambient temperature. The TEM image was obtained using a JEOL JEM-2010 (JEOL Ltd., Akishima, Tokyo, Japan) electron microscope operating at 160 kV. The fibril disruption assay was performed as previously described [6]. Preformed fibrils were prepared using acid-mediated aggregation assay and formation of fibrils was confirmed by TEM. The pre-formed fibrils were further incubated with or without BME in the dark at 37 °C for 24 h. Thereafter, fibril disruption activity was confirmed by TEM and glutaraldehyde cross-linking assay followed by 10% Tricine-SDS-PAGE.

2.7. Transthyretin Quaternary Structural Alterations Determined by Glutaraldehyde Cross-Linking Assay

The quaternary structure of human TTR or L55P TTR subjected to urea-induced denaturation or human TTR after acid-mediated denaturation stress was determined by chemical cross-linking assay using glutaraldehyde. Aliquot of protein solution was obtained denaturation at stress. Glutaraldehyde was added to the protein solution (final concentration of 2.5%) and cross-linking allowed for 4 min at ambient temperature. Cross-linking reaction was quenched by addition of 7% $NaBH_4$ in 0.1 M NaOH (of equal volume to glutaraldehyde). The mixture was solubilized with 4× SDS sample loading buffer (final SDS concentration of 2%) and boiled for 10 min before resolving on 10% Tricine-SDS-PAGE gel. Protein bands were detected using Coomassie brilliant blue staining.

2.8. Determination of Inhibitor Binding by ANS Displacement Fluorescence Assay

The small fluorescent probe 8-anilino-1-naphthalene sulfonic acid (ANS), is widely used in monitoring ligand or inhibitor binding to the thyroxine-binding site of native tetrameric TTR [23]. ANS binding assay was performed on Synergy HT (BioTek Instruments, Winooski, VT, USA) microplate reader. The ANS stock solution (2.47 mM) was prepared in 10 mM phosphate buffer, pH 7.4 and its concentration was determined by absorbance (E_{350} = 5000 $M^{-1}cm^{-1}$) [24]. Human TTR (0.055 μg/μL) was incubated in the presence of 10 μM ANS and varying concentrations of BME (0.0055–0.55 μg/μL). Fluorescence intensity was measured after 10 min at excitation of 360/40 nm and emission at 460/40 nm at a temperature of 37 °C.

2.9. Statistical Analysis

Statistical analysis was performed with the aid of Graph Pad Prism version 7 for Microsoft windows (Graph Pad Software, San Diego CA, USA). The data was statistically analyzed by one-way analysis of variance (ANOVA) followed by multiple comparison analysis using Tukey's test. Statistical significance was defined as * $p < 0.05$, ** $p < 0.01$, and *** $p < 0.001$. All determinations were performed in triplicate and results represented as means ± SD.

3. Results

3.1. BME Prevented TTR Amyloid Fibril Formation

Amyloidogenesis and fibril formation by TTR is closely associated with the development of the devastating clinical features that characterize ATTR amyloidosis. In order to determine whether BME is able to modulate TTR amyloidogenesis, we accessed its effect on human TTR fibrillation in vitro using acid-mediated aggregation and fibril formation assay. In vitro, human TTR is capable of forming mature amyloid fibrils under mildly acidic conditions at a temperature of 37 °C. As revealed by the TEM image in Figure 1A, human TTR did not only form amorphous aggregates, but also formed mature amyloid fibrils after incubation for 14 days in the absence of BME (Figure 1B). Notably, in the presence of 20 μg/μL BME (concentration of human TTR was 1 μg/μL) no oligomers nor fibrils were observed as shown in Figure 1B. From these results, it can be inferred that BME inhibited human TTR aggregation and fibril formation.

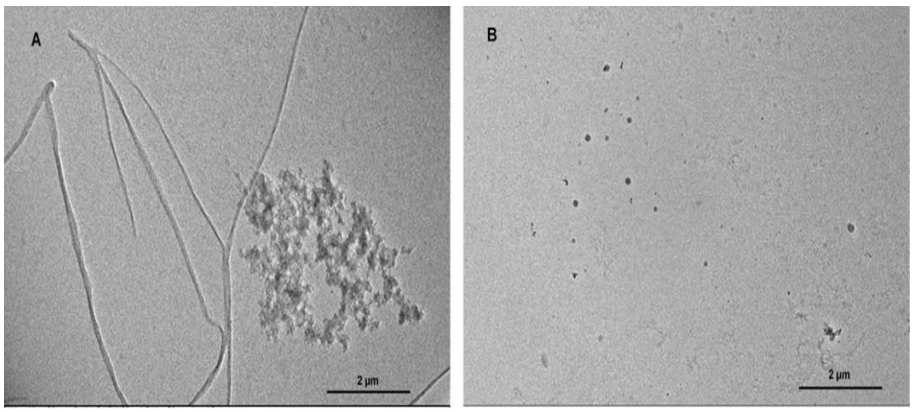

Figure 1. The effect of BME on human TTR aggregation and fibril formation. TEM images of human TTR subjected to acid-mediated aggregation assay in the absence (**A**) or presence (**B**) of BME after 14 days of incubation at 37 °C.

3.2. Effect of Native TTR Stability under Urea-Induced Denaturation Stress

Since tetramer dissociation into monomers is the required and rate-limiting step in TTR amyloidogenesis we speculated that BME might have an effect on native TTR dissociation given its inhibition of fibril formation. Thus, we determined the effect of BME on human TTR and L55P TTR resistance to urea-mediated denaturation stress as described in the Materials section. As shown in Figure 2A (and its representative Tricine-SDS-PAGE image, Figure 2C), in the absence, but not in the presence of BME, human TTR was substantially dissociated after 72 h of incubation in 6 M urea at 4 °C. The percent of folded human TTR (i.e., tetramers, trimers and dimers) left after denaturation stress was higher in the presence of 13.33 μg/μL BME (106 ± 4.77) compared to in its absence (73.49 ± 2.06). Quantitatively the percentage of folded human TTR left after denaturation in BME was not different from that of the control. Correspondingly, there was no formation of human TTR monomers in the presence but not in the absence of BME as indicated by the lack of appearance of the 16 kDa protein band on the gel (Figure 2C). The same trend of results was observed when L55P TTR was subjected to urea mediated denaturation with or without 13.33 μg/μL BME (Figure 2B,C), however, dissociation of L55P TTR was not completely abrogated by BME as indicated by the presence of protein bands around 14–20 kDa corresponding to monomers. These results thus suggest that BME mitigated the dissociation of both human TTR and L55P TTR into monomers.

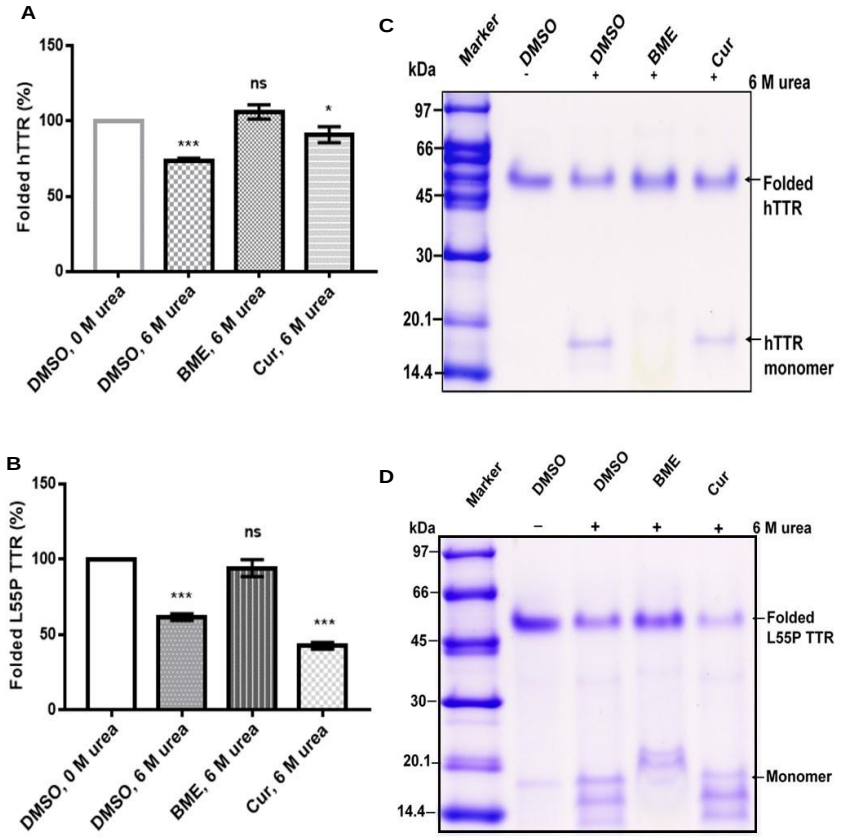

Figure 2. The effect of BME on native TTR dissociation under urea mediated denaturation stress. Bar charts (**A**,**B**) represent folded human TTR (hTTR) and L55P TTR, respectively, in percentage left after 72 h of incubation in the presence or absence of BME. Images (**C**,**D**) are representative of Tricine-SDS-PAGE images of human TTR and L55P TTR, respectively, after denaturation.

3.3. Effect of Human TTR Tetramer Stability under Mildly Acidic Denaturation Condition

TTR undergoes amyloidogenesis in vitro under mildly acid pH. However, this process requires the dissociation of native TTR tetramers into monomers which are susceptible to amyloidogenic transformation by partial unfolding. To ascertain the effect of BME on human TTR stability under acid-mediated denaturation conditions, the amount of tetramer left after aging the protein for 14 days with or without BME was quantified as described in above. As shown in Figure 3, incubation of human TTR under mild acidity markedly reduced the percentage of tetramers in the absence but not in the presence of 20 μg/μL BME. Correspondingly, the content of monomers produced due to acid mediated denaturation of human TTR was higher in the absence than in the presence of BME as revealed by the monomer band intensity (Figure 3B). These results suggest that BME mitigated human TTR tetramer dissociation under mildly acidic conditions and further supports the earlier results observed under urea mediated denaturation conditions.

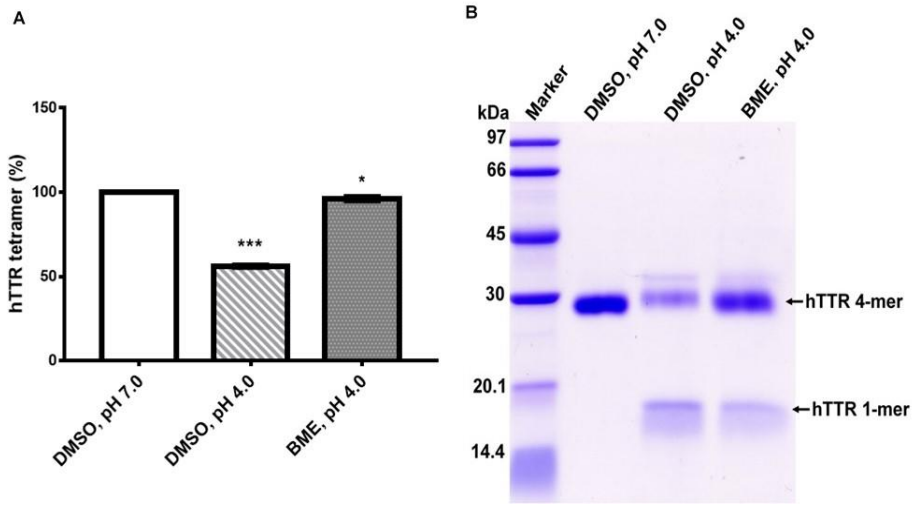

Figure 3. (**A**) Quantitative analysis of the effect of BME on human TTR (hTTR) tetrameric resistance to moderate acidic denaturation conditions. (**B**) Representative Tricine-SDS-PAGE gel image of human TTR (hTTR) resistance to acid mediated denaturation without (Lane 3) or with (Lane 4) BME. Lane 1—protein molecular weight marker.

3.4. Impact of BME on TTR Quaternary Structural Stability and Dose-Dependent Effect

As earlier stated, the key to TTR amyloidogenesis is its transition from tetramer to monomer, thus the stability of the native tetramer is crucial in mitigating its amyloidogenesis. To determine the effect of BME on the quaternary structural stability of human TTR, the protein solution with or without the extract was subjected to urea mediated denaturation stress followed by cross-linking with glutaraldehyde. Glutaraldehyde cross-linking assay gives a reflection of the protein in its different conformations upon resolving on Tricine-SDS-PAGE [25]. As shown in Figure 4, the human TTR solution with or without BME after denaturation stress contained tetramers, trimers, dimers, and monomers, albeit in different proportions. In both the acid and urea mediated denaturation conditions (Figure 4A,B, respectively), the proportion of human TTR tetramer left at the end of the denaturation stress was greater in the presence than in the absence of BME as indicated by the protein band intensities. The opposite was reflected with regards to the proportion of monomers left, especially in the case of urea mediated denaturation (Figure 4B). However, based on the protein band intensities, the content of monomers left after acid mediated denaturation appear to be lesser in the absence of BME. Presumably, this may be due to their rapid conversion to amyloid competent species that are rapidly transformed into higher molecular weight aggregates and fibrils [26] as earlier shown in Figure 1. Thus, it is possible to deduce from these results that BME resisted the dissociation of TTR tetramer to monomers under tetramer-dissociating acid and urea mediated denaturation stress conditions.

The dose-dependent effect of BME on human TTR stability was determined by varying the concentrations of the extract in human TTR denaturation solution. As shown in Figure 4C, there was a substantially higher percentage of human TTR tetramers left after denaturation stress in the presence and not the absence of BME. However, the increase in the amount of human TTR in the presence of increasing amounts of BME was not remarkably different. These observations may be due to fact that the bioactive ligands responsible for tetramer stability was already saturated in its interactions with human TTR at every concentration of BME tested. These results thus seem to suggest that it is possible for BME to stabilize human TTR tetramer.

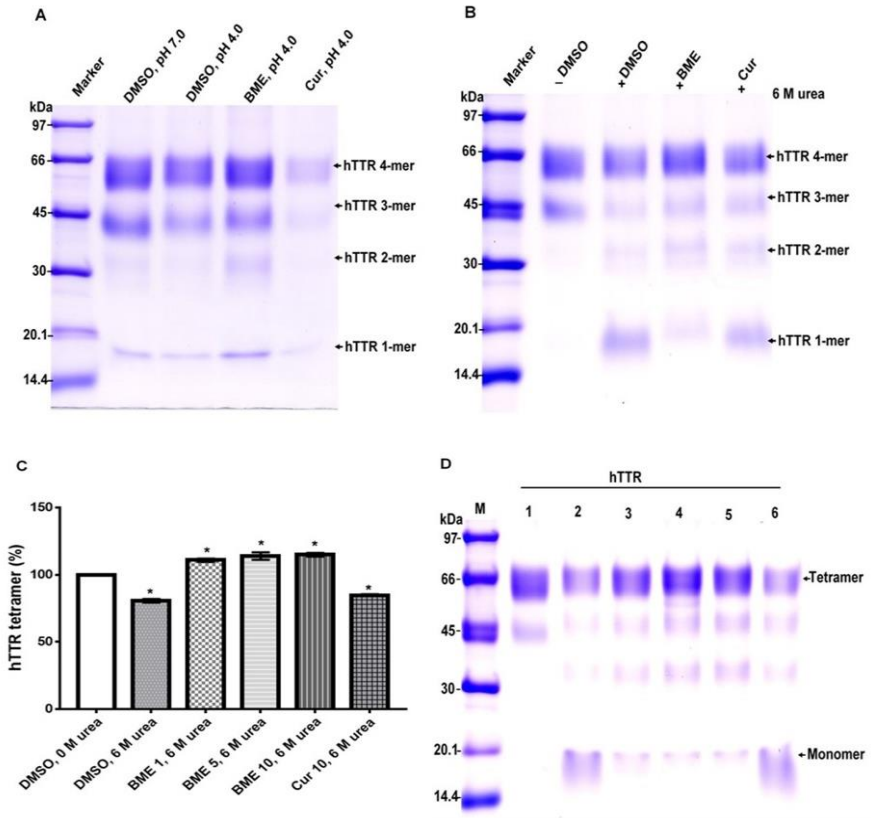

Figure 4. The effect of BME on human TTR (hTTR) quaternary structural stability and its dose-dependent effect. Representative Tricine-SDS-PAGE gel images of glutaraldehyde cross-linked protein samples with or without BME after acid-mediated denaturation (**A**) and urea-mediated denaturation (**B**) assays. (**C**) Quantitative analysis of dose-dependent activity of BME on urea-mediated denaturation of human TTR. (**D**) Representative Tricine-SDS-PAGE gel image of the effect of increasing BME amounts on human TTR tetramer stability. M—molecular weight marker; 1—human TTR in DMSO, without urea; 2—human TTR in DMSO, 6M urea; 3—human TTR in 1 µg/µL BME, 6M urea; 4—human TTR in 5µg/µL BME, 6M urea; 5—human TTR in 10µg/µL BME, 6M urea; 6—10µg/µL curcumin, 6M urea.

3.5. Determination of Human TTR Amyloid Fibril Disrupting Activity of BME

In order to ascertain whether BME had any effect on already formed human TTR amyloid fibril, the soluble protein was first converted into mature fibrils by aging for 14 days in 200 mM acetate buffer, pH 4.0 at 37 °C. Formation of mature human TTR amyloid fibrils was confirmed using TEM. The preformed human TTR fibrils was the co-incubated with or without BME at 37 °C for an additional 24 h. Thereafter, aliquot of the fibril solution was obtained and diluted by 100 times with Milli-Q water and spotted on formvar coated copper TEM grid followed by negative staining with 2% uranyl acetate. Electron micrographs were later obtained. From the TEM images obtained (Figure 5), it could be seen that the presence of BME did not alter the fibril morphology. There was no disruption in the mature preformed human TTR fibrils after 24 h of incubation of the given concentration of BME. Thus, it can be concluded that BME did not possess any fibril disrupting activity on mature human TTR fibrils.

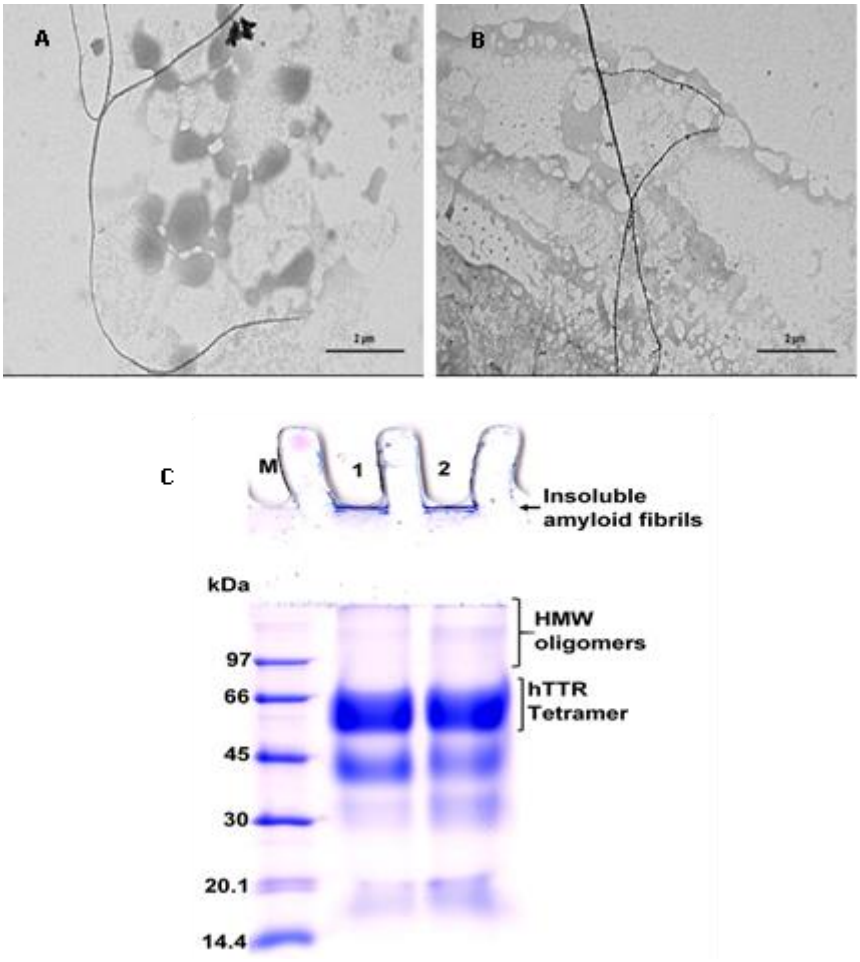

Figure 5. Images of pre-formed human TTR amyloid fibrils in the absence (**A**) or presence of BME (**B**) after incubation for 24 h. (**C**) Tricine-SDS-PAGE gel representation of human TTR fibril disruption activity of BME. Lane 1—protein molecular weight marker; Lane 2—human TTR pre-formed fibrils without BME; Lane 3—human TTR pre-formed fibrils with BME.

3.6. Determination of BME Binding to TTR

Binding interaction between BME and human TTR was monitored using the small fluorescent probe ANS. ANS is very sensitive to the polarity of its environment. In aqueous environments, ANS has a weak fluorescence and displays an emission of maximum at 500 nm. Upon binding to the hydrophobic patches of proteins it produces a blue shift in its emission wavelength and an increase in its fluorescence intensity the extent of which is dependent on the protein structure and milieu surrounding ANS [27]. In the presence of human TTR tetramer, ANS binds specifically to the thyroxine-binding sites within the hydrophobic cavity with a consequent increase in fluorescence intensity at about 480 nm [28]. As shown in Figure 6, human TTR and ANS separately in phosphate buffer had very weak fluorescence intensities. However, upon co-incubation of human TTR and ANS in phosphate buffer, there was a dramatic increase in the fluorescence intensity. This can be attributed to the binding of ANS to the thyroxine-binding sites of human TTR tetramers as previously reported [7,28]. Interestingly, introduction of BME reduced the ANS fluorescence intensities dose-responsively. These seem to suggest that BME binds to the thyroxine binding sites of the tetramers and prevents ANS from its preferred binding location on the protein. Out of the hydrophobic T4-binding sites, ANS thus gives reduced fluorescence intensity.

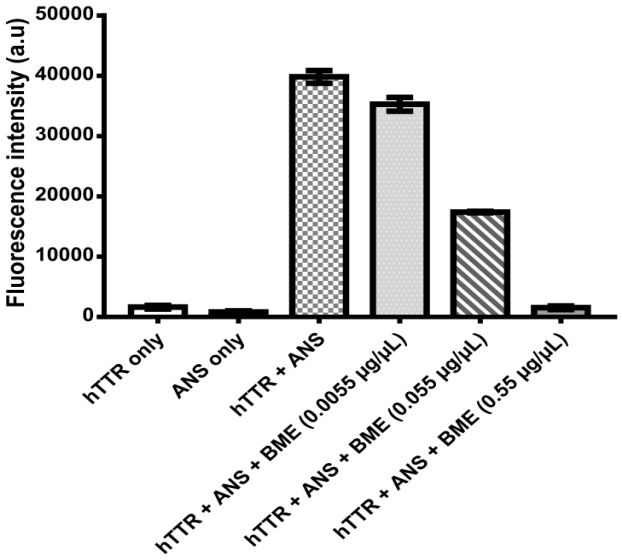

Figure 6. Human TTR-ANS fluorescence intensity without or with increasing concentrations of BME for the determination of ANS displacement from human TTR T4-binding sites by BME.

3.7. Chemical Characterization of BME

The major bioactive phytoconstituents in BME were determined by RP-HPC quantitative analysis as described in the Methods section. BME was found to contain Bacoside A (Bacoside A3 (2.22% *w*/*w*), Bacopaside II (4.68% *w*/*w*), Bacopaside X (3.25% *w*/*w*)) and Bacopaside I (3.54% *w*/*w*), giving a total saponin content of 16.03% *w*/*w* of dried extract. Previously it had been reported that the total Bacoside A content of methanol extract of in vitro culture of *Bacopa monnieri* was 8.73 mg/g of dry weight [29]. The superior content of BME may be due to difference in our extraction method and solvent composition. BME contain over sixty individual compounds. The metabolite profile of saponins, phenolics, and other components present were previously determined by LC-ESI-qTOF-MS [15]. The total phenolic content of BME was also determined using the widely accepted Folin–Ciocalteu assay. BME recorded a phenolic content of 26.45 mg gallic acid equivalent/gram of dry weight. Compared to the phenolic content of thirty common culinary herbs in Thailand previously reported, BME had a higher phenolic content than twenty-three of them including *Cucurbita moschata* (pumpkin) leaves, *Allium sativum* (garlic) cloves, *Mentha canalenisa* (peppermint) leaves, *Curcuma longa* (turmeric) rhizome. However, the phenolic content of *Ocimum basilicum* (sweet basil) leaves, *Ocimum sanctum* (holy basil) leaves and *Acacia penneta* (acacia) shoot tips were higher than BME. Given that flavonoids constitute a major proportion of polyphenols in several plant species, the total flavonoid content in BME was determined and found to be 17.6 mg quercetin equivalent/g of BME [30].

The antioxidant capacity of BME was determined using DPPH and FRAP assays, two of the most commonly reported in vitro methods for ascertaining antioxidant content in fruits, vegetables, and plant-derived constituents. The FRAP assay measures the reductive ability of all the redox-active constituents in BME via single electron transfer (SET) mechanism while the DPPH assay determines radical scavenging activity of the extract toward the DPPH radical by SET and hydrogen atom transfer (HAT) mechanisms [31]. As shown in Table 1, BME had a FRAP value of 306.82 µmol Fe(II)/g, which is indicative of its ability to reduce ferric-TPTZ complex to its ferrous form. The DPPH IC_{50} value for BME was 90.89 mg/L. Konczak et al. observed a high degree of correlation between the FRAP value (in µmol Fe(II)/g dry weight) of commercially grown native Australian herbs and spices and their phenolic content (in mg gallic acid equivalent/g dry weight), which validated the notion that antioxidant capacity of bioactive components from food and plants is a function of their natural phenolic content [32]. Given that many of the health benefits associated with the consumption of fruits, vegetables and bioactives from plant sources have been attributed to antioxidants, it can be

speculated that the presence these small-molecule natural antioxidant phenolics and saponins might be responsible for the anti-amyloidogenic properties of BME.

Table 1. Chemical profile and antioxidant activity of Brahmi extract.

Chemical Property	Brahmi Extract
Total saponin content (% *w*/*w* of dried extract)	16.03 ± 0.01
Total phenolic content (mg gallic acid/g BME)	26.45 ± 0.34
Total flavonoid content (mg quercetin/g BME)	17.6 ± 1.5
Ferric reducing antioxidant power (μmol Fe (II)/g BME)	306.82
DPPH radical scavenging activity IC_{50} (mg/L)	90.84 ± 0.44

4. Discussion

The objective of this work was to determine the ability of *Bacopa monnieri* extract (BME) to modulate transthyretin amyloidogenesis and fibril disaggregation in vitro. The results obtained strongly suggest that BME inhibited the formation of human TTR aggregates and mature fibril by stabilizing and preventing the dissociation of native tetramers through binding at the thyroxine-binding sites of the protein. However, BME could not disrupt preformed TTR fibrils. These findings suggest that BME contained bioactive metabolites with potential therapeutic implications for the modulation of ATTR amyloidosis.

Normal physiological native TTR is made up of four identical monomers often annotated A-D. Each monomer is consisted of eight B-strands (A–H) and a short alpha helix, EF helix. Interaction between monomers via hydrogen bonds produces dimers. The dimers self-associate furnished by hydrogen bonds and hydrophobic interactions to form the functional tetramer which possesses a central hydrophobic channel that contains two binding sites for thyroxine (T4) created by amino acid residues from both dimers [33]. TTR is also capable of acquiring a gain-in-toxic function by becoming amyloidogenic in human [34]. Indeed, TTR amyloidogenesis is associated with the development of severe clinical complications including peripheral neuropathy, autonomic dysfunctions, cardiomyopathy, or death in some cases, a condition which is generally referred to as ATTR amyloidosis. Unlike in several other similar multifactorial diseases such as Alzheimer's disease and Parkinson's disease where there are a lot of controversies surrounding their origin, in ATTR amyloidosis the consensus is that the key molecular event underpinning its etiopathogenesis is destabilization of the homotetrameric structure leading to its dissociation to monomers [1]. Given the pivotal role of tetramer dissociation in initiating the TTR amyloid cascade, there had been a strong momentum in research focused on the identification and development of kinetic stabilizers i.e., small-ligand agents which binds to (typically at the T4-binding sites) and prevents dissociation of tetrameric transthyretin [4]. The kinetic stabilization strategy led to the development of the regulatory approved drug Tafamidis, for the treatment of early-stage FAP [1] or cardiomyopathy of ATTRw amyloidosis. However, with limitations in Tafamidis such as its inability to prevent progression in neuropathy as well as its lack of effectiveness in late-stage TTR amyloidosis and nonV30M ATTRv amyloidosis [35], it is, therefore, vital to continue investigations aimed at identifying and developing effective and safe therapeutic alternatives.

In vitro, transthyretin is known to form amyloid fibrils under mildly acidic pH (5–4) at physiological temperature [36]. Using the well-established acid-mediated aggregation and fibril formation assay, we found that BME completely abrogated the formation of oligomers and mature amyloid fibrils by human TTR after 14 days of incubation as shown by the electron micrographs of the aged protein solutions. These findings are supported by earlier studies demonstrating the anti-amyloidogenic potential of BME on α-Synuclein [37]. Parkinson's disease is recently being considered as a type of amyloidosis—of which the main neuropathological diagnostic feature is the accumulation of cross-β sheet-rich aggregates of α-Synuclein as Lewy bodies in the brain [38]. The crucial step in the pathogenesis of Parkinson's disease is the aggregation of α-Synuclein [39], which is reportedly attenuated by *B. monnieri* extract [37]. However, unlike α-Synuclein and beta-amyloid which aggregate

and form fibrils via a nucleation-dependent polymerization mechanism, TTR follows a downhill polymerization of amyloid competent monomers [40]. The implication here is that formation of these amyloidogenic monomers mandates the dissociation of tetramers—the critical step in TTR amyloidogenesis. Additionally, since this process is concentration-driven, a viable strategy to prevent the TTR amyloidogenesis and fibrillation would certainly involve preserving the quaternary structural integrity of tetramers [41]. Results from this study shows that BME indeed mitigated the urea-induced dissociation of human TTR and its most pathogenic variant L55P TTR, into their constituent monomers. These results were further supported by the resistance of human TTR in the presence but not in the absence of BME against acid-mediated denaturation and fibril formation. However, BME was incapable of disrupting preformed mature human TTR amyloid fibrils. These seem to suggest that the inhibition of human TTR fibril formation by BME was due to the prevention of the rate-limiting tetramer dissociation. Previous studies in the recent past have shown that natural products such as curcumin from *Curcuma longa* (Turmeric), propolis from honeybee were able to prevent the dissociation of TTR tetramers and, thus, modulate its amyloidogenesis [7,28]. The prevailing molecular mechanism, especially in the case of propolis involved the binding of the small-molecule ligand at the T4-binding site within the central hydrophobic channel of TTR tetramer with consequent increase in the tetramer stability. BME binds to and displaced the fluorescent probe ANS from the T4-binding sites in native tetrameric TTR as revealed by ANS displacement assay. The binding of BME at the T4-binding sites presumably creates further interactions between the dimers which might explain the plausible increase in stability of TTR tetramer observed in the glutaraldehyde cross-linking assay. This is supported by similar observations in several previous studies, i.e., increased TTR tetramer stability by binding of small-ligands at the T4-binding sites [7,19,28,42], as well as by mutations which fill the T4-binding cavity [3].

BME possessed a high content of triterpenoid saponins as revealed by the RP-HPLC quantitative analysis, as well as phenolics, especially flavonoids. These findings were in accord with previous reports on the phytochemical constituents of *B. monnieri* extracts [15]. It is plausible that the tetramer stabilizing and anti-amyloidogenic effects of BME are due to the binding interactions mediated by these small-molecule ligands. In addition, BME also demonstrated a strong radical scavenging and antioxidant capacity. The radical scavenging effect of plant bioactives rich in phenolics is based on their ability to initiate single electro transfers, donate hydrogen atoms, or chelate transition metals [31]. In addition to BME binding directly and stabilizing TTR tetramers, its antioxidant bioactives might also be relevant in modulating TTR amyloidogenesis. For instance, it has been well reported that, similar to beta-amyloid in Alzheimer's disease and α-Synuclein in Parkinson's disease, TTR amyloidogenesis is also influenced by environmental or physiological factors, such as post-translational modifications [41]. This is supported by the fact that aging is the most relevant risk factor in these pathologies, and aging-associated oxidative modifications have been shown to modulate transthyretin amyloidogenesis and disease onset [43]. The free thiol group on Cys-10 residue has been shown to be one of the most susceptible free thiols in human plasma to oxidative modifications. Given its unique location close to the surface of the tetramer and near the thyroxine binding site, oxidative modifications of Cys-10 alters the structure of the homotetramer and reduces its stability [44]. The antioxidant and radical scavenging attributes of BME might provide an indirect protection on TTR by altering the redox potential of the milieu. A similar positive impact on TTR amyloidogenesis by natural agents with potent antioxidant activities had been previously observed in carvedilol, TUDCA, curcumin, and green tea extracts, which were shown to significantly reduce deposition of amyloid TTR despite their less impressive effect on tetramer stability [45–48]. Previous studies have reported the neuroprotective effects of *B. monnieri* in diseases such as Alzheimer's disease [49], Parkinson's disease [37], and neurotoxicant-induced brain dysfunction [50]. Our investigation for the first time provides in vitro evidence for the protective role of BME in modulating transthyretin amyloidogenesis.

5. Conclusions

In conclusion, this mechanistic investigation using biochemical assays suggested that BME inhibited TTR amyloidogenesis by attenuating the rate-limiting step in TTR amyloidogenesis pathway, that is the dissociation homotetramers into monomeric constituents by binding at the thyroxine-binding sites of and possibly stabilizing the native tetramer. Although these studies unveiled the potential of BME in countering the causative mechanism of ATTR pathology, further investigations are warranted, such as determining its potency and safety profile in disease animal models.

Author Contributions: F.N.E. planned and conducted experiments, analyzed and organized the data, generated figures, interpreted the results, and wrote the manuscript. K.I. prepared and performed analysis of *B. monnieri* extract (BME). P.P. conceptualized the idea, administrated the project, supervised the study, planned the experiments, and co-interpreted and reviewed the manuscript.

Funding: This research was supported by the National Research Council of Thailand, Prince of Songkla University and the Excellent Biochemistry Program Fund of Prince of Songkla University, Thailand. F.N.E. is a recipient of scholarship for his PhD research from Thailand's Education Hub for ASEAN Countries (TEH-AC 055/2014) and the Graduate School of Prince of Songkla University, Thailand.

Conflicts of Interest: The authors declare no conflict of interest. The funders had no role in the design of the study; in the collection, analyses, or interpretation of data; in the writing of the manuscript; or in the decision to publish the results.

References

1. Johnson, S.M.; Connelly, S.; Fearns, C.; Powers, E.T.; Kelly, J.W. The Transthyretin Amyloidoses: From Delineating the Molecular Mechanism of Aggregation Linked to Pathology to a Regulatory Agency Approved Drug. *J. Mol. Biol.* **2012**, *421*, 185–203. [CrossRef] [PubMed]
2. Hortin, G.L.; Sviridov, D.; Anderson, N.L. High-abundance polypeptides of the human plasma proteome comprising the top 4 logs of polypeptide abundance. *Clin. Chem.* **2008**, *54*, 1608–1616. [CrossRef] [PubMed]
3. Sant'Anna, R.; Almeida, M.R.; Varejão, N.; Gallego, P.; Esperante, S.; Ferreira, P.; Pereira-Henriques, A.; Palhano, F.L.; de Carvalho, M.; Foguel, D.; et al. Cavity filling mutations at the thyroxine-binding site dramatically increase transthyretin stability and prevent its aggregation. *Sci. Rep.* **2017**, *7*, 44709. [CrossRef] [PubMed]
4. Johnson, S.M.; Wiseman, R.L.; Sekijima, Y.; Green, N.S.; Adamski-Werner, S.L.; Kelly, J.W. Native state kinetic stabilization as a strategy to ameliorate protein misfolding diseases: A focus on the transthyretin amyloidoses. *Acc. Chem. Res.* **2005**, *38*, 911–921. [CrossRef]
5. Kapoor, M.; Rossor, A.M.; Laura, M.; Reilly, M.M. Clinical Presentation, Diagnosis and Treatment of TTR Amyloidosis. *J. Neuromuscul. Dis.* **2019**, *6*, 189–199. [CrossRef]
6. Chaudhary, N.; Sasaki, R.; Shuto, T.; Watanabe, M.; Kawahara, T.; Suico, M.A.; Yokoyama, T.; Mizuguchi, M.; Kai, H.; Devkota, H.P. Transthyretin Amyloid Fibril Disrupting Activities of Extracts and Fractions from Juglans mandshurica Maxim. var. cordiformis (Makino) Kitam. *Molecules* **2019**, *24*, 500. [CrossRef]
7. Yokoyama, T.; Kosaka, Y.; Mizuguchi, M. Inhibitory activities of propolis and its promising component, caffeic acid phenethyl ester, against amyloidogenesis of human transthyretin. *J. Med. Chem.* **2014**, *57*, 8928–8935. [CrossRef]
8. Yokoyama, T.; Mizuguchi, M. Inhibition of the Amyloidogenesis of Transthyretin by Natural Products and Synthetic Compounds. *Biol. Pharm. Bull.* **2018**, *41*, 979–984. [CrossRef]
9. Tungphatthong, C.; Somnuek, J.; Phadungcharoen, T.; Ingkaninan, K.; Denduangboripant, J.; Sukrong, S. DNA barcoding of species of Bacopa coupled with high-resolution melting analysis. *Genome* **2018**, *61*, 867–877. [CrossRef]
10. Sivarajan, V.V.; Balachandran, I. *Ayurvedic Drugs and Their Plant. Sources*; Oxford & IBH Publishing Company: New Delhi, Delhi, India, 1994.
11. Russo, A.; Borrelli, F.; Campisi, A.; Acquaviva, R.; Raciti, G.; Vanella, A. Nitric oxide-related toxicity in cultured astrocytes: Effect of Bacopa monniera. *Life Sci.* **2003**, *73*, 1517–1526. [CrossRef]
12. Jain, P.; Khanna, N.K.; Trehan, N.; Pendse, V.K.; Godhwani, J.L. Antiinflammatory effects of an Ayurvedic preparation, Brahmi Rasayan, in rodents. *Indian J. Exp. Biol.* **1994**, *32*, 633–636. [PubMed]

13. Aguiar, S.; Borowski, T. Neuropharmacological Review of the Nootropic Herb Bacopa monnieri. *Rejuvenation Res.* **2013**, *16*, 313–326. [CrossRef] [PubMed]
14. Sireeratawong, S.; Jaijoy, K.; Khonsung, P.; Lertprasertsuk, N.; Ingkaninan, K. Acute and chronic toxicities of Bacopa monnieri extract in Sprague-Dawley rats. *BMC Complement. Altern. Med.* **2016**, *16*, 249. [CrossRef] [PubMed]
15. Nuengchamnong, N.; Sookying, S.; Ingkaninan, K. LC-ESI-QTOF-MS based screening and identification of isomeric jujubogenin and pseudojujubogenin aglycones in Bacopa monnieri extract. *J. Pharm. Biomed. Anal.* **2016**, *129*, 121–134. [CrossRef] [PubMed]
16. Prapunpoj, P.; Richardson, S.J.; Schreiber, G. Crocodile transthyretin: Structure, function, and evolution. *Am. J. Physiol.-Regul. Integr. Comp. Physiol.* **2002**, *283*, R885–R896. [CrossRef]
17. Leelawatwattana, L.; Praphanphoj, V.; Prapunpoj, P. Effect of the N-terminal sequence on the binding affinity of transthyretin for human retinol-binding protein. *FEBS J.* **2011**, *278*, 3337–3347. [CrossRef]
18. Phrompittayarat, W.; Putalun, W.; Tanaka, H.; Jetiyanon, K.; Wittaya-Areekul, S.; Ingkaninan, K. Determination of pseudojujubogenin glycosides from Brahmi based on immunoassay using a monoclonal antibody against bacopaside I. *Phytochem. Anal.* **2007**, *18*, 411–418. [CrossRef]
19. Eze, F.N.; Leelawatwattana, L.; Prapunpoj, P. Structural Stabilization of Human Transthyretin by Centella asiatica (L.) Urban Extract: Implications for TTR Amyloidosis. *Biomolecules* **2019**, *9*, 128. [CrossRef]
20. Benzie, I.F.; Strain, J.J. Ferric reducing/antioxidant power assay: Direct measure of total antioxidant activity of biological fluids and modified version for simultaneous measurement of total antioxidant power and ascorbic acid concentration. *Meth. Enzymol.* **1999**, *299*, 15–27.
21. Lesjak, M.M.; Beara, I.N.; Orčić, D.Z.; Anačkov, G.T.; Balog, K.J.; Francišković, M.M.; Mimica-Dukić, N.M. Juniperus sibirica Burgsdorf. as a novel source of antioxidant and anti-inflammatory agents. *Food Chem.* **2011**, *124*, 850–856. [CrossRef]
22. Robinson, L.Z.; Reixach, N. Quantification of Quaternary Structure Stability in Aggregation-Prone Proteins under Physiological Conditions: The Transthyretin Case. *Biochemistry* **2014**, *53*, 6496–6510. [CrossRef] [PubMed]
23. Yokoyama, T.; Mizuguchi, M. Crown Ethers as Transthyretin Amyloidogenesis Inhibitors. *J. Med. Chem.* **2019**, *62*, 2076–2082. [CrossRef] [PubMed]
24. Stryer, L. The interaction of a naphthalene dye with apomyoglobin and apohemoglobin. A fluorescent probe of non-polar binding sites. *J. Mol. Biol.* **1965**, *13*, 482–495. [CrossRef]
25. Sekijima, Y.; Dendle, M.A.; Kelly, J.W. Orally administered diflunisal stabilizes transthyretin against dissociation required for amyloidogenesis. *Amyloid* **2006**, *13*, 236–249. [CrossRef]
26. Reixach, N.; Deechongkit, S.; Jiang, X.; Kelly, J.W.; Buxbaum, J.N. Tissue damage in the amyloidoses: Transthyretin monomers and nonnative oligomers are the major cytotoxic species in tissue culture. *Proc. Natl. Acad. Sci. USA* **2004**, *101*, 2817–2822. [CrossRef]
27. Choudhary, S.; Save, S.N.; Vavilala, S.L. Unravelling the inhibitory activity of Chlamydomonas reinhardtii sulfated polysaccharides against α-Synuclein fibrillation. *Sci. Rep.* **2018**, *8*. [CrossRef]
28. Pullakhandam, R.; Srinivas, P.N.B.S.; Nair, M.K.; Reddy, G.B. Binding and stabilization of transthyretin by curcumin. *Arch. Biochem. Biophys.* **2009**, *485*, 115–119. [CrossRef]
29. Łojewski, M.; Pomierny, B.; Muszyńska, B.; Krzyżanowska, W.; Budziszewska, B.; Szewczyk, A. Protective Effects of Bacopa Monnieri on Hydrogen Peroxide and Staurosporine: Induced Damage of Human Neuroblastoma SH-SY5Y Cells. *Planta Med.* **2016**, *82*, 205–210. [CrossRef]
30. Wongsa, P.; Chaiwarit, J.; Zamaludien, A. In vitro screening of phenolic compounds, potential inhibition against α-amylase and α-glucosidase of culinary herbs in Thailand. *Food Chem.* **2012**, *131*, 964–971. [CrossRef]
31. Nimse, S.B.; Pal, D. Free radicals, natural antioxidants, and their reaction mechanisms. *RSC Adv.* **2015**, *5*, 27986–28006. [CrossRef]
32. Konczak, I.; Zabaras, D.; Dunstan, M.; Aguas, P. Antioxidant capacity and phenolic compounds in commercially grown native Australian herbs and spices. *Food Chem.* **2010**, *122*, 260–266. [CrossRef]
33. Munro, S.L.; Lim, C.F.; Hall, J.G.; Barlow, J.W.; Craik, D.J.; Topliss, D.J.; Stockigt, J.R. Drug competition for thyroxine binding to transthyretin (prealbumin): Comparison with effects on thyroxine-binding globulin. *J. Clin. Endocrinol. Metab.* **1989**, *68*, 1141–1147. [CrossRef]

34. Cornwell, G.G.; Sletten, K.; Johansson, B.; Westermark, P. Evidence that the amyloid fibril protein in senile systemic amyloidosis is derived from normal prealbumin. *Biochem. Biophys. Res. Commun.* **1988**, *154*, 648–653. [CrossRef]
35. Lozeron, P.; Théaudin, M.; Mincheva, Z.; Ducot, B.; Lacroix, C.; Adams, D. French Network for FAP (CORNAMYL) Effect on disability and safety of Tafamidis in late onset of Met30 transthyretin familial amyloid polyneuropathy. *Eur. J. Neurol.* **2013**, *20*, 1539–1545. [CrossRef]
36. Lashuel, H.A.; Lai, Z.; Kelly, J.W. Characterization of the transthyretin acid denaturation pathways by analytical ultracentrifugation: Implications for wild-type, V30M, and L55P amyloid fibril formation. *Biochemistry* **1998**, *37*, 17851–17864. [CrossRef]
37. Jadiya, P.; Khan, A.; Sammi, S.R.; Kaur, S.; Mir, S.S.; Nazir, A. Anti-Parkinsonian effects of Bacopa monnieri: Insights from transgenic and pharmacological Caenorhabditis elegans models of Parkinson's disease. *Biochem. Biophys. Res. Commun.* **2011**, *413*, 605–610. [CrossRef]
38. Araki, K.; Yagi, N.; Aoyama, K.; Choong, C.-J.; Hayakawa, H.; Fujimura, H.; Nagai, Y.; Goto, Y.; Mochizuki, H. Parkinson's disease is a type of amyloidosis featuring accumulation of amyloid fibrils of α-synuclein. *Proc. Natl. Acad. Sci. USA* **2019**, *116*, 17963–17969. [CrossRef]
39. Wood, S.J.; Wypych, J.; Steavenson, S.; Louis, J.C.; Citron, M.; Biere, A.L. alpha-synuclein fibrillogenesis is nucleation-dependent. Implications for the pathogenesis of Parkinson's disease. *J. Biol. Chem.* **1999**, *274*, 19509–19512. [CrossRef]
40. Hurshman, A.R.; White, J.T.; Powers, E.T.; Kelly, J.W. Transthyretin aggregation under partially denaturing conditions is a downhill polymerization. *Biochemistry* **2004**, *43*, 7365–7381. [CrossRef]
41. Eisele, Y.S.; Monteiro, C.; Fearns, C.; Encalada, S.E.; Wiseman, R.L.; Powers, E.T.; Kelly, J.W. Targeting Protein Aggregation for the Treatment of Degenerative Diseases. *Nat. Rev. Drug Discov.* **2015**, *14*, 759–780. [CrossRef]
42. Yokoyama, T.; Ueda, M.; Ando, Y.; Mizuguchi, M. Discovery of γ-Mangostin as an Amyloidogenesis Inhibitor. *Sci. Rep.* **2015**, *5*, 13570. [CrossRef]
43. Zhao, L.; Buxbaum, J.N.; Reixach, N. Age-related oxidative modifications of transthyretin modulate its amyloidogenicity. *Biochemistry* **2013**, *52*, 1913–1926. [CrossRef]
44. Pereira, C.D.; Minamino, N.; Takao, T. Free Thiol of Transthyretin in Human Plasma Most Accessible to Modification/Oxidation. *Anal. Chem.* **2015**, *87*, 10785–10791. [CrossRef]
45. Macedo, B.; Magalhães, J.; Batista, A.R.; Saraiva, M.J. Carvedilol treatment reduces transthyretin deposition in a familial amyloidotic polyneuropathy mouse model. *Pharmacol. Res.* **2010**, *62*, 514–522. [CrossRef]
46. Macedo, B.; Batista, A.R.; Ferreira, N.; Almeida, M.R.; Saraiva, M.J. Anti-apoptotic treatment reduces transthyretin deposition in a transgenic mouse model of Familial Amyloidotic Polyneuropathy. *BBA-Mol. Basis Dis.* **2008**, *1782*, 517–522. [CrossRef]
47. Ferreira, N.; Gonçalves, N.P.; Saraiva, M.J.; Almeida, M.R. Curcumin: A multi-target disease-modifying agent for late-stage transthyretin amyloidosis. *Sci. Rep.* **2016**, *6*, 26623. [CrossRef]
48. aus dem Siepen, F.; Bauer, R.; Aurich, M.; Buss, S.J.; Steen, H.; Altland, K.; Katus, H.A.; Kristen, A.V. Green tea extract as a treatment for patients with wild-type transthyretin amyloidosis: An observational study. *Drug Des. Devel. Ther.* **2015**, *9*, 6319–6325. [CrossRef]
49. Uabundit, N.; Wattanathorn, J.; Mucimapura, S.; Ingkaninan, K. Cognitive enhancement and neuroprotective effects of Bacopa monnieri in Alzheimer's disease model. *J. Ethnopharmacol.* **2010**, *127*, 26–31. [CrossRef]
50. Shinomol, G.K.; Mythri, R.B.; Srinivas Bharath, M.M. Muralidhara Bacopa monnieri Extract Offsets Rotenone-Induced Cytotoxicity in Dopaminergic Cells and Oxidative Impairments in Mice Brain. *Cell Mol. Neurobiol.* **2012**, *32*, 455–465. [CrossRef]

VITAE

Name **Eze Fredrick Nwude**

Student ID **5710230031**

Educational Attainment

Degree	Name of Institution	Year of Graduation
Master of Science, (Biochemistry)	University of Benin, Ugbowo	2014
Bachelor of Science (Biochemistry)	Joseph Ayo Babalola University, Ikeji-Arakeji	2010

Scholarship Awards during Enrolment

Thailand's Education Hub for ASEAN Countries (TEH-AC 055/2014) and the Graduate School of Prince of Songkla University, Thailand

List of Publications

Eze, F. N., Ingkaninan, K. and Prapunpoj, P. 2019 Transthyretin anti-amyloidogenic and fibril disrupting activities of *Bacopa monnieri* (L.) Wettst (Brahmi) extract. *Biomolecules* 2019,9, 845.

Eze, F. N., Leelawatwattana, L. and Prapunpoj, P. Structural Stabilization of Human Transthyretin by *Centella asiatica* (L.) Urban Extract: Implications for TTR Amyloidosis. *Biomolecules 2019*, 9, 128.

Oral presentation

Eze F. N., Prapunpoj P. Profile of phenolic content of Brahmi and semi-purification of tannins from *C. asiatica*. Oral presentation at: The 5th International Biochemistry and Molecular Biology Conference; 2016 May 26-27; Songkhla, Thailand.